Automatic Skin Cancer Detection system

By
Azadeh Noori Hoshyar

Submitted in partial fulfilment of the requirements for the
Master of Engineering

Faculty of Engineering and Information Technology
UNIVERSITY OF TECHNOLOGY, SYDNEY

November, 2014

CERTIFICATE OF AUTHORSHIP/ORIGINALITY

I certify that the work in this thesis has not previously been submitted for a degree nor has it been submitted as part of requirements for a degree except as fully acknowledged within the text.

I also certify that the thesis has been written by me. Any help that I have received in my research work and the preparation of the thesis itself has been acknowledged. In addition, I certify that all information sources and literature used are indicated in the thesis.

Signature of Candidate

Acknowledgment

Over the last two years I have had the privilege of working with a variety of people who have made my time at University of technology, Sydney an enjoyable and intellectually stimulating experience.

I would like to thank all the people who have helped me along the way and contributed to this dissertation. I am especially grateful to my Supervisor Associate Professor **Dr. Adel Al-Jumaily**. In working with Adel, I have learned how to pursue research problems with intellectual rigor and how to critically evaluate my work.

Finally, I would like to acknowledge the endless love of my husband and family; who have been constant source of support also who have provided guidance, love and encouragement throughout my life.

Table of Contents

List of Figures

Chapter 1

Chapter 2

Chapter 3

Chapter 4

Chapter 5

List of Tables

Chapter 4

Chapter 5

List of Abbreviations

Adaptive histogram equalization (AHE)

Artificial Neural Networks (ANN)

Analysis of variance (ANOVA)

Diagnostic odds ratio (DOR)

Epilumence microscopy (ELM)

Fuzzy c-means thresholding (FCM)

Gray Level Coocurrence Matrix (GLCM)

Gray Level Non-Uniformity (GLNU)

Gradient vector flow (GVF)

Histogram Equalization (HE)

High Grey-Level Zone Emphasis (HGZE)

Inverse difference normalized (INN)

Inverse difference (INV)

Inertia based Particle Swarm Optimization (IPSO)

K-means-level set (KLS)

K-nearest-neighbourhood (K-NN)

Low Grey-Level Zone Emphasis (LGZE)

Leave One Out (LOO)

Long Zones Emphasis (LZE)

Long Zone High Gray-Level Emphasis (LZHGE)

Long Zone Low Gray-Level Emphasis (LZLGE)

Non-melanoma skin cancer (NMSC),

Optical Coherence Tomography (OCT)

Peak signal-to-noise ratio (PSNR)

Particle Swarm Optimization (PSO)

Reflectance confocal microscopy (RCM)

Self-Advising Support vector machine (SA-SVM)

Symmetry distance (SD)

Sequential Floating Backward Selection (SFBS)

Sequential Floating Forward Selection (SFFS)

Sequential fature selection (SFS)

Short Zone High Gray-Level Emphasis (SZHGE)

Short Zone Low Gray-Level Emphasis (SZLGE)

Support vector machine (SVM)

Short Zones Emphasis (SZE)

Side transillumination (TLM)

Traditional level set (TLS)

Unsharp Masking (UM)

Ultraviolet (UV)

Cross-polarization epiluminescence (XLM)

Zone Length Non-Uniformity (ZLNU)

Zone Percentage (ZP)

ABSTRACT

During recent decades, the incident of malignant melanoma as the lethal form of skin cancer has been raised. The occurrence in Australia is much higher than US, UK, and Canada with the cases more than 10,000 diagnosis and annual mortality of 1250 people. The persistent raise of this cancer in the worldwide, the high medical cost and death rate have prioritized the early diagnosis of this cancer. The anticipation and cure of melanoma is strictly relevant to its thickness, if it can be detected early, the survival rate would be increased. Although lots of effort has been made to advance the detection of skin cancers, the challenging concerns still about it.

The computer-based detection systems can improve the diagnosis rate of melanoma by 5–30% in comparison with the naked-eye. Since the visual perception often involve some faults, the necessity of second opinion with higher accuracy and reliability is highlighted. On the other hand, it reduces the task and responsibilities that are performed by physicians.

Many researches have been developed in automated detection of melanoma. The potential advantages of such studies are significant and incalculable. Moreover, the difficulties entangle are a lot, and the new contributions in the area are highly appreciated. However, it is extensively acknowledged that the more trustful and reliable detection systems require higher accuracy. The purpose of this thesis is to propose an algorithm for skin cancer diagnosis that is able to classify lesions as malignant or benign automatically.

The different components in an automated diagnosis of skin cancer includes: Pre-processing, segmentation, feature extraction and selection, and classification. In this thesis, after selecting the best image enhancement techniques which are achieved by applying and comparing different noise removal and contrast enhancement techniques on images, the segmentation stage is performed. In this stage, a fully automated segmentation algorithm in dermoscopy images based on k-mean and level-set algorithms are proposed and compared with other algorithms mentioned in this thesis using statistical tools. Proposed algorithm shows the improvement in the results.

In the next stage, after extracting the various features of images, a fully automated feature selection algorithm, Smart PSO-SVM, which optimizes the feature selection stage, is proposed. Comparative study of proposed algorithm with other algorithms is performed to analyse the performance of proposed algorithm among others. The results obtained in the best subset of features which feed the classification stage. In classification stage, the use of SA-SVM as a new classifier in the area of skin cancer detection systems is proposed. The average accuracy and F-score are estimated as 87.0611% and 0.9167 respectively. The statistical evaluation using t-test also shows the superiority of proposed algorithm when compares with other algorithms in this thesis.

CHAPTER I

INTRODUCTION

1.1.Motivation

During recent decades, the incident of malignant melanoma as the lethal form of skin cancer has been raised. In 2010, the American Cancer Society presented around 68,130 new incidents of skin cancer in USA with the mortality of 8,700 people while it was 8,420 in 2009[1].Skin cancer has become a common cancer in different countries specially in Australia in ages between 15-44.The occurrence is much more higher than US, UK, and Canada with the cases more than 10,000 diagnosis and annual mortality of 1250 people. Its portion is 10% among all cancers [2, 3]. The persistent raise of this cancer in the worldwide [4], the high medical cost and death rate have prioritized the early diagnosis of this cancer.

There are two reasons which make the early diagnosis of this cancer very important [5, 6, 7]: Firstly, the diagnosis of skin cancer is very simple due to its localization on the skin. Anyway melanoma is more presumably to metastasise and propagate to other organs in comparison with other skin cancers. Secondly, the anticipation of melanoma is strictly relevant to its thickness. In early stages in which the thickness is less than 1 mm, the melanoma can be cured successfully. However, it is not very obvious to detect the melanoma in early stages even by experienced dermatologists [8, 9, 10].

Lots of effort has been made to develop the detection of skin cancers. It includes different detection algorithms like pattern analysis [11], Menzies method [12], CASH algorithm [13] and the ABCD rule of der- moscopy [14], 7-point checklist [15] and many techniques based on imaging technologies like dermoscopy [8].

Different studies have demonstrated that the detection algorithms can improve the diagnosis rate of melanoma by 5–30% in comparison with the naked-eye [4, 8]. The

diagnosis of melanoma is relative and depends on visual perception and clinical experience of dermatologists. Although today the dermoscopy is used, the accuracy of detection still about 75–85% [16]. It highlights the necessity of second advice to reduce the number of false detections. However it would be very beneficial for dermatologist to have an objective evaluation of melanoma as well. Such a system can automate the analysis and help physicians to do fewer tasks and provide higher accuracy than they do.

1.2.Research Objectives

The significant interest has been raised in computer-based detection of skin cancer during recent decades. The purpose of such systems is to provide second opinion on diagnosis with less error and higher accuracy and reliability than the results achieve normally by a human expert [17].

Many investigations have been developed in automated detection of melanoma. The potential advantages of such studies are significant and incalculable. Moreover, the difficulties entangle are a lot, and the new contributions in the area are highly appreciated. However, it is extensively acknowledged that the more trustful and reliable detection systems require higher accuracy.

Generally, an automated diagnosis of skin cancer includes several components: Pre-processing, segmentation, feature extraction and selection, and classification. Figure 1.1 represents this process.

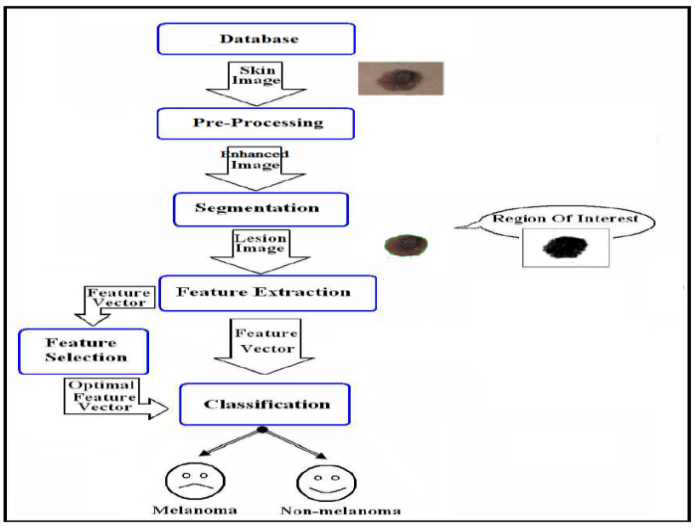

Figure 1.1. Schematic diagram of automatic diagnosis of skin cancer.

In summary, the objectives of this thesis include:

1. Designing a trustful and reliable skin cancer detection system
   - Investigating and experimenting the different steps of detection system as mentioned above in figure 1.1.
2. Proposing an algorithm for skin cancer diagnosis that is able to classify lesions as malignant or benign automatically
   - Advising on using the best filters for pre-processing step
   - Proposing an algorithm for segmentation step
   - Proposing an algorithm for classification step

1.3. Thesis Structure

The rest of the thesis is organised as follows:

In *chapter 2*, some general aspects of skin cancer are presented. Although, the investigation on details of skin cancer cannot be considered, this chapter provide some fundamental and necessary knowledge required for engineers to work with.

In *chapter 3*, the literature relevant to the methods in different stages of computer-based detection systems along with the required stages in such systems are reviewed.

In *Chapter 4*, the proposed algorithms of this thesis along with the explanation of applied techniques are indicated.

In *Chapter 5*, the results obtained in all stage of proposed algorithm have been presented. Different experiments are examined in this chapter to determine the performance of proposed algorithms.

The last chapter, *chapter 6*, is to conclude this thesis work by reviewing all the procedure which is followed, results, and the future works in the area.

1.4.Research Contributions

The contribution of this thesis is to propose and evaluate the new and creative medical expert algorithm that automatically able to classify skin cancer tumours as inoffensive or dangerous, precisely; If possible, with less errors than human experts. This purpose can be mentioned in detail as follows.

- The usage of different effective noise removal filters to optimize the skin cancer images.

- The usage of different effective contrast enhancement techniques to optimize the skin cancer images.
- Comparative study with other noise removal filters and contrast enhancement techniques to provide the best algorithm to use in pre-processing stage.
- Propose a fully automated segmentation algorithm in dermoscopy images based on k-mean and level-set algorithms.
- Analysis and comparative study of proposed algorithm with other algorithms mentioned in this thesis using statistical tools.
- The use of various properties for feature extraction in a skin cancer image.
- Propose a fully automated feature selection algorithm, Smart PSO-SVM, which optimizes the feature selection stage.
- Comparative study of proposed algorithm with other algorithms. Analytical framework consist of statistical analysis, optimisation and cross validation.
- Propose the use of SA-SVM in the area of skin cancer detection systems.
- Implementing the SA-SVM.
- Comparative study between SA-SVM and SVM along with proposed algorithm.
- Analytical analysis of proposed algorithm.

1.5.Research Scope

- This study does not consider contextual variables related to the composition of a group with respect to any factors like: age, gender, abilities, color or experience level.
- This study will not consider specific software as an independent variable.
- This study believes that the engineering design process at the level researched can be generalize to other detection systems.

1.6.Publications Resulting from the Thesis

1. Azadeh N. Hoshyar, Adel Al-Jumaily, “The Beneficial Techniques in Preprocessing Step of Skin Cancer”, Procedia Computer Science, Volume 42, 2014, Pages 25–31, Elsevier.

2. Azadeh N. Hoshyar, Adel Al-Jumaily, “Comparing the Performance of Various Filters on Skin Cancer Images”, Procedia Computer Science, Volume 42, 2014, Pages 32–37, Elsevier.

3. Azadeh N. Hoshyar, Adel Al-Jumaily,” Pre-Processing of Automatic Skin Cancer Detection System: Comparative Study”, International Journal on Smart Sensing and Intelligent Systems. , Vol. 7, NO. 3, September 2014, pp 1364-1377.

4. Azadeh N. Hoshyar, Adel Al-Jumaily,” A Binary Level Set Method Based on K-Mean for Contour Tracking on Skin Cancer Images”, The 11th IASTED International Conference on Biomedical Engineering (BioMed 2014)), Zurich, Switzerland, Jun 23-Jun 25, 2014, pp 89-95.

5. Azadeh N. Hoshyar, Adel Al-Jumaily, Review on automatic early skin cancer detection, 2011 International Conference on Science and Service System (CSSS), IEEE, 2011 , Page(s): 4036 – 4039.

CHAPTER 2

AN OVERVIEW ON HUMAN SKIN, SKIN CANCER AND DIAGNOSIS TECHNIQUES

2.1 Introduction

Skin Cancer as one of the leading cause of death is the threat to human beings in entire world. This cancer can be cured if it is diagnoses in early stages .With respect to the raises in statistical foundation of skin cancer, the importance of its early detection has been considered as a vital issue and the computer based diagnosis is an important tool for this purpose.

The early detection of skin cancer has attracted much concern from different fields. Since the work presented in this thesis lies on the automatic detection system for skin cancer, the knowledge about human skin along with the different available techniques for detection systems are the necessary information in this area.

The chapter is divided into two parts; the first part describes the structure of human skin, different types of Skin cancer and the second part focuses on diagnosing techniques in detail.

2.2 Human Skin

The skin keeps human body safe from heat, injury, infection and damages occur by ultraviolet (UV) radiation. Also it can produce vitamin D, keep water and fat.

There are different layers in human skin. Epidermis and Dermis are the two main layers in human skin which are described as follows [18,19]:

• ***Epidermis***: This layer as the top layer in human skin is built of squamous cells which are flat cells in skin. The round cells below the squamous cells are called basal cells.

The cells in a deepest part of epidermis are called melanocytes which have been located between the basal cells. The pigment (color) in skin is appeared by Melanocytes.

• ***Dermis***: The second main layer of skin is dermis which is located below the epidermis. It includes different types of cells such as lymph vessels, blood vessels and glands.Some glands help the skin to dry out, some others help to cool the body and make sweetening. The figure 2.1 indicates the layers and cells of skin:

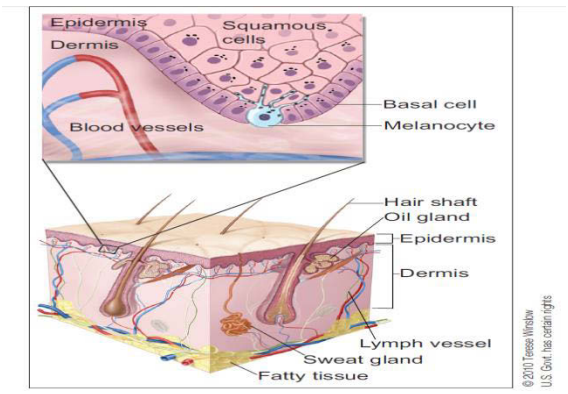

Figure 2.1. A squamous cell, basal cell, and melanocyte and epidermis and dermis layers in Human skin [18]

2.3 Cancer

Trillions of living cells consists the human body. These cells grow, and divide into new cells in normal bodies and die orderly. In adults, the cells division is to substitute worn-out, damaged, and also dying cells. When the growing of abnormal cells in a part of body increase out of control causes to cancer [20]. The growth in cancer cells will make new cancer cells and able to invade other tissues as well [18, 19].

Mostly cancer cells build a tumor, but in some cancers such as leukemia, the tumors are built rarely. The cells in these types of cancers are found in blood and bone marrow [20]. Not all the tumors are cancers, those are called benign which can grow and make problems and pressure on healthy organs. They are not able to invade into other tissues [20].

2.4 Skin Cancer

Skin cancer as the most common cancer in human begins in the skin [21]. Some cancers also can start in other organs and spread on the skin, but these cancers are not considered as skin ones [22].

The different types of skin cancers commonly can be categorized as malignant melanoma and non-melanoma skin cancer (NMSC), the latter including Basal Cell Carcinoma and Squamous Cell Carcinoma as the major subtypes.

2.4.1 Malignant melanoma

Malignant melanoma, as one of the types of skin cancer, is increasing worldwide and leads to death of 65% of its victims. Between 1991 and 2000 in UK, the patients of melanoma grew by 59% and 41% in men and women, respectively. In 2010, Australia, the mortality of Skin cancer and melanoma with projected incidence being 11,500 and 1500 respectively. The high occurrence of both melanoma and non-melanoma skin cancer in Australia provide this country as a place of research in the area [23, 24, 25]

It is derivative from epidermal melanocytes and can arise in any tissue which contains these cells, but commonly it is appeared on the lower limbs in females and on the back in males [23, 24]. As it occurs on the skin surface; therefore it is detectable by visual inspection. The clinical appearance is different according to the type and site of the tumour. Figure 2.2 shows the sample image of malignant melanoma [24].

Figure 2.2. Malignant melanoma

Malignant melanoma can occur by the phenotypic factors such as sun exposure habits, intermittent and ultraviolet radiation. The other risk factors are the fair skin type, having the history of malignant melanoma in personal or first-degree relative [23, 24]. The different types of malignant melanomas are [23]:

- ***Superficial spreading and nodular melanomas:*** The lesions are commonly asymmetrical with irregular border. It has more than one colour and the diameter is more than 0.6 cm. It may be swollen and ulcerate.

- ***Lentigo maligna and lentigo maligna melanoma***: It usually occurs on the face in elderly patients. It looks like a large and irregular mole which tends to grow slowly.
- ***Acral lentiginous melanoma:*** It usually occurs on the skin of palms and soles which doesn't have any hair. It almost diagnosed late, thus have a poorest prognosis among other types of malignant melanoma.
- ***Amelanotic melanoma:*** It usually prognosis false. The correct diagnosis is determined after biopsy.

2.4.2 Non-melanoma skin cancer

It is one of the types of skin cancer with the high incidence and costliest malignancy treated in Australia [26].

The main two types of non-melanoma skin cancer are [23, 24]:

2.4.2.1 Basal Cell Carcinoma

It is the most common malignancy in different countries. It occurs in different parts of shoulders, ears, face, back, and scalp. Its clinical appearance is different according to the type and site of tumour.

- **Nodulocystic basal cell carcinoma**

It is small, pearly nodule, translucent and often with surface telangiectasia. As the lesion is magnified, it usually ulcerates to make a rolled edge and adherent crust. Figure 2.3 is a sample of nodulocystic basal cell carcinoma.

Figure 2.3. Nodulocystic basal cell carcinoma

- **Superficial basal cell carcinoma**

It is scaly, plaque and pink which grows slowly. It is usually appear on the trunk. The telangiectasia and rolled edge are usually observable by good light. Figure 2.4 is a sample of superficial basal cell carcinoma.

Figure 2.4. Superficial basal cell carcinoma

- **Sclerosing (morphoeic) basal cell carcinoma**

It is scar-like plaque which the edge is poorly specified. It is a white lesion with a slowly expanding. Figure 2.5 is a sample of sclerosing (morphoeic) basal cell carcinoma.

Figure 2.5. Sclerosing (morphoeic) basal cell carcinoma

2.4.2.2 Squamous Cell Carcinoma

It is usually appeared in chronic solar damage include scalp, dorsum of hand, lower lip, forearm and ear. It starts from small and crusted plaque and becomes indurated and

nodular. It is almost with ulceration. Figure 2.6 is a sample of Squamous Cell Carcinoma.

Figure 2.6. Squamous Cell Carcinoma

2.5 Skin Lesion Imaging Methods

Imaging is the procedures and techniques to make the image and information from biological structures and functions of the body. Different imaging methods of skin lesions are used to detect the skin cancer. The common imaging techniques are as follows [27, 28]:

➢ Dermoscopy

Dermoscopy as non-invasive imaging technique has been utilized for detecting skin cancers. It is also called epilumence microscopy (ELM) and skin surface microscopy. This technique renders the skin by applying the surface reflectance dominant illumination methods. It allows visualizing the color and subsurface structures such as blood vessels or pigment to help for detection of skin cancer in early stages .The structure of dermoscopy is to utilize the cross polarized light and immersion medium such as immersion oil or alcohol to minimize surface reflections.

➢ Ultrasound

In this technique, the ultrasound waves reflected from the tissue is used to visualize the skin morphology. Although this technique can penetrate to the skin deeply for measuring the thickness of tumor and evaluating the lymph nodes, but the clinical application is not extensive because of the low resolution which is not able to do histomorphologic distinction between skin lesions.

➢ Optical Coherence Tomography (OCT)

This is a non-invasive technique which is based on interferometry. It produces cross-sectional and 2-dimensional images. Although OCT images can differentiate the macromorphology as well as blood vessels and adnexial structures, is not able to visualize the subcellular details and basement membrane. Hence, it is not able to reliably detect the early incursion of tumor.

➢ Reflectance confocal microscopy (RCM)

This technique is non-invasive and painless technique which can visualize the skin's cellular details in vivo without artefacts' processing. RCM can differentiate the refraction indices to detect the skin chromophores include water, hemoglobin and melanin. A small spot in a tissue is irradiated by a point light source and after reflection is conducted to the detector.

2.6 Diagnosis System of Skin cancer

According to different researches, the accuracy of dermatoscopic diagnosis is 75% to 97% while it is 65% to 80% in macroscopic diagnosis. The diagnosis can be more inaccurate if it is decided by inexperienced dermatologists [5, 29, 30]. So, because of the faults , expenses involved and morbidity researchers are trying to automate this assessment to verify if it is inoffensive or dangerous, and estimate it with a small margin of error less that the human may achieve[31, 32].

2.7 Diagnosis Techniques

Based on different features achieved by dermoscopy, the following diagnostic techniques have become more reliable by clinicians.

➢ ABCD-E Rule

This model was introduced by Stolz and his colleagues in 1994 [33].The ABCD-rule of dermatoscopy is based on a semi-quantitative assessment using four dermoscopic criteria: asymmetry (A), border (B), color (C), diameter (D) and elevation/evolving (E) [34].

➢ Pattern Analysis

Pattern analysis algorithms try to identify specific patterns, which may be global (reticular, globular, cobblestone, homogeneous, starburst, parallel, multicomponent, nonspecific) or local (pigment network, dots/globules/moles, streaks, blue-whitish veil, regression structures, hypopigmentation, blotches, vascular structures) [9].

➢ The Seven-Point Checklist

It is a scoring diagnosis analysis and considers only seven standard ELM criteria includes atypical pigment network, blue-whitish veil, atypical vascular pattern, irregular streaks, irregular dots/globules, irregular blotches, and regression structures [9,15,34].

➢ The Menzies method

This method seek negative features such as symmetry of pattern and presence of a single color, also positive features such as blue-white veil, multiple brown dots, pseudopods, radial streaming, scar like depigmentation, peripheral black dots/globules, multiple (five to six) colors, multiple blue/gray dots and broadened network [9].

➢ Texture Analysis

This method try to quantify texture notions such as “fine,” “rough,” and “irregular” and to identify, measure, and utilize the differences between them[9].

➢ The Three-Point Checklist

This method seeks any two of three features of asymmetry; atypical pigment network; and blue-white structures to detect the lesion as melanoma [16, 35]

2.8 Brief Summary on Pathology based Research

There are other types of areas that researchers are working on that as well. The content of this area is briefly described as follows.

Researchers on the area of skin cancer [36, 37, 38] found the significance of anatomic portion to offense melanoma. Another research [39] proposed to measure

primary tumour thickness by optical micrometre. These two parameters are well-known prognostic variables to auspicate the biologic behaviour of melanoma [40].During 1980s, improvements in biology and pathology of melanoma made it obvious that tumours sustain particular growth phases. Specifically, radial growth phase were approved unable to generate metastatic events unless getting worse had been observed at the primitive site. University of Pennsylvania and Massachusetts General Hospital appointed further research and found that brisk mitotic activity and microscopic satellites can modify the behaviour of a tumour [36].

As mentioned before, the two main layers of skin are Epidermis and Dermis. Pathologists mostly do diagnosis the cancer tumour by focusing on the structure of epidermis layer. Therefore, the first task in such images based work is to separate the dermal and epidermal layers. They utilize microscopic to examine histo-pathological tests and obtain the required information by their observations. Figure 2.7 show the manual segmentation of pathologists obtained by 'Aperio Image Scope' software [41].

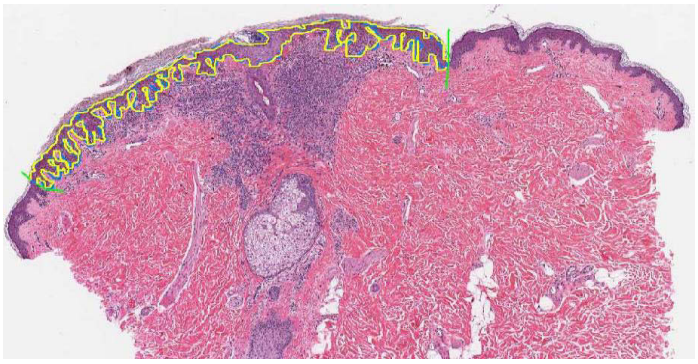

Figure 2.7. Manual Segmentation by Trained Pathologists

2.8.1 Histo-pathological Images

Histopathology images in high resolution provide dependable and accurate information to differentiate normal tissues from abnormal ones; therefore, it is an important technology to analysing and diagnosing skin cancers [42-45]. In other word, it provides more extensive view of disease and its efficacy on tissues, since the pre-processing process keep the underlying tissue architecture. The characteristics in some disease would only be discovered from histopathology image. Cancer diagnosis by a histopathology images still as a 'gold standard' in the era [52]. By analysing the histopathology imagery the spatial information can be obtained to extract specific

characterizations for cancer diagnosis [47, 48, 49]. Some of Histo-pathological information is in following sections.

➢ Radial and Vertical Growth Phase Melanoma

Cancers grow at an uncontrolled rate due to abnormalities in genes which control the growth of cells. Skin-deep forms of melanoma outspread in the epidermis layer of skin. This is reported as radial growth phase by pathologist. If melanoma cells are bounded to epidermis, it is called melanoma in situ which always cured by cutting because it is not extended round the skin. When cancerous cells outspread through the basement membrane of dermis layer in the skin, it is called invasive melanoma which is stated as vertical growth phase of tumour as shown in Figure 2.8. It is more hazardous than horizontal growth phase [50, 51].

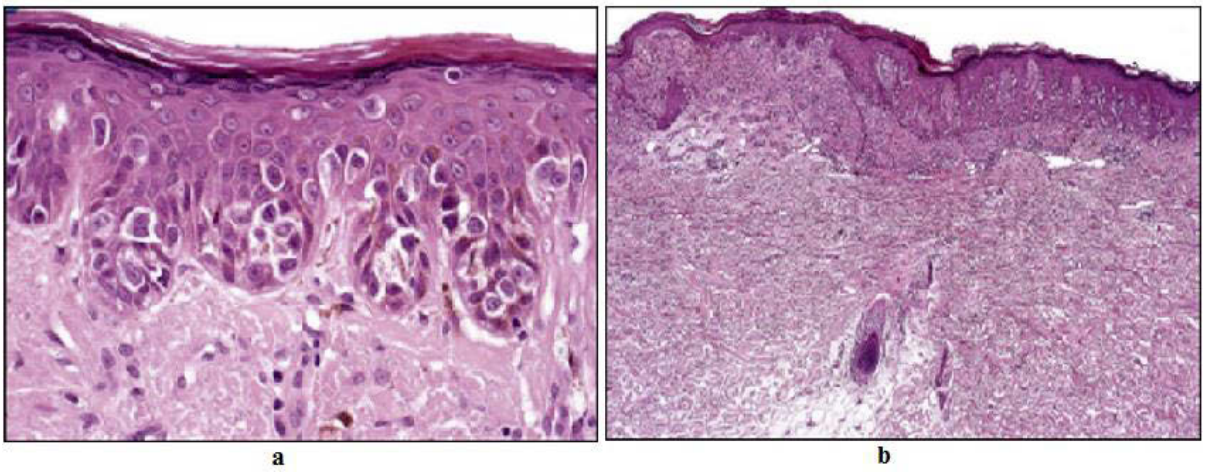

Figure 2.8. Radial and Vertical Growth Phase Melanoma [57]

➢ Histologic type (The microscopic structure) of melanoma

Histologically melanomas are categorized as superficial spreading, lentigo maligna, acral lentiginous, and nodular melanoma [38,52,53].Researchers [54,55,56]show that the less thickness of melanoma at the time of diagnosis is one of the reasons for successful curing the patients.

➢ Thickness (Breslow)

Pathologist looks at the skin biopsy to estimate the tumour thickness which can be measured by the microscope. It is known as a powerful factor to diagnosis the cutaneous melanoma and called the Breslow measurement. This helps doctors to plan an

appropriate treatment and determine prognoses[7, 39,54-66]. The thicker melanoma has the greater possibility of spreading.

➢ Microscopic Satellites

Microscopic Satellites are distinct tumour nests with diameter more than 0.05 mm in which the normal reticular dermal collagen separate it from the tumour [67,68]. Just few researches have surveyed its role as a prognostic factor in skinny melanoma [68]. They found the decrease of 89% to 36% in patients with microscopic satellites versus the patients without in the 5-year disease-free survival [68, 69, 70].

2.9 What are the pathologic features of a melanoma?

Here is the review of pathologic features in cutaneous melanoma which are including [71]:

- **Growth phases:** It has been explained in section 2.7.1.1.
- **Major histologic subtypes:**
    - Superficial spreading melanoma
    - Lentigo maligna melanoma
    - Acral lentiginous melanoma
    - Nodular melanom
- **Rare variants**
    - Nevoid melanoma
    - Desmoplastic melanoma
    - Clear cell sarcoma
    - Solitary dermal melanoma

2.10 Summary

Skin cancer is an increasing cancer in different countries. With this type of cancer, the patient can be survived if it is detected in early stages. So, early detection is the promising strategy to cut the mortality rate of skin cancer. As the background and knowledge of human skin, and also the diagnosis techniques, help researchers to do research in the area, thus, the chapter provide information about human skin, skin

cancer, and summarized the findings of previous researchers about cancer and diagnosis techniques. It is essential to recognize the comprehensive diagnostic assessment to avoid misleading results.

CHAPTER 3

LITERATURE REVIEW

3.1 Introduction

Malignant melanoma is nowadays one of the leading cancer have been increased in the last decades in Australia, America and Europe [72]. Fortunately, if the skin cancer is detected early, the curability is very high and over 92% [73]. In many cases, dermatologists must perform a biopsy (a laboratory medical procedure) to determine whether a tumour is malignant or benign. Since this procedure involves some expense and morbidity, automatic early detection techniques are being as rapid and convenient skin cancer screening [74].

Dermatology imaging researchers believe that diagnosis of skin melanoma can be automated based on certain physical features and color information that are characteristic of the different categories of skin cancer [75]. It has been revealed that the major diagnostic and prognostic parameters of melanoma are the vertical thickness, three-dimensional (3D) size and shape, and color of the lesion. The other characteristic features of early melanoma include irregularities in the boundary of the lesion, and the appearance of non-uniform pigmentation with a variety of color [75,76].

Many experimental researches [77-82] attempt to build automatic skin cancer detection and improve the accuracy of diagnosis. In the following, the literatures on these attempts are reviewed. Also, in order to achieve a reliable skin cancer detection system, the right path knowledge seems crucial.

3.2 Computer-aided diagnosis system

Automation of skin cancer detection can reduce the false positive or false negative clinical diagnosis because it adds a quantitative observation to the “clinical eye observation”. The common approach to skin lesion early detection on cancer image is

divided into four stages of pre-processing, segmentation, feature extraction, and classification [83-90].

3.2.1 Image acquisition/ methods for screening skin lesions

The visual inspection is a common clinical diagnosis in melanoma detection which may involves some error [91,92]. There are different techniques which help dermatologists to visualize morphological features that are not detectable by naked eye. These include dermoscopy [93], solar scan [94], epiluminescence microscopy (ELM) [95, 96], cross-polarization epiluminescence(XLM), and side transillumination (TLM) [97, 98].

3.2.2 Pre-Processing

Image pre-processing is an essential step of detection in order to remove noises and enhance the quality of original image. It required to be applied to limit the search of abnormalities in the background influence on the result [99]. The main purpose of this step is to improve the quality of melanoma image by removing unrelated and surplus parts in the back ground of image for further processing. Good selection of pre-processing techniques can greatly improve the accuracy of the system [100,101,102].

The objective of the pre-processing stage can be achieved through three process stages of image enhancement, image restoration and hair removal.

3.2.2.1 Image Enhancement

Image Enhancement is a crucial procedure to improve the visual appearance of the image; it is defined as provider of the “better” transform representation for further automated steps of detection [44].

Thus, the image enhancement can be categorized in three categories:

- **Image Scaling**

Image scaling techniques are applied due to the lack of same and standard size of images. Since the skin cancer images may be gathered from different sources and sizes, the first step is to resize the images to have the fixed width pixels but variable size of height [90].

➢ Color Space Transformation

Since color information plays an inevitable role in skin cancer detection systems, researchers try to extract the more corresponding color of images for further processing. Generally, the common color spaces include RGB, HSV, HSI, CIELAB and CIE-XYZ.. The most frequently presentation of colors in image processing is RGB. RGB is a color space which comprise the red, green, and blue spectral wavelength. Since RGB color space has some limitation in high level processing, other color space representations have been developed [103]. HSV and HSI color spaces imitate the human visual perception of color in terms of hue, saturation and intensity which are respectively the average wavelength of the color, the amount of white in the color and the brightness. The next color space is CIE- LAB which has been proposed to provide uniformity. CIE-XYZ is another color space which can produce every color with positive tristimulus values [104]. Since the purpose in images of skin cancer detection systems is to obtain the high level variations between intensities to detect the edges of lesions, it would be optimal to convert the image into greyscale. Since LAB is one of the useful color models which represent every color through three components of luminance, red/green and blue/yellow, it could be beneficial to transform the RGB to LAB using XYZ as an intermediate color space. In this thesis the same transformation has been applied. The luminance would present the greyscale skin image. Figure 3.1 shows the tristimulus curves of LAB color space which have been obtained by data tables of CIE 1964 Supplementary Standard Colorimetric System [105].

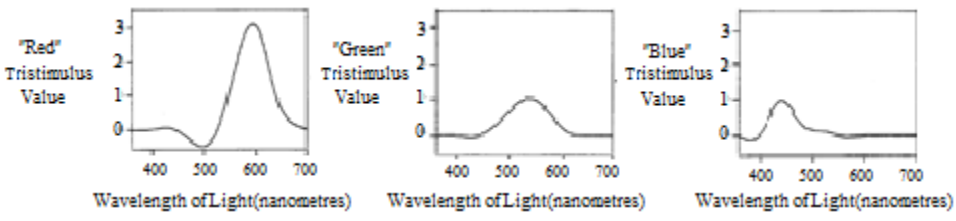

Figure 3.1. Tristimulus Curves

➢ Contrast Enhancement

Contrast enhancement is beneficial step to improve the perception for further processing; it can sharpen the image border and improve the accuracy by accentuating the brightness difference between background and foreground. Contrast enhancement plays a vital role in increasing the quality of an image [106]. The widely practiced

methods are classified into “Linear contrast enhancement” and “Non-Linear contrast enhancement” techniques [43].

- *Linear contrast enhancement techniques:* This type of contrast enhancement refers to contrast stretching techniques. The image can be transformed to higher contrast by remapping or stretching the grey-level values so that histogram spread over the full range [107]. Figure 3.2 shows the expand classification of Linear contrast Enhancement methods.

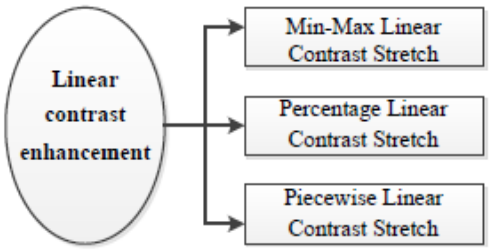

Figure 3.2. Linear Contrast Enhancement Methods

- *Non- Linear contrast enhancement techniques:* This type of contrast enhancement mostly deals with histogram equalizations and algorithms [43]. The most imperfection of such techniques is losing the correct brightness of an object due to the multiple values of output image against each value in an input image [43]. In medical purposes, non-Linear contrast enhancement techniques are commonly used [108]. The different methods of non-Linear contrast enhancement are in figure 3.3.

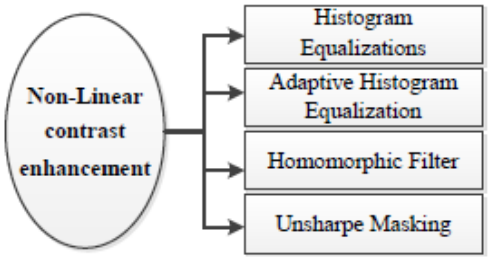

Figure 3.3. Non-Linear contrast Enhancement Methods

Since in skin cancer detection systems, local details of melanoma are more essential than global, therefore, the Histogram Equalization (HE), Adaptive histogram equalization (AHE), and Unsharp Masking as three well-known local enhancement methods are more applicable in such diagnostic [90,101-111]. Among above contrast enhancement techniques, although the HE can also sharpen the image, it reduces the surrounding detail [102]. Figure 3.4 shows the results sample of these three techniques on skin cancer images as the following.

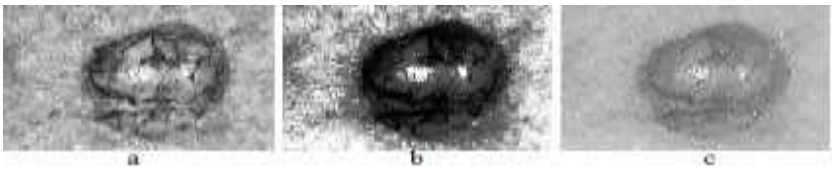

Figure 3.4. a) Adaptive Histogram Equalization b) Histogram Equalization c) Unsharp Masking

3.2.2.2 Image Restoration

Image Restoration is defined as the procedure to recover the degraded image from a blurred and noisy one [45]. It can restore the degraded images in different ways. The image degradation can happen by various defects such as imperfection of imaging system, bad focusing, motion which make an image usually noisy or blur [45]. Since the corrupted images lead to fault detection, hence, it is essential to know about noises present in an image to select the most appropriate de-noising algorithm. The image noises can be divided into four groups of Gaussian, Salt and Pepper, Poisson and Speckle [112]. The sample of such noises has been simulated in Matlab as shown in figure 3.5.

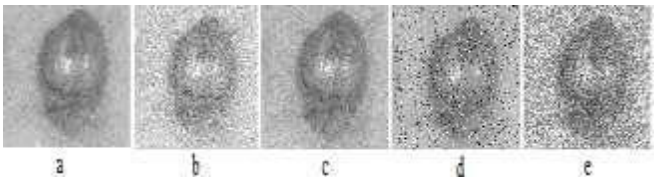

Figure 3.5. a) Image without noise b) Gussian noise c) Poison noise d)Salt and Pepper noise e) Speckle noise

3.2.2.2.1 Restoration from noise

Image de-noising is an essential step in pre-processing of an image. It is extremely difficult to apply an effective de-noising algorithm for different types of noisy images. The essential property of a good image de-noising method is to suppress the noise as well as preserving the edges [113].

There are many existing methods for de-noising an image. The basic methods can be classified as Spatial Filtering and Transform Domain Filtering [114]. Spatial filtering such as Mean filters, Median filters, Wiener filter, Lee filter, Anisotropic diffusion filter, Total variation filter and etc. include neighborhood and a predefined operation

which change the grey value of each pixel according to the pixel values of square neighborhood centered at that pixel [115]. The description of more common spatial filters for removing noises and smoothing the image are in the following [112,116-118].

- Mean filters: It works best with Gaussian noise and could be effective for salt and pepper noise. Although this filter reduces the noise, blur the image and reduce sharp edges.

– Arithmetic mean filter: This is the simplest of mean filter. It can uniform the noise and works well with Gaussian noise.

– Geometric mean filter: This filter can preserve the detail information of an image better than the arithmetic mean filter

– Harmonic mean filter: It works well with salt noise, and other types of noise such as Gaussian noise, but doesn't work well with pepper noise.

– Contraharmonic mean filter: It can preserve the edge and remove noise much better than arithmetic mean filter.

- Adaptive filters: It works best when the noise is constant-power ("white") additive noise like Speckle noise.

– Adaptive local noise reduction filter: It can be used for random noises.

– Adaptive median filter: It can preserve the details as smoothing non impulse noise such the traditional median filter that is not able to do.

- Order statistics filters

– Median filter: This filter in comparison with mean filter is less sensitive to the extreme values. Therefore, it can remove the outlier without reducing the sharpness of an image. It is an effective filter for salt and pepper noise.

– Max and min filters: This filter is useful to find the darkest points of an image.

– Mid-point filter: This filter is the best for random distributed noises such as speckle noise.

– Gaussian smoothing filter: This is a useful filter for smoothing and sharpening the image.

The second classification of de-noising methods, Transform Domain Filtering, is based on wavelet transforms. Wavelet transforms is the extended form of Fourier transform which represent the function by wavelets. Wavelets are defined as mathematical functions which analyze data based on scale or resolution [119,120]. There are different types of Transform Domain Filtering such as VisuShrink, SureShrink, BayesShrink, Neighshrink, OracleShrink, Smoothshrink and LAWML [119,120].

In medical applications, particularly in skin cancer images, the most common filters applied by researchers to suppress noises in pre-processing step of detection systems are Median filter, Adaptive Median filter, Mean filter and Gaussian smoothing filter [116,109-123].

3.2.2.2.2 Restoration from blur

As mentioned earlier, blur is a kind of image degradation which owe to the imperfect formation process of an image. It occurs by bad focusing or motion between original image and camera [124,125,126]. There exist different techniques for de-blurring such as Lucy- Richardson algorithm technique, Inverse filter, Wiener filter de-blurring technique, and Neural network Approach [124,125,126]. In medical applications, Wiener filter has been applied as one of the most powerful and common de-blurring technique which also remove the noise as well [127-130].

3.2.2.3 Removing Thick Hairs

Although the thin blood vessels and skin lines will be smoothed using most of restoration filters, the image may include the thick hairs. Thick hairs in automated analysis of small skin lesions are considered as a common impediment which are able to mislead the segmentation process [131]. To remove the thick hairs in skin cancer images, researchers applied other methods such as mathematical morphology methods [132], curvilinear structure detection [30], an inpainting based method approach [133], automated software called DullRazor [134] and Top Hat transform combined with a bicubic interpolation approach. The hair-free images are acquired using the operations. At the end of pre-processing step of skin cancer detection system, the resulting images

are distinguishable from those initial images and almost are ready to feed the segmentation stage.

3.2.3 Segmentation

A great challenge of research and development activities have recently highlighted in segmenting of the skin cancer images. Segmentation as an essential issue in digital image processing is used for image description and classification.

The various properties in shape, brightness, colour, texture may be applied to assist the segmentation of skin lesion. However, during recent decades many algorithms have been proposed for detection of lesions in skin cancer images. Celebi et al.[135] categorized the segmentation methods into

(i) Histogram thresholding which separate the area of interest (ROI) and background using one or multiple threshold values [136, 137, 138, 139].

(ii) Region-based methods which incorporate the pixels into their similar regions using region-splitting and region-merging algorithms[140, 141, 142, 143, 144, 145].

(iii) Edge-based methods in which the edges of lesions are determined using the edge operators [146].

(iv) Active-contour methods in which the contours in the shape are determined to be evolved using curve evolution techniques [147, 148, 149].

(v) Morphological methods determine the seeds and employ the watershed transform for identifying the contours in an object [150, 151].

(vi) Colour-clustering methods employ the unsupervised clustering algorithms to generate homogeneous areas by separating the colour space [152, 153, 154, 155, 156, 157, 158, 159].

(vii) Soft-computing methods employ different soft-computing techniques to classify the pixels [160].

(viii) Model-based methods in which the image is considered as random fields and the model is parameterized using optimisation methods [141].

In segmentation area, clustering as a process of classifying a set of objects into classes with similar characteristics has been widely applied in many areas such as image

processing, machine learning, pattern recognition, data mining, and statistics. Recently clustering algorithms found crucial applications in medical imaging field [17].

In these algorithms, the number of clusters, initial centers of each cluster and selecting the proper parameters are the main issues. Different researchers dedicated time and effort to improve these techniques to apply in skin cancer detection systems [161-170]. Schmid [132] presented a segmentation algorithm based on fuzzy c-means in which the histogram maxima's are employed to determine the number of clusters. In [161-173], K-means has been known as a simple and fast numerical, non-deterministic, unsupervised and iterative method which is proved to provide good clustering results. K-means is the most popular one due to its simplicity and fast running speed. Level set method is another powerful and robust segmentation technique which is flexible under challenging conditions. It depends on both extrinsic and intrinsic factors such as intensity and curvature [174,175]. Different researchers [176,177] indicated that level set method may decrease the mutability of complex segmentation tasks in medical applications. They mentioned the flexibility of level set techniques cause to long computation times and consequently will limit its application in medical area. In some other works [178,179], the level set algorithm has been proposed to not be used merely for segmentation purposes.

Many researchers have applied Active-contour methods as a successful method of segmentation. In [180], a new algorithm of multi-direction gradient vector flow (GVF) has proposed. They applied a diffusion filter with the new computation along with the adaptive threshold for noise removal. Afterward, the multi-direction GVF has been employed for the segmentation purpose. In another research [181], the radial search algorithm has been applied for borders detection. Abbas et al. [179] presented a segmentation algorithm based on the Active Contour model. They automatically set the initial value of threshold and employ the Courant-Friedreichs-Lewy as their function in an algorithm which controls the curves stability. The achievements demonstrate the better performance of this algorithm among other methods.

Some researchers have merged the different segmentation methods to improve their results. For instance, Pagadala [182] proposed a segmentation algorithm by merging the achievements of three threshold-based algorithms which have been employed independently on various channels of a skin cancer image. Ganster et al. [183]

employed a fusion process and used the combination of three segmentation method includes dynamic and global thresholding and also an algorithm which applies the 3-D colour clustering idea [184]. The results show the better performance of the algorithm while the segmentation results achieved by the global thresholding were about 80% and the other two methods provided a poor segmentation performance. In another work, Melli et al. [157] merged the supervised classification module with the component of unsupervised clustering to segment the lesion from skin. They applied different clustering algorithms of mean-shift, k-means, median-cut and fuzzy c-means and made comparison to determine the best performance. They assume that the tumour have located in the centroid of the skin and considered the corners as skin part. They used the corner pixels for classifier training and the resulted clusters were incorporated as a background if the colours have been considered as background in training procedure. The results cluster the image into skin and lesion. They compared their achievements with the ground truth skin images determined by dermatologists in 117 images. They obtained the better performance with mean-shift algorithm. Hance et al. [152] investigated on six segmentation algorithms of median cut, spherical transform, fuzzy c-means, multi-resolution, adaptive thresholding and split and merge. They compared the results achieved by these methods. Despite the other colour segmentation algorithms they kept the segmentation number in four. Their results indicated the better performance of adaptive thresholding and also median cut. Moreover, they merged these algorithms to evaluate the result. They could obtain the further improvement in their investigation.

In Chapter 4, this thesis proposes a hybrid segmentation method which successfully separates the lesion from background with less error close to one drawn by dermatologists. It achieved by applying k-mean and level-set algorithms and could outperform the results than traditional ones.

3.2.4 Feature Extraction

Feature extraction is to extract the parameters of image to characterize the dermatological features of melanoma, and performing the diagnosis based on these parameters. Clinicians rely on the features of melanoma. The method of diagnosis applies for diagnosis is important to select the features. For instance, asymmetry and pigmented network are respectively the features in ABCD-rule and pattern analysis.

Actually the features evaluation of melanoma diagnosis is visually very difficult, because the content of information in dermatoscopic images is very complicated and entirely requires the experienced physicians. The diagnosis methods to determine melanoma lesions in screening process by non-dermatologists are listed as ABCD rule [170], ABCD-E criteria [185], and Glasgow 7-point checklist [186]. ABCD rule proposed by Friedman et al.[170] consist four criteria: Asymmetry, Border irregularity, Color variegation and Diameter ≥6 mm. ABCD-E is the extended type of ABCD which incorporate "evolving" lesion over time. Glasgow 7-point checklist consist 7 criteria: size, shape, color, inflammation, sensory change, diameter≥7 mm, crusting or bleeding. The diagnosis methods to determine melanoma lesions by dermoscopic images has been developed as ABCD rule, ABCD-E criteria, ABC-point list [A(A)BCDE], 7-point checklist, 7 features for melanoma, 3-point checklist, Pattern analysis, Menzies' method [187]. The ABCD rule of dermoscopy consist four criteria: Asymmetry, Border sharpness, Color variegation and Differential structures. The ABCDE consist: Border irregularity, Color variegation, Diameter, Evolving and Other features .The 7-point checklist consist seven criteria: Atypical pigment network, Blue-whitish veil, Atypical vascular pattern, Irregular streaks, Irregular dots/globules, Irregular blotches and Regression structures. Pattern analysis consists: Global patterns and Local features [187].

According to [14], Symmetry has achieved the highest weight in ABCD rule of dermatoscopy. Stolz et al. [17] indicated that, the 96% of asymmetry in melanoma cases had score 2 (both axes represent asymmetry) while it was just about 24.2% in benign images. Many researches have considered the asymmetry according to the axis of symmetry in the tumour. In such studies, the axis of symmetry may be identified using Fourier transform [188], best-fit ellipse [189, 190], diameter length [191], principal axis [192, 193, 194]. Thereafter, the both created areas by the axis are differentiated. In many studies, the roundness, compactness and thinness of lesion have been considered as appropriate properties of the skin cancer images [191, 195, 196, 197] and in [198], have been considered as accurate geometry variables. In [199,200], the symmetry distance (SD) has been introduced as another measure in images. Seidenari et al. [201] presented a method to estimate the distribution in skin lesions. They purpose was to determine the effectiveness of distribution parameters to identify the melanoma from

the normal ones. They found out about the non-homogeneity of lesion region; they computed the mathematical parameters such as mean, variance, and Euclidean distance. Manousaki et al. [198] proposed to estimate the distribution irregularity using the fractal dimension in the surface of the lesion. Also, they computed the standard deviation to measure the sharpness of borders. Lee et al. [202, 203, 204], presented an algorithm to search a convex and curvature maxima's locations in an image. In [205], the standard deviation and mean are calculated in six colour spaces. In another approach [206], the different statistical properties of standard deviation, energy, mean and entropy are computed as extracted features. The Neural Network has been trained using these features and the accuracy of 79% was achieved.

The Gray Level Coocurrence Matrix (GLCM) as another popular method to extract the image features has been employed by different researchers in various applications [207-215].

Many other researches have been reported on feature extraction of skin cancer in the literature [216-221].

In chapter 4, this thesis proposes an optimal combination of various features which can be extracted to feed classification.

3.2.5 Feature Selection

Feature selection as an important process is performed prior to lesion classification. Its purpose is to reduce the computational cost of classification by decreasing the extracted feature descriptors in number. Although this decrement is not trivial due to eliminating redundancy which may make negative effect on discriminatory power.

Feature selection process may be explained as the following [222]. Firstly, the search procedure as subset generation is performed to provide various subset candidates of features [223, 224]. An evaluation criterion is considered to evaluate the subset candidates. This is compared and replaced with the estimated performance of the prior best subset in a case of preference. As illustrated in Figure 3.6, this process is repetitious till the stopping criterion is met. In the final stage, the validation and testifying the best selected subset is performed [225].

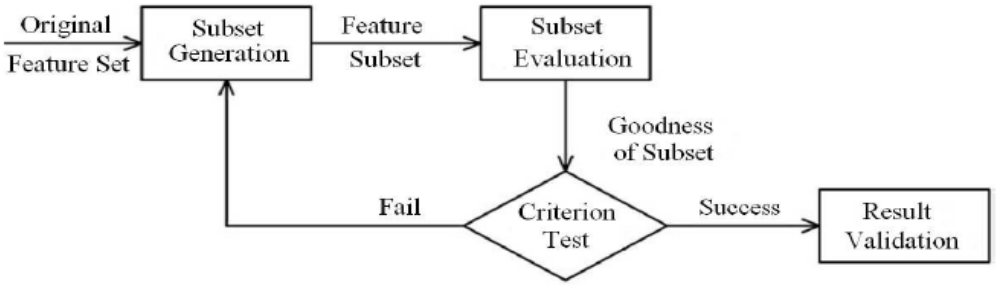

Figure 3.6.Common Feature selection process [225]

To develop the procedure of feature selection, different researches have been take approaches [226,227,228]. In 2009, a very useful review on feature descriptors was revealed by Maglogiannis and Doukas [9]. Walvick et al. [229] applied the Principal component analysis to achieve the optimal subset from the set of eleven features. Ro et al [230] employed sequential forward selection (SFS) to decrees the set of eighty seven features to five. In [231], a statistical feature selection algorithm has optimized the vector of 34 features to five. In another study [138], the neural network along with node pruning has been employed to cut down the number of features to optimize the solution. Ganster et al. [183] optimized the number of features by applying the statistical approaches. The methods include Sequential Floating Backward Selection (SFBS), Leave One Out (LOO) and Sequential Floating Forward Selection (SFFS) were considered for this purpose.

Particle Swarm Optimization (PSO) is extensively applied in feature selection problems to search for the optimal feature subset of a large database of possible candidates [232,233,234]. Binary Particle Swarm Optimization is another extension for PSO that particles are considered by a point in a binary multidimensional space. This type of PSO also is widely applied in feature selection [235,236,237]. In [238,239] the authors represented an algorithm for feature subset selection by employing PSO along with the fuzzy evaluation function. In [240], a PSO algorithm has been developed using artificial neural network for feature subset selection. Yashar et al. [241] proposed a Particle Swarm Optimization - Support Vector Machines (PSO-SVM) feature selection algorithm in their study in Sleep Apnea. They could effectively reduce the number of features and select the best subset for their purpose. PSO computationally is less expensive than other methods and can quickly do convergence. Thus, PSO is used as an effective technique in many fields such as feature selection [242,243,244].

In chapter 4, this thesis proposes a feature selection algorithm in which the optimal subset of feature will effectively selected and feed the classification stage.

3.2.6 Classification

Lesion classification as a final step in computerized analysis is to estimate whether the lesion is malignant or benign. To follow out the classification task, the existing systems utilize different classification methods to feature descriptors have been extracted in prior stage. The efficiency of these methods appertains on both extracted descriptors and selected classifier [245].

There are exist different classifiers such as Discriminant Analysis, Artificial Neural Network, K-Nearest Neighbourhood, Support Vector Machine, Decision Trees and Self-Advising SVM.

In Different researches [193, 231, 246-249], Discriminant analysis have been applied as a classifier to make predefined classes from a set of observations. It works by the values of determined measurements which are called predictors. Artificial Neural Networks (ANN) as another tool has been employed in [143, 193,229, 230, 246, 250]. This approach connects the inputs and outputs for detecting the patterns in data. It is usually employed in classification problems. In [139, 143,183, 229, 251] another algorithm called k-nearest-neighbourhood (K-NN) has been considered for classifying the lesions into melanoma or benign. This classifier employs the distance measure like Euclidean distance to evaluate the distribution of data and classify the objects according their closeness to the training set. SVM showed its powerful ability to solve problems of nonlinear classification in many applications even in high dimension. Furthermore, SVMs prevent over fitting by selecting a particular hyperplane among many which can separate the data in feature space [193]. SVM has been used as a popular technique in [9, 193, 205, 250, 252, 253] for classifying skin cancer melanoma. In some other researches [139, 254, 255], Decision trees separate the data set into different groups according to its disparity and make the classification schema.

Dreiseitl et al. [250] compared the different classification techniques of artificial neural network, k- nearest neighbourhood, support vector machine, logistic regression and decision tree in skin cancer detection systems. The results achieved the effective performance of SVM, ANN, and logistic regression. In Maglogiannis and Doukas'

research [9], they employed and compare the performance of SVM, multinomial logistic regression, ANN, CART and Bayes networks to classify the lesions in the skin. Their experimental results emphasised the superiority of SVM followed by Bayes networks and regression. Yashar et al.[256] has developed a new SVM algorithm as Self-Advising Support vector machine (SA-SVM) which has been applied as a classifier in the area of sleep Apnea. The experimental results show the better performance than SVM.

In chapter 4, this thesis explains the SA-SVM and SVM as two effective classifiers in proposed algorithm. According to the literature SA-SVM has not been employed in skin cancer detection systems before.

3.2.7 Performance Indicators

The two criteria mostly used for assessing the quality of a classification are discrimination and calibration. Discrimination is defined as a measure to know the well separation of two classes in the data set and calibration is defined as a measure to know the closeness probability of predicted and real model based on expert knowledge. Some of the general measures to analyse the discriminatory power in different methods are Accuracy, Diagnostic accuracy, F-score, T-Test, Positive predictive value, Negative predictive value, ROC curve, Classification rate, Error probability, Index of suspicion, LR+, LR-, Diagnostic odds ratio.[257, 258, 259]. These Performance evaluators can be defined as follows:

- *Accuracy*: This measure records the correct and incorrect recognized samples of each class according to "confusion matrix" to evaluate the classification quality. A confusion matrix is shown in table 3.1.

label / result	As positive	As negative
Positive	*tp*	*fn*
Negative	*fp*	*tn*

Table 3.1: Confusion matrix for a binary classification

tp: true positive , *fp* : false positive, *fn* : false negative, *tn* : the true negative amount(s) .

$$accuracy=(tp+tn)/(tp+fp+tn+fn) \quad (3.1)$$

- *F-score* : Another indicator is F-score which can be calculated as follows [260]:

$$\text{Precision}=tp/(tp+fp)\ ,\ \text{recall}=tp/tp+fn \quad (3.2)$$

$$\text{F-score}=(\beta^2+1)*\text{Precision}*\text{recall}/\ \beta^2*(\text{Precision}+\text{recall}) \quad (3.3)$$

Three above measures differentiate the correct classification of labels among different classes because the concentration would be only on one class (positive samples). Recall is a function of samples which are classified correctly (true positives) and its misclassified samples (false negatives). Precision is a function of true positives and the samples which are misclassified as positives (false positives). The F-score is equally balanced in a case $\beta = 1$ because it considers precision in a case $\beta > 1$, and recall otherwise [261].

- *T-Test:* This statistical test is measure to determine whether the results obtained by these approaches are statistically different.

The other performance evaluators are defined in summary as follows:

- *Diagnosis Accuracy*: Diagnostic Accuracy=TP/(TP+FP+FN) (3.4)
- *Positive predictive value*: $\text{Positive Predictive Value} = \frac{\text{TP}}{\text{TP+FP}}$ x 100% (3.5)
- *Negative predictive value*: $\text{Negative Predictive Value} = \frac{\text{TN}}{\text{TN+FN}}$ x 100% (3.6)
- *ROC curve*: $\text{ROC curve} = \frac{\text{P(x|positive)}}{\text{P(x|negative)}}$ (3.7)

Where P(x|C)*:* is the conditional probability in which a data entry include the class label C

- *Classification rate*: No of images correctly classified/ total no of images (3.8)
- *Error probability*: $\text{Error Probability} = \frac{\text{FP+FN}}{\text{TP+TN+FP+FN}}$ x 100% (3.9)
- *Index of suspicion*: $\text{Index od Suspicion} = \frac{\text{TP+FP}}{\text{TP+FN}}$ x 100% (3.10)
- *LR+* : $\text{LR}_+ = \frac{\text{Sensitivity}}{1-\text{Specificity}}$ (3.11)
- *LR-* : $\text{LR}_{--} = \frac{1-\text{Sensitivity}}{\text{Specificity}}$ (3.12)
- *Diagnostic odds ratio*: $\text{Diagnostic odds ratio(DOR)} = \frac{\text{TP/FN}}{\text{FP/TN}}$ (3.13)

Among above measures, the three popular measurement factors of Accuracy, F-score and T-Test have been selected in this thesis to improve the precious and reliability of the algorithm estimations.

3.3 Summary

This chapter has a review on the literature of skin cancer detection systems. It provided information for designing the components of automatic skin cancer systems and their methods with the purpose of improvement and increasing the accuracy of skin cancer detection systems. Furthermore, at the end of each section, the selected techniques resulted from the discussed literature have been mentioned to use in proposed detection system in chapter 4 and 5.

CHAPTER 4

METHODOLOGY REVIEW and PROPOSED SYSTEM

4.1 Introduction

This chapter proposes an algorithm for Automatic diagnostics of skin cancer which is one of the most challenging problems in medical image processing. It helps physicians to decide whether a skin melanoma is benign or malignant. So, determining the more efficient methods of detection to reduce the rate of errors is a vital issue among researchers.

The contribution of this work is to propose and evaluate the new and creative medical expert systems that automatically able to classify skin cancer tumours as inoffensive or dangerous, precisely; If possible, with less errors than human experts.

The proposed Algorithm of this thesis utilizes a novel approach for classifying the skin melanomas. It does so by enhancing the quality of skin cancer images, segmenting the tumours from the skin, extracting and selecting the best characteristic features of tumour and finally its classification into melanoma or non-melanoma. Different methods in different steps have been used to achieve this efficient system. The purpose of this research is to propose contributions in different stages of this system. The algorithms try to speed up the detection with less error than other traditional ones. It is intended that the proposed algorithms have contribute in public health systems and help medical experts to screen tumours in early stages.

In summary, the topic of discussion can be categorized in stages as illustrated in figure 4.1:

- Pre-processing
- Segmentation process
- Feature extraction and Selection
- Classification

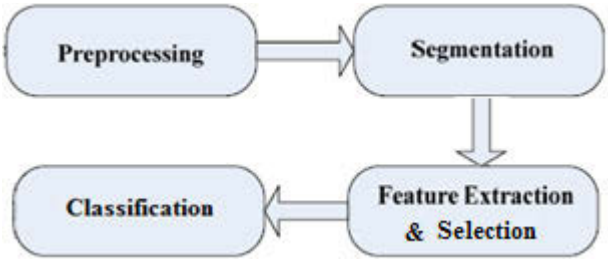

Figure 4.1.Skin Cancer detection system

Generally, the results are analysed by comparing the proposed algorithm with the existing ones to prove the accuracy of results and reducing the computational cost.

4.2 Pre-Processing

The image has been taken has noises which needs to be reduced for getting better quality to improve segmentation. Two function of ‘filter2’ and’medfilt2’for image enhancement are used. Using Matlab the comment is defined as;

h = fspecial (type) (4.1)

This command creates a two-dimensional filter h of the specified type. 'fspecial' returns h as a correlation kernel, which is the appropriate form to use with filter2. Type is a string having one of these values; 'average', 'disk', 'gaussian', 'laplacian', 'log', 'motion', 'prewitt', 'sobel', 'unsharp'. By experimenting all of these filters, the ‘average’ filter is considered as the best and effective one for this application.

Y = filter2 (h, I2) (4.2)

This command filters the data in I2 with the two-dimensional FIR filter in the matrix h. It computes the result, Y, using two-dimensional correlation, and returns the central part of the correlation that is the same size as X. Another filter has been used is Median filtering. It is a nonlinear operation often used in image processing to reduce "salt and pepper" noise. A median filter is well effective when the goal is to simultaneously reduce noise and preserve edges.

B = medfilt2 (Y, [m n]) (4.3)

This command performs median filtering of the matrix Y in two dimensions. Each output pixel includes the median value in m-by-n neighbourhood around corresponding

pixel in the input image. Medfilt2 pads the image with 0s on the edges, so the median values for the points within [m n]/2 of the edges might appear distorted.

After using filters, the image contrast is increased using the AHE command in Matlab;

I= adapthisteq (B) (4.4)

The total chart for Image enhancement is shown in figure 4.2.

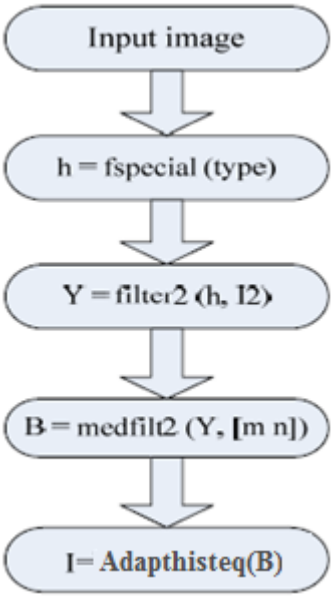

Figure 4.2.Image enhancement process

All the above process leads to image enhancement, hence, the skin image is ready to feed the next stage.

4.3 Segmentation

In this stage, the enhanced skin image is segmented to separate the tumour from the background (skin). As mentioned in chapter 2, there are different methods for segmentation. As one of the contributions in this thesis a segmentation algorithm is proposed to improve the segmentation results. For this purpose two segmentation algorithm of K-mean and Level-set, are applied.

In traditional level set methods, initialization has extensively an essential role in curve evolution process. Re-initialization of level set function, has significantly used as

a numerical remedy to keep the curve evolution more stable and to achieve effective results. Though, as pointed out by Gomes, many presented re-initialization schemes provide undesirable results with computational cost [262]. On the other hand, it is becoming significantly obvious that none of the methods alone are adequate and that the application of different approaches will clear the various aspects of data to be explored [41, 166, 263, 264]. Thus, this thesis attempts to incorporate the strength of two techniques and discard the disadvantages. Here, an implicit algorithm based on k-means and level set algorithms for classifier decision boundaries is presented. It applies k-means algorithm to get initial label estimation for level-set algorithm. In other words, k-mean is used as an initial curve or surface function of level-set algorithm. Summarizing, the contribution of this thesis at segmentation stage is to propose a new and creative segmentation algorithm which develops the medical expert systems for precision diagnosis. The algorithm increases the accuracy of segmentation while decrease the computational cost.

The performance of proposed algorithm is compared with traditional level set algorithm and Fuzzy C-mean thresholding method in two cut off, in the data set of eighty six skin cancer images. It is performed using four factors of False positive error, Hammoude distance, True detection rate and Similarity and found the results which are competitive with the mentioned methods in this practice. The k-mean and level set frameworks followed by the proposed algorithm are explained as follows.

4.3.1 The K-means Algorithm

K-means algorithm is a clustering algorithm which firstly presented by MacQueen in 1967 [265]. This algorithm divides the pixels into k clusters and heavily relies on selecting the number of clusters k and initial cluster centroids v_i, i = 1, ... 2, k. The centroids of clusters are calculated based on the average of pixel intensities in each cluster. These initial centres have effectively influence on number of iterations in k-means algorithm. After calculating the centroids v_i, the distance of pixels and centres are estimated and each pixel x_j is iteratively assigned to the closest cluster as in equation (4.5).

$$d_{ij}=||x_j-v_i|| \tag{4.5}$$

The matrix of U with the membership values are determined by

$$U=|u_{ij}| \tag{4.6}$$

Where $u_{ij} \in \{0,1\}$ for all i and j. $\sum_{t}^{k}=1 \ u_{ij}=1$ for all j and $0<\sum_{j=1}^{n} u_{ij}<n$ for all i (k=number of clusters, t=0, n=number of pixels).

The cluster centres are updated by computing the mean of each cluster as in equation (4.7).

$$V_i=\frac{\sum_{j=1}^{n} u_{ij}x_j}{\sum_{j=1}^{n} u_{ij}} \quad forall\, i \tag{4.7}$$

This process is repeated till reaching the centre values same as the prior values since it indicates the current values are the optimal results.

This algorithm optimize the objective function J_w (U, v) in a manner that

$$J_W(U,V)=\sum_{i=1}^{k}\sum_{j=1}^{n}\left\|X_j-V_i\right\|^2. \tag{4.8}$$

It is spotted that the algorithm is sensitive to cluster initialization and distance measure [161, 266, 267].

4.3.2 The Level Set Framework

Level set algorithms, firstly presented by Osher and Sethian [268,269], offer an impressive implementation of curve evolution. This approach is based on enchasing contour C as the zero level set of the graph of a higher dimensional function Ø(x,y,k), as in equation (4.9).

$$C_k=\{(x,y)\ l\ Ø(x,y,k)=0\} \tag{4.9}$$

Where k represents an artificial time-marching parameter, and then evolves the graph as moves pursuant to the prescribed flow. Therefore, the level set can change topology and expand singularities as remains smooth and preserve the form of a graph. In this manner, the curve evolution is defined as equation (4.10).

$$\partial c/\partial k=VN \tag{4.10}$$

Where V is the speed of curve evolution, N is the normal vector of inward unit. From $Ø(C_k,k)$, the following equation is achieved:

$$(\partial Ø/\partial k)+\blacktriangledown Ø \bullet (\partial c/\partial k)=0 \tag{4.11}$$

According to the level set function definition described above, the vector N may be written as $\mathbf{N} = -\nabla\phi / \|\nabla\phi\|$. Then it can be implemented corresponding to curve evolution equation (4.12):

$$\partial Ø/\partial k = V||\blacktriangledown Ø|| \quad (4.12)$$

The initial level set function is generated using the initial given curve. In addition, the function requires to be re-initialized consecutively during the update process which generally takes a lot of computing time.

4.3.3 The Proposed Active Contour Tracking Method

The presented method seeks a new target location t1 in the current frame exploiting the k-means procedure and initializing the level set segmentation algorithm from the location t0 of the target in prior frame. The weighs are computed based on the scale of bandwidth h centred at t0. In other word, the initial curve of each sample is set up and evolved based on the target location t0 obtained by the k-means algorithm. The energy function is refined using the previous knowledge of target model achieved by k-means. The presented active contour tracking algorithm is explained in detail as follow. The proposed algorithm have been published in the proceeding of "The 11th IASTED International Conference on Biomedical Engineering (BioMed 2014)"

4.3.3.1 The Proposed Algorithm

As described above, k-means clustering algorithm needs K clusters which should be initialized manually. The number of clusters is 3 in this algorithm because the skin cancer images are expected to be clustered into less or equal to 3 parts consisting the background (skin), tumour, and possible extra parts. That is, the first cluster is named cluster 1 and the last one is cluster 3. Since the skin cancer image is greyscale image in which the minimum intensity value is equal to 0 and the maximum intensity value is equal to 255, the centroid of cluster 1 is 0 and the centroid of cluster 3 is 255. Equation (4.13) indicates the calculation of centroid in cluster k, $C_{k,}$ while pseudo code 4.1 shows k-means clustering procedure.

$$C_k = \text{rand} * 255 \quad (k => 1 \text{ and } k <= 3) \quad (4.13)$$

Pseudo code 4.1 shows the total procedure of k-means clustering of this work. After determining the initial centroid values of the clusters, the pixels are distributed to one of

Input: *The original skin cancer image*
Output: *Initial Segmented image*

1. *Initialize centroid of clusters randomly*
2. *loop while CTr=CTr-1*
   - *If CTr=CTr-1, then disk,i=|CTk-I_{ij}| for all pixels*
   - *Assign pixels to the closest distance*
   - *Estimate the new centroid for 3 clusters ctk=Avg(I_k)*

   End loop

3. *The segmented skin lesion is achieved at location t1 with the scale of h*

CTr : Cluster centroid at round r
I_{ij}: Pixel in an image

Pseudo code 4.1 pseudo code of K-means clustering with 3 clusters

3 clusters which the centroid value is the most closest to that pixel intensity. The centroids of clusters are updated by the mean intensity values of its pixels. This process is repeated till reaching the constant value. The target segmented location t1 achieved by this algorithm is used to initialize the level set algorithm.

For each sample s_k^i in level set framework, a curve is initialized by a target segmented location t1 with the scale of h achieved by k-means segmentation algorithm. Thence, the curve is evolved using level set algorithm upon the time k, I_k , and the target model t as appeared in equation (4.14):

$$C_k^i = evo\ (s_k^i, I_k, t) = S_k^i(M) \tag{4.14}$$

Where S_k indicate the contour at time k and iterate M times to the direction of reducing the energy function E_{img}. in equation (4.15).

$$E_{img} = E_R(c1, c2, \partial) \tag{4.15}$$

Where c1, c2 indicate positive constant, ∂ is the indicator of regions (∂= 1 lesion, ∂= -1 background)

By the end of this process, the true target segmentation is achieved which includes the energy smaller than other samples in evolution process. Therefore, the algorithm of this process is illustrated in pseudo code *4.2*.

Input: *target segmented location t1with a scale of h achieved by k-means segmentation*

algorithm
***Output**: True target segmentation t2*

1. *Initialize a curve by a target segmented location t1*
2. *Run curve evolution in M iterations toward the direction of energy reduction*
3. *Calculate the weights*
4. *If the (t2-t1) < ε and mark t2 as the result*

Pseudo code 4.2 Level set segmentation algorithm initializing by k-means clustering algorithm

4.4 Feature Extraction

Feature extraction plays a vital role in recognition systems. To classify the images into benign or melanoma, the extraction of features is needed to feed the classification stage. Therefore, to characterize the various types of lesions, a parametric approach has been considered. In such kind of approach, the skin mole is resumed by a vector of features that its dimension depends on the number of extracted properties. In this thesis, several statistical properties are computed as features. These obtained features have been considered as a source data for the following stages. The features properties are very important due to the different ways of taking pictures by physician; the lesions may have different sizes and properties. Full list of proposed features are represented as follows.

4.4.1 Texture properties

This feature allows characterizing the discontinuity of the mole by differentiating between the colors in the mole, that is a beneficial tool applied by physicians to recognize weather a mole is malignant or not. To represent the texture, local binary pattern (LBP) of the skin image that creates a code of variability in the neighbourhood of each pixel is employed. The texture properties have been extracted are in table 4.1 and table 4.1.

Autocorrelation	Contrast	Correlation	Cluster Prominence	Cluster Shade
Dissimilarity	Energy	Entropy	Homogeneity	Maximum probability
Sum of squares	Sum average	Sum variance	Sum entropy	Difference variance
Difference entropy	Information	Information	Inverse difference	Inverse difference

	measure of correlation1	measure of correlation2	(INV) is homom	normalized (INN)
Variance	Inverse difference moment normalized			

Table 4.1.GLCM features

In table 4.1 GLCM features are calculated using the 'GLCM_Features1' function. The reference to this function is accessible in: http://au.mathworks.com/matlabcentral/fileexchange/22187-glcm-texture- features/ content// GLCM_Features1.m. Although in Matlab, there is a function called 'graycoprops()' which computes Contrast, Energy, Correlation and Homogeneity, this function 'GLCM_Features1' provide the computation of whole features in table 4.1.On the other hand, it should be noticed that there is no preference consideration in table 4.1.

Table 4.2 shows the additional properties which are used in this thesis for image analysis.

Short Zones Emphasis (SZE)	Long Zones Emphasis (LZE)	Low Grey-Level Zone Emphasis (LGZE)
High Grey-Level Zone Emphasis (HGZE)	Short Zone Low Gray-Level Emphasis (SZLGE)	Short Zone High Gray-Level Emphasis (SZHGE)
Long Zone Low Gray-Level Emphasis (LZLGE)	Long Zone High Gray-Level Emphasis (LZHGE)	Gray Level Non-Uniformity (GLNU)
Zone Length Non-Uniformity (ZLNU)	Zone Percentage (ZP)	

Table 4.2. Volumetric zone length type texture

In table 4.2 Volumetric zone length type texture features are calculated using the 'grayrlprops' function. The reference to this function is accessible in: http://au.mathworks.com/matlabcentral/fileexchange/17482-gray-level-run- length-matrix-toolbox. Using this function, the high order run length features are extracted. On the other hand, it should be noticed that there is no preference consideration in table 4.2.

4.4.2 Shape properties

This feature characterizes the shape properties in the mole which gives how circular or irregular and elliptic is the mole. This feature is very important in the classification of a mole. This feature indicates not only the shape, but the mole uniformity as the internal shape as well. The extracted shape properties which have been considered are in table 4.3.

Area	BoundingBox	ConvexHull	ConvexImage	SubarrayIdx
ConvexArea	Eccentricity	EquivDiameter	EulerNumber	WeightedCentroid
Extent	Extrema	FilledArea	FilledImage	
Image	MajorAxisLength	MaxIntensity	MeanIntensity	
MinIntensity	MinorAxisLength	Orientation	Perimeter	
PixelIdxList	PixelList	PixelValues	Solidity	

Table 4.3.Extracted shape properties

In table 4.3, shape properties are calculated using the following function in Matlab :

STATS=Regionprops (image, 'All') (4.16)

Where STATS is the structure array which its cells show the different properties. It should be noticed that there is no preference consideration in table 4.3.

4.5 Feature Selection

The feature selection is the key point of classification which should be adequate in order to achieve an accurate detection rate. As there can exist complex interaction among features, feature selection has been a difficult task. An individually redundant or irrelevant feature may become relevant when working outright with other features and vice versa. Thus, the optimal feature subsets have to be a group of supplementary features which span over the various properties of the classes to make them properly discriminate. On the other hand, feature selection task has been challenging due to the large search space. This search space may increase exponentially based on the number of features available in the data set [270]. Thus, a thorough search in most situations is practically impossible.

The robust and discriminative subset of the extracted features of previous stage will be selected by the Smart Feature Selection algorithm. This proposed algorithm is Sequential Feature selection/ Particle Swarm Optimization - Support Vector Machines (SFS/PSO-SVM) which attempts to represent the best subset of characteristics to feed classification stage. It specifies the best subset of measurements out of a set of total measurements. The experimental results are reported in Chapter 5. For explaining the proposed algorithm in this stage; the following components are firstly defined as follows.

4.5.1 Sequential Feature selection (SFS)

The SFS [271] is an ascendant search method of the set of superlative discriminative parameters among an initial set of parameters (Ei) as in equation 12:

$$\begin{aligned} &Ei = \{pj,\ j = 1, 2,\ \ldots,\ N\} \\ &E_{SFSn} \subset Ei\ ,\ n \leq N \qquad E_{SFS0} = \varphi \end{aligned} \tag{4.17}$$

In this method, one parameter p_j is appended at a time to E_{SFS} subset. SVM is trained using the corresponding subset and the corresponding classification error (Err) is calculated in equation (4.17), the remaining parameters p_j in E_i is added into E_{SFS} in each step and the corresponding classification error (Err) is also calculated.

$$Err = \frac{1}{q}\sum_{i=1}^{q}(d_i - a_i)^2 \tag{4.18}$$

Where q: total image number of the training database. di: desired output. ai: real output. In every step, the selected parameter (pj) is the one in which the new ESFS subset allow minimizing the classification error:

$$Err(E_{SFS}U_{pj}) \leq Err(E_{SFS}U_{pj}') \tag{4.19}$$

Therefore, the first selected parameter is the more discriminative of the initial set of parameters. The parameters selection is curbed by increasing the classification error in a condition of adding a new parameter to ESFS.

4.5.2 Particle Swarm Optimization

Particle Swarm Optimization (PSO), firstly presented by Kennedy and Eberhart in 1995 [272, 273].This technique works by simulating the social behaviours such as fishes schooling or birds flocking to a promising position for achieving accurate objectives [274]. This population-based stochastic technique is based on swarm intelligence. The PSO technique includes a set of particles or agents which are known as swarm, it “flies” over the solution space attempting to locate promising regions. These particles are represented as possible solutions in the optimization problem and are indicated as points in the n-dimensional search space.

In standard PSO, every particle (X_i) include its own velocity (V_i) bounded with a maximum value (V_{max}), the memory of its best obtained position is (P_i) and the best

found neighbourhood solution is considered as (G). In this search process, PSO updates its population of particles with respect to their internal velocity and position that are achieved by the experiment of all particles. Each particle adjusts its position based on the equations (4.20) and (4.21):

$$V_i^{(k+1)} = V_i^{(k)} + c_1 r_1 (P_i - X_i^{(k)}) + c_2 r_2 (G - X_i^{(k)}) \quad (4.20)$$

$$X_i^{(k+1)} = X_i^{(k)} + V_i^{(k+1)} \quad (4.21)$$

Where k: the current generation, c_1 and c_2 : positive constants, r_1 and r_2 : random numbers on the interval [0,1].

In this thesis, the Inertia based Particle Swarm Optimization (IPSO) is used. Shi et al. [275] has modified the standard PSO as "Inertia based Particle Swarm Optimization (IPSO)" by adding inertia weight (ϖ) as a parameter to it. This inertia weight is multiplied by the prior velocity in the standard velocity equation. A nonzero inertia weight moves the particle to the same direction it was in the prior iteration as shown in equation (4.22).

$$v^{k+1}{}_{id} = w * v_{id}^k + c_1 rand\ () * (p_{id}^k - x_{id}^k) + c_2 * Rand\ () * (p_{gd}^k - x_{id}^k) \quad (4.22)$$

Where w: the none zero inertia weight.

It is set based on the equation (4.23):

$$w = \frac{w_{\max} - w_{\min}}{iter_{\max}} * iter \quad (4.23)$$

where $iter_{max}$: the maximum number of iterations , *iter* : the number of current iteration.

The interpolation of this parameter insures the balance between the capacities of global and local search. The wrong value selection of this parameter will effect on the speed of algorithm convergence. So, the initial selection would be very important [276].

4.5.3 Support Vector Machine

Recently, the strong and powerful theoretical foundation and superb practical performance of Support Vector Machines have possessed a great consideration in machine learning community [205]. It has been applied in various applications of biomedical and automatic recognition systems of different diseases [277]; like, micro-classification detection in mammograms, polyps in CT colonography, cancer in optical

images, and many melanoma detection in dermoscopic images [9]; This study has also adopted this technique as one required component in feature selection algorithm.

Support vector machine (SVM) is a statistical machine learning method was presented by Vapnik in 1995 [278]. It applies a linear separating hyperplane for creating a classifier to maximize the margin. The width of margin between the classes is considered as the optimization criterion. Margin is defined as the distance of optimal hyperplane and nearest training data points of a class. In cases of non-linearly separation of original input space, in 1992, Guyon, Boser and Vapnik presented an approach to generate nonlinear classifiers using kernel functions [279]. SVM firstly transforms the original feature to a higher dimensional feature space. The transformation may be obtained using different nonlinear mappings. The kernel function K(x; y) may be chosen to suit the problem. The common kernels include in equations from (4.24) to (4.29) [280]:

- Linear Kernel $(K(x,y) = x \cdot y)$ (4.24)
- Radial Basis Kernel $(K(x,y) = \exp(-\gamma\|x - y\|^2), \gamma > 0)$ (4.25)
- Polynomial Kernel $(K(x,y) = (\gamma(x \cdot y) + \beta)^d)$ (4.26)
- Gaussian Kernel $(K(x,y) = \exp(\frac{-\|x-y\|^2}{2\sigma^2}), \sigma \neq 0)$ (4.27)
- Radial Basis Kernel $(K(x,y) = \exp(-\gamma\|x - y\|^2), \gamma > 0)$ (4.28)
- Sigmoid $(K(x,y) = \tanh(\gamma(x \cdot y) + \beta))$ (4.29)

After this transformation, the optimal hyperplane may easily found. The achieved hyperplane is the optimal case with respect to a maximal margin [281].

In this thesis, SVM is selected as the method of choice as it linearly classifies data in a high dimensional feature space which is related nonlinearly to the input space using specific Radial Basis (RBF) kernel. The RBF kernel has been adopted due to various reasons [205]: (i) the Linear kernel is unable to handle the problems of nonlinearly separable classification, and actually it is a particular form of RBF kernel [282]; (ii) computation of RBF kernel is much more stable than Polynomial kernel, that may return values of zero or infinity in various cases; (iii) the Sigmoid kernel may only valid (i.e., satisfies Mercer's conditions [283]) in some certain parameters; (iv) the RBF kernel require less parameters to be calculated than Sigmoid and Polynomial kernels.

➢ **SVM Theoretical Background**

Consider a set D of n training data points as [256]:

$$D = \left\{(x_i, y_i)|x_i \in \Re^d, y_i \in \{-1, +1\}, i = 1, 2, ..., n\right\} \quad (4.30)$$

Where x_i: a point in d-dimensional space (d-dimensional vector), y_i: a two-class label.

Assume a hyperplane which separates the positive and negative samples. The points x on this hyperplane satisfies the following condition:

$$w.x + b = 0 \quad (4.31)$$

Where w : the normal vector to the hyperplane , dot(.) : the dot products of the two vectors.

The parameter $\frac{|b|}{||w||}$ is considered as the perpendicular distance (offset) of hyperplane to the origin along with the normal vector (||w|| is assumed as the Euclidean norm of w. If two such hyperplanes is assumed between the positive samples and negative ones, the SVM maximise the distance among them. Considering d+ and d− are the shortest distance of hyperplanes with the closest samples (positive and negative), the margin is determined as d+ + d−. In a linearly separable sample sets, the training data may satisfy the following constraints:

$$x_i.w + b \geq +1 \quad for \quad y_i = +1 \quad (4.32)$$

$$x_i.w + b \leq -1 \quad for \quad y_i = -1 \quad (4.33)$$

That can be composed to yield:

$$y_i(x_i.w + b) - 1 \geq 0 \quad \forall i \quad (4.34)$$

The samples which satisfy Equation (4.34) fall on the hyperplane H1: $x_i.w$+b = 1 with the distance $\frac{|b|}{||w||}$ from the origin, and those samples satisfying the Equation (4.34) are considered as a member of hyperplane H2 : $x_i.w$ + b = −1 with the distance $\frac{|-1-b|}{||w||}$. Therefore, $d_+ = d_- = \frac{1}{||w||}$ and the margin would be $\frac{2}{||w||}$. To find the pair of maximum margin hyperplanes, $||w||^2$ may minimised, considering the given constraints

in Equation (4.34). The training samples which are satisfying those are called support vectors.

The optimisation problem may convert to a dual form by applying the following formulation:

$$L_{linear} = \sum_{i=1}^{n} \alpha_i - \frac{1}{2} \sum_{i=1}^{n} \sum_{j=1}^{n} y_i y_j \alpha_i \alpha_j x_i x_j \tag{4.35}$$

By considering the inequality constraints:

$$\alpha_i \geq 0 \quad \forall_i \tag{4.36}$$

And equality constraint:

$$\sum_{i=1}^{n} \alpha_i y_i = 0 \tag{4.37}$$

In nonlinear separable cases, positive slack variables $\xi_i, (i = 1, 2, ..., n)$ are appended to the constraints. In addition, the user selected parameter C could be placed as the upper bound of α as a penalty parameter related to classification errors.

$$y_i(x_i.w + b) \geq 1 - \xi_i \ , \ \xi \geq 0 \forall_i \tag{4.38}$$

4.5.4 The Proposed Algorithm

In this thesis, an approach is proposed for reducing the dimension of extracted features. This approach is achieved by SFC-IPSO-SVM implementation. According to the details of Sequential Feature Selection (SFC), Inertia based Particle Swarm Optimization presented (IPSO) and Support Vector Machine, explained above, the proposed algorithm in detail is as follows.

- **SMART IPSO-SVM Approach:**

In this thesis, a “Smart IPSO-SVM” approach is proposed for feature selection. The main task of “Smart IPSO-SVM” algorithm is to choose a best subset of features and tuning the parameters of SA-SVM in classification.

- *Initialization:*

In this achievement, each particle is defined as an array with two parts. The first part of particle is an array includes two cells in relation to gamma and cost parameters of SVM which can get a value between $2^{-5}$to 2^{5}. The second part includes an array of 53 cells, refers to 53 features, which contains weights, numbers in range of 0 and 1. These weights indicate the significance of corresponding features;

In first population, the first particle of PSO is initialized by Sequential feature extraction algorithm. In other word, the SFC would propose its best selected subset of features and feed the first particle of PSO. The other particles in first population of PSO are initialized by generating a random vector with the same dimensionality.

- *Selection of features in particle :*

In each iteration, features with the weight more than a specified threshold are chosen. All the particles are sent to SVM for calculating their accuracy based on corresponding features.

- *Fitness function*

To compute the fitness of each particle; SVM algorithm is trained by the training set and the selected features from the corresponding particle and the performance of the SVM on the test set with the corresponding feature set is considered as the fitness of that particle. For implementing this algorithm, cross validation is used to generate the training and testing set.

After achieving the accuracy of particles, the best accuracy in a population would be considered as “gbest” and the best accuracy in the history of that particle would be as “pbest”. The particles in next populations are generated according to the detailed formulas which have been described in 4.4.2. Apparently, in the first population “pbest” and “gbest” are same. By reaching to maximum number of iteration the process is stopped and the obtained “pbest” with its corresponding features is considered as the best solution candidate.

By finishing this algorithm, the best subset of features and setting for the SVM and SA-SVM in the next step is reported to do classification. Pseudo code 4.2 and Figure

4.3 demonstrates the proposed algorithm of "Smart IPSO-SVM" for feature selection stage.

1-Specify data sets of features to feed SFC

2-Initialize the IPSO

- *i. The first particle using the proposed subset of SFC*
- *ii. The other particles using a random vector*

3-Do until the maximum number of iterations is reached

{

4. For each particle

i. Specify the corresponding features subset, and SVM parameters according to the particle.

ii. Use SVM to calculate accuracy as the fitness of the particle.

5. Update particles

6. Go to 3.

7-End Do

}

8-Report the best features subset and SVM parameters

Pseudo code 4.2 The proposed algorithm for feature Selection

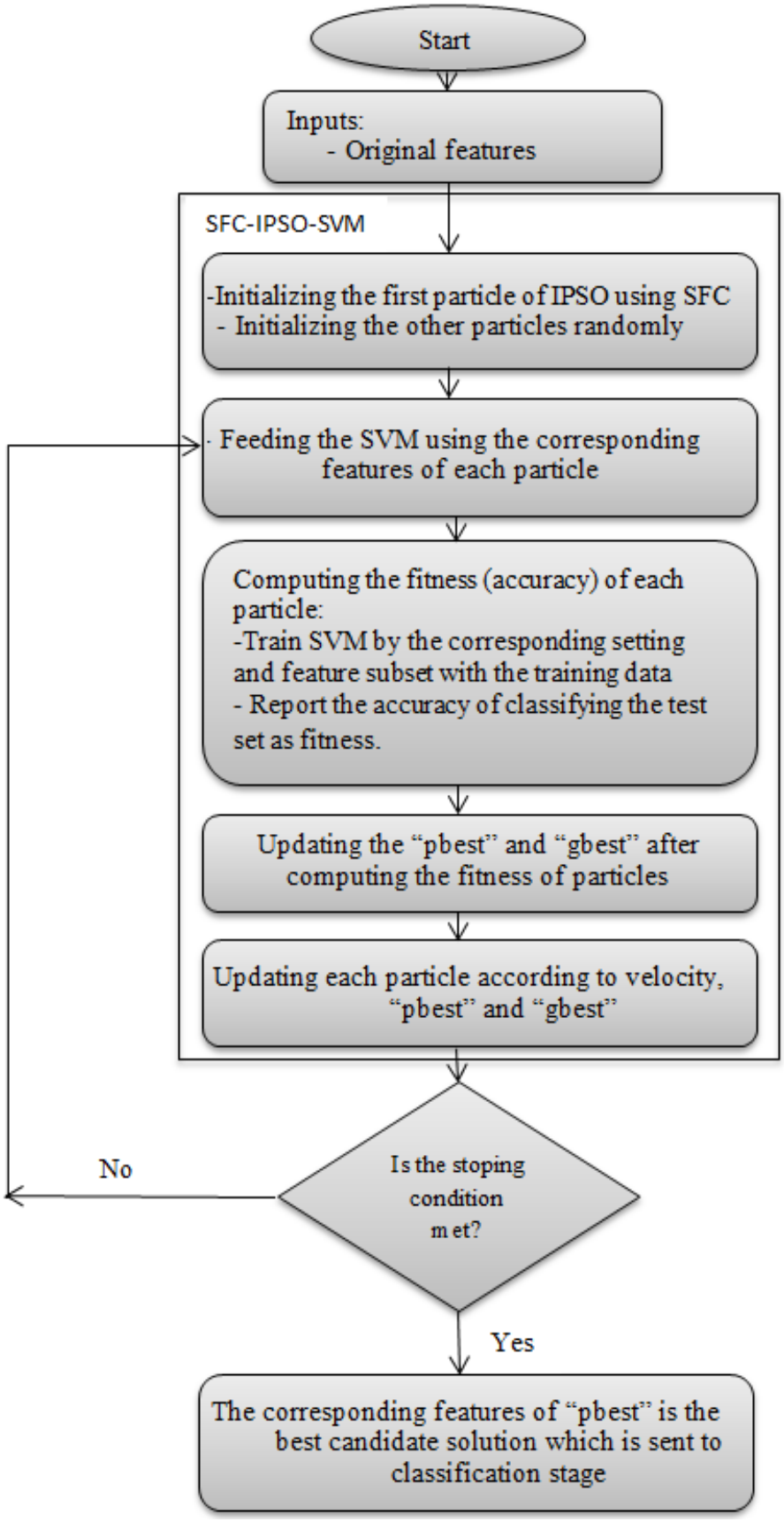

Figure 4.3.Flowchart of proposed SMART IPSO-SVM

4.6 Classification

In this thesis, two types of classifiers including SVM and Self-advising SVM (SA-SVM) are examined. The details of SVM can be found in section 4.4.3. The details of SA- SVM are explained in the following.

4.6.1 Self-advising SVM

The SA-SVM is a developed version of SVM had been introduced by Yashar et al [256], in 2014. It is a non-iterative method which may extracts pursuant knowledge from training phase. According to [256], the SA-SVM provide more promising results than SVM, as it can produce subsequent knowledge from the misclassified data. Thus, this thesis is using the SA-SVM as an efficient classifier in the area of skin cancer detection. In SA-SVM, pursuant knowledge may be in the form of any additional information derived about the first or second type of support vectors, e.g. distribution. More specifically, SA-SVM intends to obtain subsequent knowledge through misclassified data in SVM's training phase. These misclassified data may achieve through two potential sources such as outliers or data which could not separate linearly by applying any type of kernels. This classifier advices weights according to the usage of misclassified data in training phase to employ it along with the decision values in the SVM's test phase. The weights assist the algorithm to omit the outlier data.

To find the misclassified data it is defined in equation (4.39) as follows:

$$MD = \bigcup_{i=1}^{n} \boldsymbol{x}_i | y_i \neq sign\left(\sum_{\alpha_j>0} y_j \alpha_j k(\boldsymbol{x_i}, \boldsymbol{x_j}) + b\right) \tag{4.39}$$

Consider a training set of N samples ($\boldsymbol{x}$,y),…,($\boldsymbol{x}$,y),…,($\boldsymbol{x}$,y)∈$\mathcal{R}$ ×*±1+, where $\boldsymbol{x}$ is the input vector corresponding to the i sample that is labelled by y_i depending on its class. $k\ (x_i, x_j)$ is the kernel function. The 3 most common kernel functions in SVM are:

Polynomial Kernel: $K(x_i x_j) = (x_i x_j + 1)^q$ (4.40)

RBF Kernel: $K(x_i x_j) = e^{-\gamma |x_i - x_j|^2}$ (4.41)

Sigmoid Kernel: $K(x_i x_j) = tanh(\gamma x_i^T x_j + c)$ (4.42)

Here q, y are kernel parameters.

Any SVM decision function and kernel in the right side of equation may be employed. In training phase, although the happening of misclassified data is prevalent, it can be null as well.

The neighbourhood length (NL) of each x_i in MD is described in equation (4.43):

$$NL(\boldsymbol{x}_i) = minimum_{\boldsymbol{x}_j}\left(||\boldsymbol{x}_i - \boldsymbol{x}_j|| | y_i \neq y_j\right) \tag{4.43}$$

Where x_j , j=1,…, n are the training data.

The distance of x_i and x_j may be calculated according to the following equation when the training data is mapped to a higher dimension.

$$||\boldsymbol{\theta}(\boldsymbol{x}_i) - \boldsymbol{\theta}(\boldsymbol{x}_j)|| = \left(k(\boldsymbol{x}_i, \boldsymbol{x}_i) + k(\boldsymbol{x}_j, \boldsymbol{x}_j) - 2k(\boldsymbol{x}_i, \boldsymbol{x}_j)\right)^{0.5} \tag{4.44}$$

Finally, the advised weight is calculated as follows:

$$\begin{cases} 0, & \forall \boldsymbol{x}_i \in MD,\ ||\boldsymbol{x}_k - \boldsymbol{x}_i|| > NL(\boldsymbol{x}_i)\ or\ MD = NUL \\ 1 - \frac{\sum_{\boldsymbol{x}_i} ||\boldsymbol{x}_k - \boldsymbol{x}_i||}{\sum_{\boldsymbol{x}_i} NL(\boldsymbol{x}_i)} & \boldsymbol{x}_i \in MD,\ ||\boldsymbol{x}_k - \boldsymbol{x}_i|| \leq NL(\boldsymbol{x}_i) \end{cases} \tag{4.45}$$

The advised weights are in a range of [0, 1]. It determines the closeness of test data to misclassified data.

4.7 Experimental Evaluation and Comparison of Results

To assess and evaluate the performance of machine learning algorithms, different measures may be applied [285]. The different performance evaluation methods in supervised machine learning approaches have been described in section 3.2.7.

In this study, for a more reliable evaluation of results, Accuracy and F- score along with T-test has been employed to determine the performance and efficiency of proposed algorithm.

The Accuracy and F-score are calculated in various observations between the following cases:

- No feature selection with SVM classification

- Sequential feature selection with SVM classification

- Sequential feature selection with SA-SVM classification

- IPSO-SVM feature selection with SA-SVM classification

- Smart IPSO-SVM feature selection with SA-SVM classification

Finally, the T-test is applied to do statistical comparison for determining the performance of proposed method whether it is significant or not. The p-values achieved by T-test show the significant difference between the obtained results of proposed algorithm and the other practical approaches employed in this thesis as will be shown in chapter 5.

4.8 Summary

This chapter reviewed the proposed algorithms in different stages of skin cancer detection system. This process consists of pre-processing, segmentation, feature extraction and selection, and classification. In pre-processing stage, different comparisons were performed to select the suitable method for proposed algorithm in which Adaptive Median and Adaptive histogram Equalization have been considered in this process. In segmentation stage, a new algorithm based on K-mean and level set algorithms has been proposed and the results are compared with traditional Level set and Fuzzy c-means thresholding (in two cut off, sw=0 and sw=1) in next chapter. In next step, after extracting the different features from images, the proposed algorithm for feature selection (Smart PSO-SVM Feature Selection) is performed to choose the best subset of features to feed the classification stage. This proposed algorithm is compared with 4 other feature extraction algorithms in chapter 5 (Sequential feature selection with SVM classification, Sequential feature selection with SA-SVM classification, IPSO-SVM feature selection with SA-SVM classification and when there is no feature selection in the algorithm). In classification stage, SA-SVM is selected as a suitable classifier in proposed algorithm. It is compared with SVM (next chapter) to prove its better performance of algorithm. The Accuracy, F-score and T-test are explained to estimate the performance of proposed algorithms.

CHAPTER 5

DISCUSSION OF RESULTS

5.1Introduction

This chapter discuss about the results obtained from proposed algorithms in this thesis. During this research, it was necessary to propose different algorithms based on specific application of skin cancer detection system. However, new ideas and algorithms in segmentation and feature selection stages have been proposed to improve the accuracy of the system. Since these algorithms can be applied in different areas of machine learning, they are presented separately in this chapter.

5.2 Pre-Processing

In this section, the five different filters on different noises have been experimented to get the better filter for improving the images' quality. The results have been published in the paper titled "Comparing the Performance of Various Filters on Skin Cancer Images" in Journal Procedia Computer Science, Volume 42, 2014, Pages 32-37, Elsevier.

The following figures represent the Skin cancer image after simulating of Gaussian, Salt & Pepper , Speckle and Poisson noise, and de-noising the results using Median filter, Adaptive Median filter, Mean filter, Adaptive Mean filter, Gaussian smoothing filter and Wiener filter to evaluate the best de-noising filter on different noisy images as shown in figures 5.1 to figure 5.4. The Simulation is run by MATLAB 7.12.0 (R2011a).

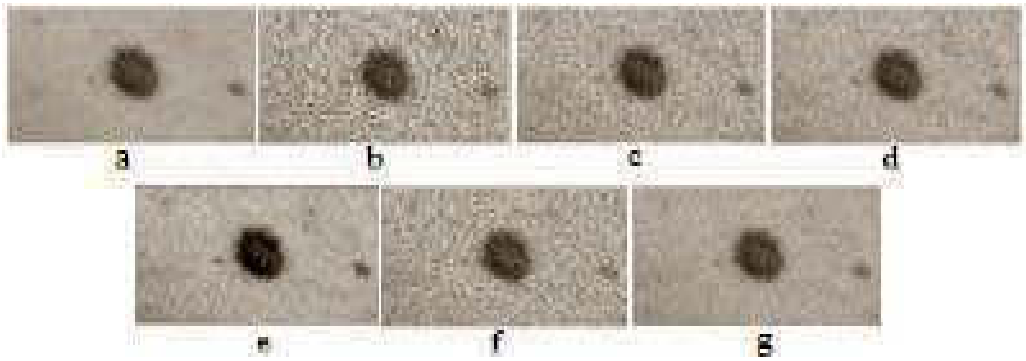

Figure 5.1. a) Original image b) Simulated Speckle noise and de-noising by c) Gaussian Filter d) Median Filter e) Mean Filter f) Adaptive Median Filter g) Adaptive Wiener

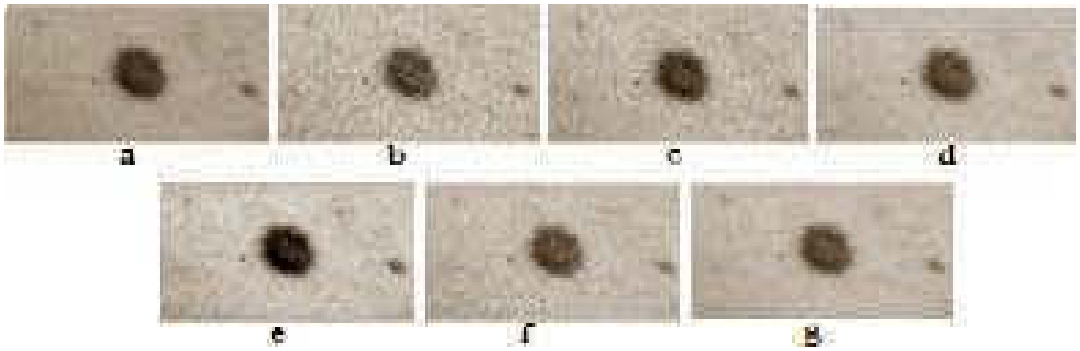

Figure 5.2. a) Original image b) Simulated Gaussian noise and de-noising by c) Gaussian Filter d) Median Filter e) Mean Filter f) Adaptive Median Filter g) Adaptive Wiener

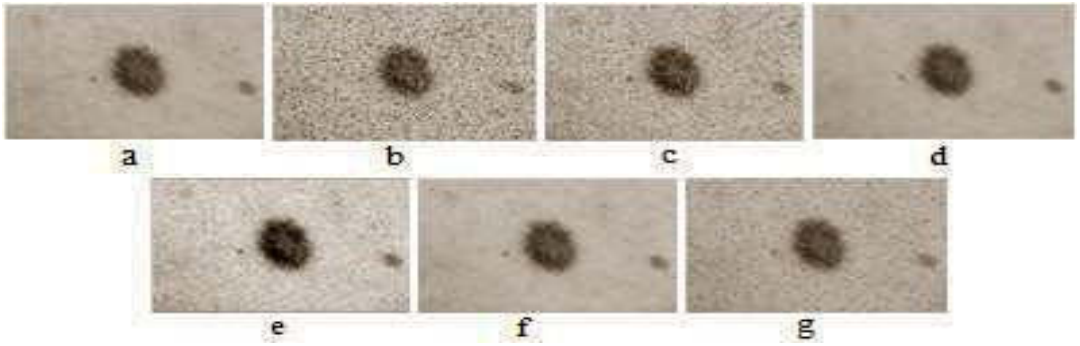

Figure 5.3. a) Original image b) Simulated Salt & Pepper noise and de-noising by c) Gaussian Filter d) Median Filter e) Mean Filter f) Adaptive Median Filter g) Adaptive Wiener

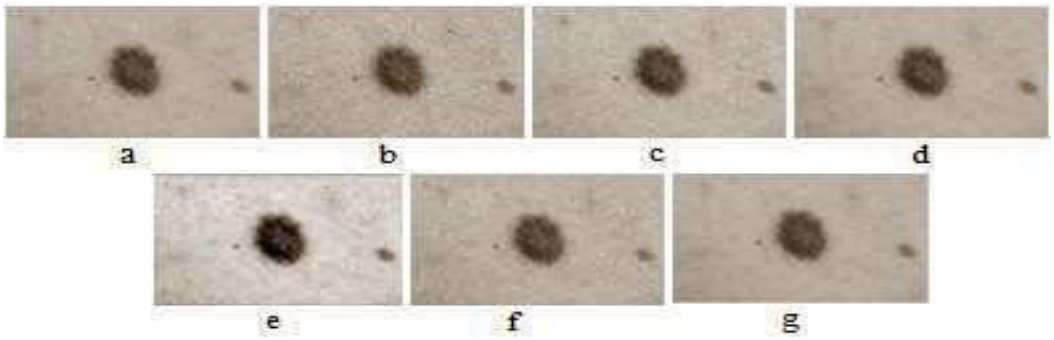

Figure 5.4. a) Original image b) Simulated Poison noise and de-noising by c) Gaussian Filter d) Median Filter e) Mean Filter f) Adaptive Median Filter g) Adaptive Wiener

The comparison of images to achieve the most effective filter on different noises in different densities has been evaluated by peak signal-to-noise ratio (PSNR) which is the popular and well-known index to compare the original and de-noised image. Mostly, the higher PSNR conduct a higher quality and less noisy image [286]. The experiments have been tested on 15 digital images. Since these images have been evaluated in 8 different densities, each image is like a new image. The following table shows the PSNRs for a sample Skin cancer image which has been simulated by Gaussian, Salt & Pepper , Speckle and Poisson noise, and then de-noised using Median filter, Adaptive Median filter, Mean filter, Adaptive Mean filter, Gaussian smoothing filter and Wiener filter to compare their noise removal performance and to choose the most effective filter which are the main purpose of this section. Table 5.1 has been classified according to 10% - 80% densities.

Density	10 %				20 %				30 %			
Noise / Filters	Speckle	Gussian	Salt & Pepper	Poison	Speckle	Gussian	Salt & Pepper	Poison	Speckle	Gussian	Salt & Pepper	Poison
Gussian	+30.72	+30.64	+38.59	+32.83	+29.38	+31.54	+36.83	+32.83	+28.87	+32.53	+35.53	+32.83
Median	+32.71	+34.20	+34.72	+33.99	+31.58	+35.97	+34.72	+33.99	+30.90	+37.79	+34.72	+33.99
Mean	+33.75	+34.65	+33.72	+34.07	+33.08	+36.34	+32.93	+34.07	+32.55	+37.84	+32.30	+34.07
Adaptive Median	+29.94	+30.33	+40.98	+32.10	+29.00	+31.14	+40.96	+32.10	+28.60	+32.00	+40.94	+32.10
Adaptive Wiener	+34.24	+34.97	+35.67	+34.71	+33.35	+36.90	+35.49	+34.71	+32.59	+38.86	+34.97	+34.71
Density	40 %				50 %				60 %			
Noise / Filters	Speckle	Gussian	Salt & Pepper	Poison	Speckle	Gussian	Salt & Pepper	Poison	Speckle	Gussian	Salt & Pepper	Poison
Gussian	+28.58	+33.59	+34.55	+32.83	+28.40	+34.73	+33.80	+32.83	+28.26	+35.94	+33.14	+32.83
Median	+30.43	+39.60	+34.71	+33.99	+30.10	+41.36	+34.71	+33.99	+29.84	+43.03	+34.70	+33.99
Mean	+32.12	+39.11	+31.74	+34.07	+31.75	+40.12	+31.30	+34.07	+31.41	+40.89	+30.82	+34.07
Adaptive Median	+28.37	+32.92	+40. 94	+32.10	+28.22	+33.59	+40.93	+32.10	+28.10	+34.93	+40.86	+32.10
Adaptive Wiener	+31.99	+40.78	+34.20	+34.71	+31.51	+42.61	+33.43	+34.71	+31.12	+44.33	+32.67	+34.71
Density	70 %				80 %							
Noise / Filters	Speckle	Gussian	Salt & Pepper	Poison	Speckle	Gussian	Salt & Pepper	Poison				
Gussian	+28.16	+37.23	+32.61	+32.83	+28.07	+38.60	+32.15	+32.83				
Median	+29.63	+44.62	+34.69	+33.99	+29.47	+46.12	+34.68	+33.99				
Mean	+31.10	+41.47	+30.44	+34.07	+30.80	+41.94	+30.09	+34.07				
Adaptive Median	+28.00	+36.00	+40.81	+32.10	+27.92	+37.14	+40.76	+32.10				
Adaptive Wiener	+30.75	+45.92	+32.13	+34.71	+30.48	+47.38	+31.68	+34.71				

Table 5.1.Comparison of PSNR for a skin cancer image after simulating different noises and de-noising by filters in different densities

In table 5.1: when the noise is speckle with the density of 10%, the adaptive wiener shows the highest PSNR which means the better performance of this filter in de-noising the speckle noises; when the noise is gussian with the density of 10%, the mean filter shows the highest PSNR which means the better performance of this filter in de-noising the gussian noises; when the noise is salt & pepper with the density of 10%, the adaptive median shows the highest PSNR which means the better performance of this filter in de-noising the salt & pepper noises; when the noise is poison with the density of 10%, the adaptive wiener shows the highest PSNR which means the better performance of this filter in de-noising the poison noises. The same illustration is considered for the whole table. After analysing Table 5.1, the most effective filters for removing different types of noises with densities of 10% - 80% have been summarized as Table 5.2.

After analysing Table 5.1, the most effective filters for removing different types of noises with densities of 10% - 80% have been summarized as Table 5.2.

Noise / Density	Speckle	Gussian	Salt & Pepper	Poison
10 % - 30 %	Adaptive Wiener	Adaptive Wiener	Adaptive Median	Adaptive Wiener
40 % - 80 %	Mean	Adaptive Wiener	Adaptive Median	Adaptive Wiener

Table 5.2. The most effective Filters on different noises with densities between 10% - 80%

According to table 5.2, Adaptive Wiener filter has the best performance (highest PSNR) in different intensities of Gaussian, Poison, and lower intensities of Speckle noise. In Speckle, when the intensities of noise increased more than 40%, Mean Filter performs the best. In all densities of salt & pepper noise, the Adaptive Median is the best candidate. So, according to images, the best candidate for proposed algorithm of skin cancer detection in this thesis is Adaptive Median.

In the following of noise removal, the experiments on three contrast enhancement techniques “Histogram Equalization (HE) “,”Adaptive Histogram Equalization (AHE) “ and “Unsharp Masking (UM) “are performed to determine the best technique for employing in the pre-processing stage of proposed algorithm as shown in figure 5.5. The results have been published in another paper “Pre-Processing of Automatic Skin Cancer Detection System: Comparative Study “in International Journal of Smart Sensing and Intelligent Systems, Vol. 7, No. 3, September 2014, PP 1364-1377.

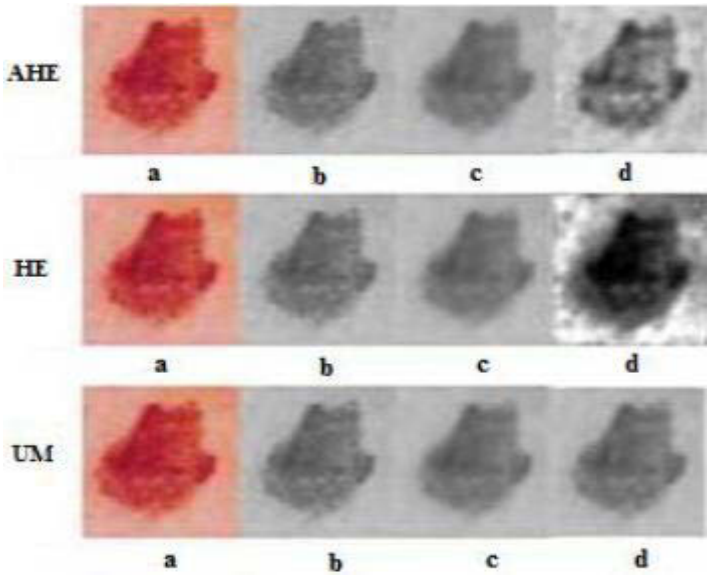

Figure 5.5.Comparison of AHE,HE and UM

Experimental results on skin cancer images show although the performance of UM and AHE are very close, the AHE is more effective than UM in most of images. The Modified Hausdorff Distance, Euclidean distance and Correlation are applied as measurement indexes.

Since the smaller value in Modified Hausdorff Distance indicates more similarity to the pattern, in Table 5.3 and Figure 5.6, the values show the better performance of UM in more images than AHE and HE. In addition, the close values of UM and AHE in most of images in the result table represent the close performance of these two contrast enhancement techniques as well.

CET	Images									
	1	*2*	*3*	*4*	*5*	*6*	*7*	*8*	*9*	*10*
AHE	3.9766	3.4512	3.0123	3.4034	3.6488	3.9388	3.9835	3.6015	3.9639	4.2252
HE	4.2461	3.5113	4.2581	4.2148	5.2215	4.2177	4.0117	3.5079	3.7818	4.1161
UM	3.9495	3.4535	3.0088	3.4056	3.4130	3.9398	3.9990	3.4593	3.8198	4.1538
CET	Images									
	11	*12*	*13*	*14*	*15*	*16*	*17*	*18*	*19*	*20*
AHE	3.5256	4.1458	3.8700	3.9046	4.4621	4.1226	4.1058	4.5828	3.9715	4.1927
HE	3.8086	4.1541	3.9255	3.9862	4.6387	4.0633	4.2427	4.5342	4.6431	4.5659
UM	3.5265	4.1253	3.8623	3.8820	4.4604	4.0633	4.1063	4.5917	3.9528	4.1664

Table 5.3 .Result table of Modified Hausdorff Distance

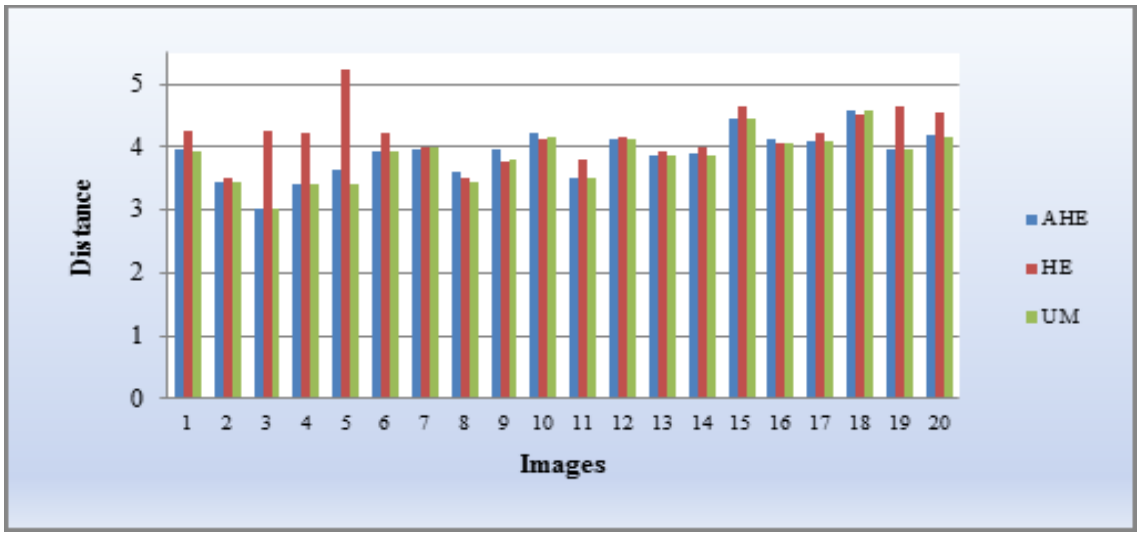

Figure 5.6. Modified Hausdorff Distance

In Euclidean Distance measurement, the smaller value shows the degree of mismatch between the resulted image and pattern. Therefore, the values in Table 5.4 and Figure 5.7 depict the better performance of AHE in more images than UM and HE. Moreover, the more similar values in the result table show the close performance of UM and AHE in most of images as well.

CET	Images									
	1	*2*	*3*	*4*	*5*	*6*	*7*	*8*	*9*	*10*
AHE	0.8529	0.8708	0.8969	0.8992	0.8942	0.9085	0.8620	0.8465	0.8504	0.9588
HE	0.9516	0.9284	0.9250	0.9435	0.9239	0.9120	0.9169	0.8671	0.8761	0.8942
UM	0.8522	0.8755	0.9028	0.9042	0.8447	0.9105	0.9161	0.8847	0.8691	0.8892
CET	Images									
	11	*12*	*13*	*14*	*15*	*16*	*17*	*18*	*19*	*20*
AHE	0.8860	0.8977	0.8904	0.8426	0.9224	0.8687	0.8459	0.8225	0.9006	0.8392
HE	0.8974	0.8981	0.8930	0.9041	0.9237	0.8771	0.8858	0.8255	0.9229	0.9491
UM	0.8860	0.8766	0.8799	0.8554	0.8919	0.8410	0.8595	0.8594	09186	0.8475

Table 5.4.Result table of Euclidean Distance

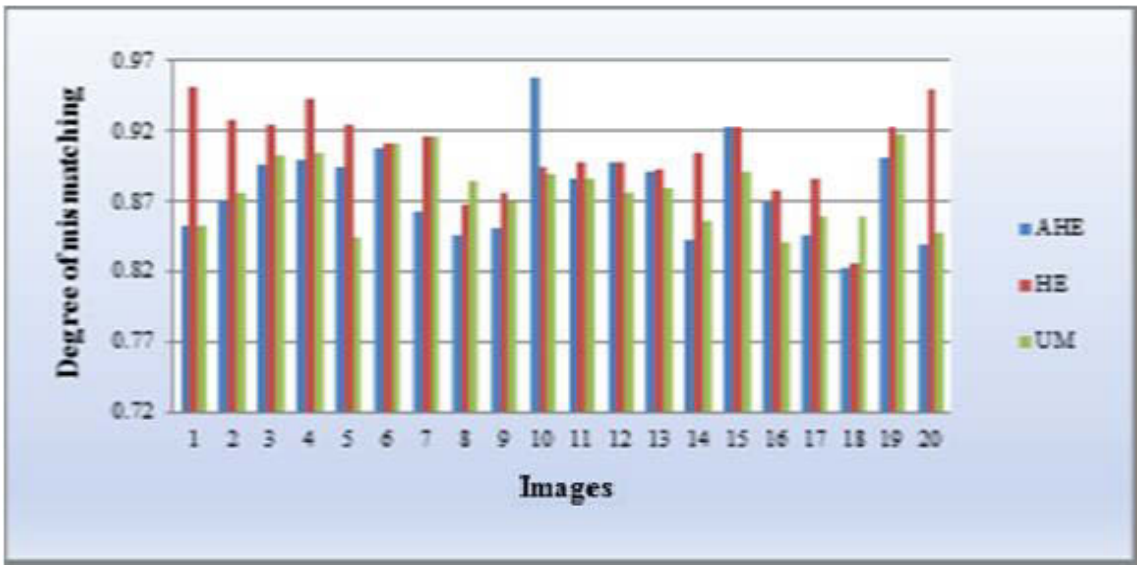

Figure 5.7. Euclidean Distance

The results of third quality measurement are represented in Table 5.5 and Figure 5.8. In Correlation, the larger value shows the degree of matching between the resulted image and pattern. Therefore, the better performance of AHE among other techniques is obvious in most of images. On the other hand, the results of Correlation in Table 5.5 are much closer to the results of Euclidean distance measurement in Table 5.4. In other words, according to the result tables, both measurements indicate the better performance of AHE among these three contrast enhancement techniques.

CET	Images									
	1	*2*	*3*	*4*	*5*	*6*	*7*	*8*	*9*	*10*
AHE	0.7084	0.8521	0.8714	0.8566	0.6423	0.8873	0.9438	0.8602	0.9137	0.6645
HE	0.6818	0.7502	0.4310	0.4481	0.2885	0.5366	0.5604	0.7620	0.8461	0.8116
UM	0.8132	0.8474	0.8789	0.8541	0.7501	0.8864	0.9324	0.9023	0.8683	0.7363
CET	Images									
	11	*12*	*13*	*14*	*15*	*16*	*17*	*18*	*19*	*20*
AHE	0.8864	0.8755	0.9046	0.8562	0.7962	0.7764	0.7769	0.6856	0.8599	0.5653
HE	0.7085	0.7096	0.6480	0.7011	0.3932	0.6922	0.5898	0.4517	0.3949	0.4797
UM	0.8804	0.9178	0.8890	0.8167	0.8349	0.8721	0.7003	0.5456	0.7591	0.6816

Table 5.5: Result table of Correlation

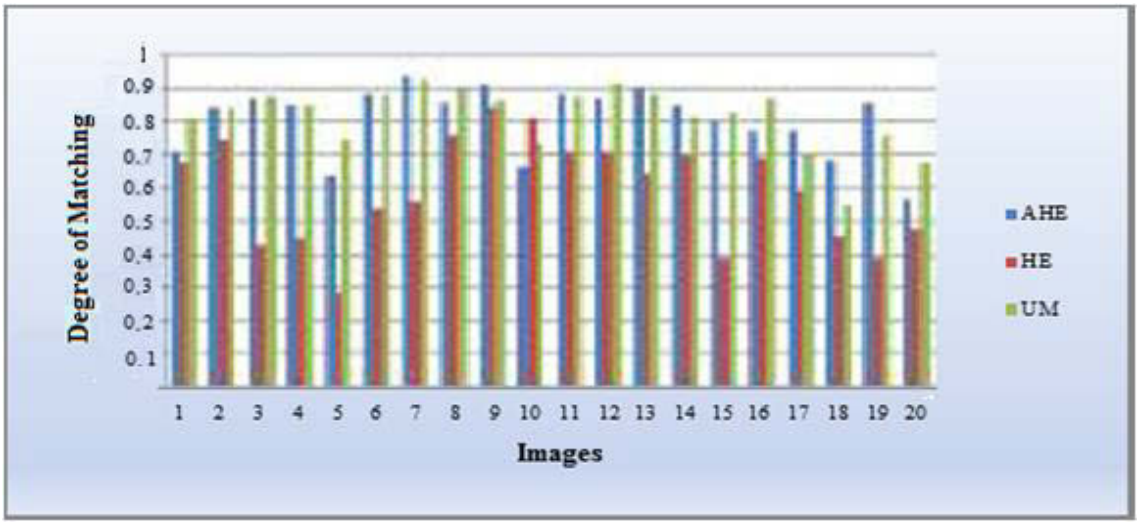

Figure 5.8. Correlation

The above three Tables show the good performance of AHE and UM, and the worse performance of HE as a contrast enhancement technique. Although AHE and UM have a close performance, two measurements of Euclidean Distance and Correlation among three applied measurements show the better performance of AHE in most of

images. Therefore, in this thesis, the AHE is selected to perform as a contrast enhancement technique of proposed algorithm.

This stage is performed to minimise the effect of background skin on analysis and maximise the concentration on lesion pixels.

5.3 Segmentation

In this section, the proposed algorithm is tested on eighty six images taken from digital cameras. In order to demonstrate the improved method, a multiple algorithms have been run with the same condition. The first algorithm is the traditional level set (TLS), proposed in [269], the second is Fuzzy c-means thresholding (FCM) [162] in two cut off (sw=0, cut between the small and middle class, sw=1, cut between the middle and large class), and the last one is the proposed algorithm for segmentation stage.

Figure 5.9 shows the segmentation results achieved by the proposed algorithm in which the k-means segmentation results have been considered as an initial curve or surface function of level set algorithm.

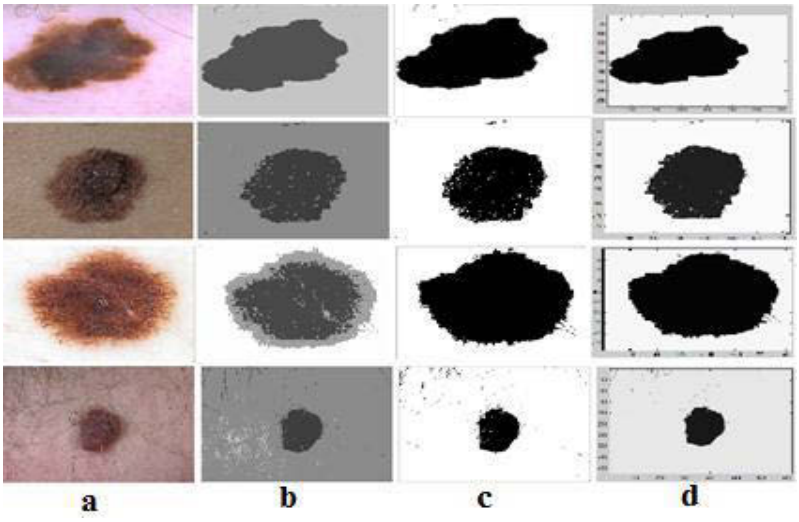

Figure 5.9. a) Original Image b) Initial k-means segmentation c) Converting the segmented image to binary d) Segmented result of proposed algorithm after initializing the level set segmentation technique by k-means algorithm

To perform the comparison of segmented results with the ground truth images, let SR and GT indicate the result of automatic segmentation method and the ground truth segmentation, respectively. Figure 5.10 indicates this comparison.

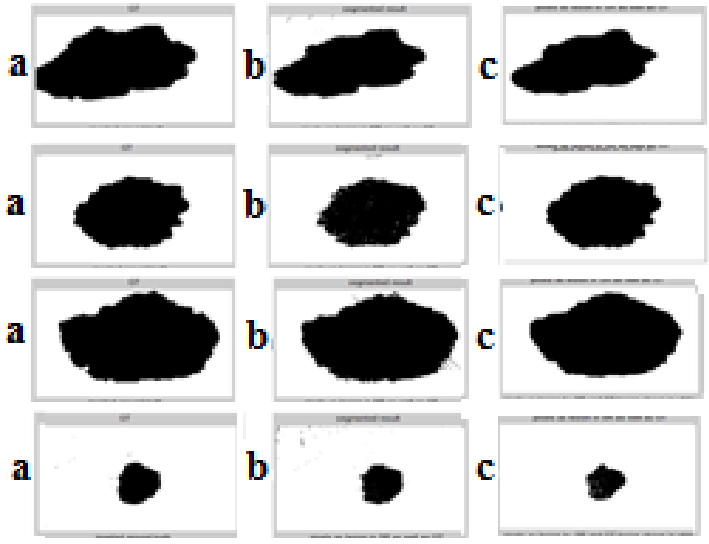

Figure 5.10. Comparison of ground truth image with the segmented image of proposed algorithm a) Ground truth image b) Segmented result c) Pixels in segmented lesion as well as ground truth (Subscription of 'a','b' images)

Figure 5.11 demonstrates the results achieved by "Fuzzy c-means thresholding" method which has been applied to compare with the proposed algorithm.

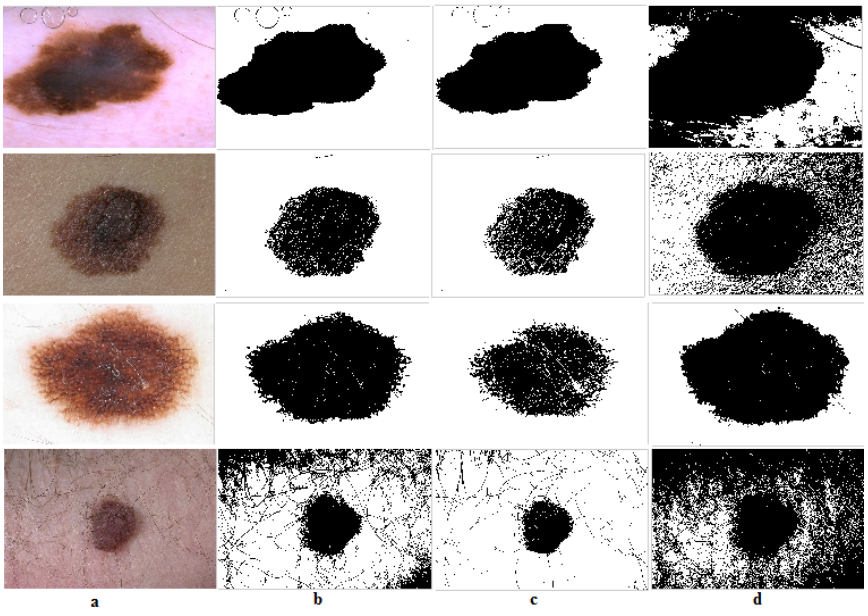

Figure 5.11. Fuzzy c-means thresholding in two cut-off position a) Original image b) Otsu thresholding c) FCM (sw=0) d) FCM (sw=1)

Figure 5.12 show the comparison of segmented images with different segmentation methods and proposed algorithm.

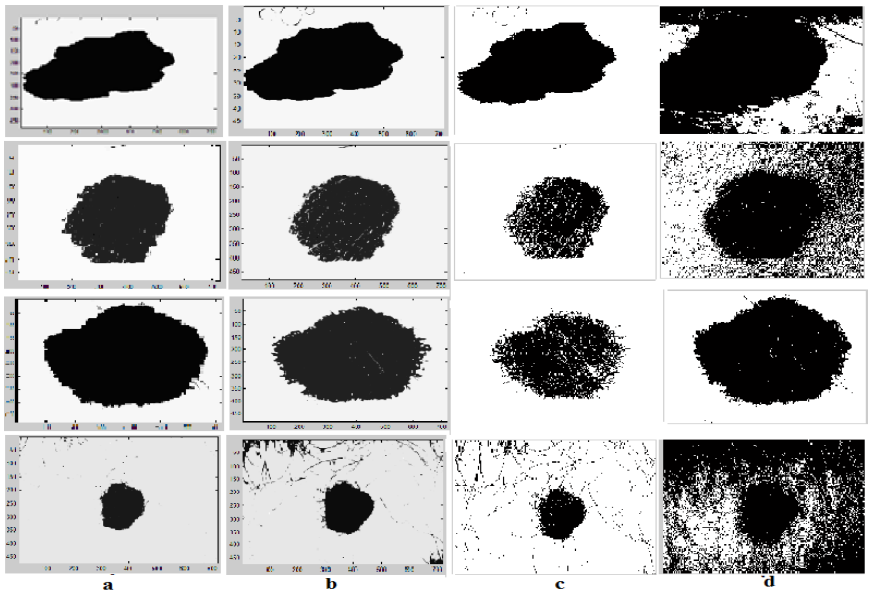

Figure 5.12.Comparison of a) the proposed segmentation method b) traditional level set method c) Fuzzy c-means thresholding (sw=0) d) fuzzy c-means thresholding (sw=1)

Four different metrics of Border error, Similarity, Hammoude distance and Rms error are used to quantify the boundary differences. Each metric is calculated between the segmented results achieved by TLS, KLS, FCT (sw=0) and FCT (sw=1) with ground truth images. Table 5.6 shows the statistical comparison of mentioned algorithms by these metrics. As it is obvious from table 5.6, in KLS, the average Border error, Hammoude distance and Rms Error between the ground truth and segmented images have the lowest values and similarity has the highest value. It shows the better performance of KLS among other algorithms.

	TLS	KLS	FCT (sw=0)	FCT (sw=1)
Bordererorr	0.10301628	0.0740709	0.09167442	0.33709060
Similarity	0.91481977	0.94976046	0.93741395	0.69192209
Hammoude distance	0.33093837	0.26466872	0.30811977	0.56523721
RmsError	0.20566395	0.15874302	0.19043721	0.48864069

Table 5.6 .Comparison of Proposed method, TLS, FCT (w=0), FCT (w=1) by the Bordererror, Similarity, Hammoude distance and Rms error

To determine the statistical difference of proposed algorithm with others, one-way analysis of variance (ANOVA) as a statistical inference is applied with a 0.05 significance level. It is known as a popular and powerful tool which is robust to non-homogeneity of the data [40]. The Anova test compare “the border errors achieved by TLS segmentation algorithm” with “the border errors achieved by KLS segmentation algorithm” with “the border errors achieved by FCT (sw=0) segmentation algorithm”,

and finally with "the border errors achieved by FCT (sw=1) segmentation algorithm". The purpose is to find out how significant is the results' difference of proposed algorithm with others. Table 5.7 represents the p-values achieved by Anova test on the Border error, Similarity, Hammoudedis and rmsErr metrics between "KLS and TLS", "KLS and FCT (sw=0)", and "KLS and FCT (sw=1)". As it can be observed in table 5.7, on the first column, all the mean values are less than 0.05, which shows the significant difference between KLS and TLS. In second column, the mean values of "Border Error" and "Rms Error" show the significant difference between KLS and FCT (sw=0), while the other metrics show although there is improvement (according to table 5.6), it is not significant. The mean values of third column show the significant difference between KLS and FCT (sw=1).

	KLS , TLS	KLS , FCT (sw=0)	KLS, FCT (sw=1)
Border Erorr	0.001297208	0.054251731	1.74945E-28
Similarity	0.001634137	0.100855147	3.67806E-27
Hammoude distance	0.012623932	0.093412074	3.67806E-27
Rms Error	0.020616402	0.054273962	3.44266E-30

Table 5.7. Anova test on Bordererror, Similarity, Hammoude distance and Rmserror metrics between "KLS and TLS", "KLS and FCT (w=0)" , "KLS and FCT (w=1)"

The experimental results achieved by Anova test are illustrated separately in tables 5.8 to 5.19.

Border Error Metric :

Anova: Single Factor						
SUMMARY						
Groups	Count	Sum	Average	Variance		
LS	86	8.8594	0.103016	0.004299		
KLS	86	6.3701	0.074071	0.002435		
ANOVA						
Source of Variation	SS	df	MS	F	P-value	F crit
Between Groups	0.036027	1	0.036027	10.70006	0.001297	3.896742
Within Groups	0.572386	170	0.003367			
Total	0.608413	171				

Table 5.8.Difference of Border error achieved by LS and KLS

Table 5.8 shows that, when LS segmentation method is performed on images, the average and variance of border error are 0.103016 and 0.004299, while in a case of KLS segmentation, the average and variance of border error are 0.074071 and 0.002435

respectively. Anova test shows the significant difference of average and variance of border errors between these two groups (p-value).Since it is equal or less than 0.05, it is considered as significant difference.

Anova: Single Factor						
SUMMARY						
Groups	Count	Sum	Average	Variance		
KLS	86	6.3701	0.074071	0.002435		
FCT (w=0)	86	7.884	0.091674	0.004659		
ANOVA						
Source of Variation	SS	df	MS	F	P-value	F crit
Between Groups	0.013325	1	0.013325	3.756737	0.054252	3.896742
Within Groups	0.602982	170	0.003547			
Total	0.616307	171				

Table 5.9.Difference of Border error by achieved KLS and FCT(w=0)

Table 5.9 shows that, when KLS segmentation method is performed on images, the average and variance of border error are 0.074071and 0.002435, while in a case of FCT(w=0) segmentation, the average and variance of border error are 0.091674and 0.004659respectively. Anova test shows the significant difference of average and variance of border errors between these two groups (p-value).Since it is equal or less than 0.05, it is considered as significant difference.

Anova: Single Factor						
SUMMARY						
Groups	Count	Sum	Average	Variance		
KLS	86	6.3701	0.074071	0.002435		
FCT (w=1)	86	28.9898	0.337091	0.030569		
ANOVA						
Source of Variation	SS	df	MS	F	P-value	F crit
Between Groups	2.974714	1	2.974714	180.2603	1.75E-28	3.896742
Within Groups	2.805395	170	0.016502			
Total	5.780109	171				

Table 5.10. Difference of Border error achieved by KLS and FCT(w=1)

Table 5.10 shows that, when KLS segmentation method is performed on images, the average and variance of border error are 0.074071and 0.002435, while in a case of FCT(w=1) segmentation, the average and variance of border error are 0.337091and

0.030569 respectively. Anova test shows the significant difference of average and variance of border errors between these two groups (p-value).Since it is equal or less than 0.05, it is considered as significant difference.

Similarity Metric :

Anova: Single Factor						
SUMMARY						
Groups	Count	Sum	Average	Variance		
LS	86	78.6745	0.91482	0.008057		
KLS	86	81.6794	0.94976	0.002189		
ANOVA						
Source of Variation	SS	df	MS	F	P-value	F crit
Between Groups	0.052497	1	0.052497	10.24691	0.001634	3.896742
Within Groups	0.870939	170	0.005123			
Total	0.923435	171				

Table 5.11. Difference of Similarity achieved by LS and KLS

Table 5.11 shows that, when LS segmentation method is performed on images, the average and variance of Similarity are 0.91482and 0.008057, while in a case of KLS segmentation, the average and variance of Similarity are 0.94976and 0.002189respectively. Anova test shows the significant difference of average and variance of similarity between these two groups (p-value).Since it is equal or less than 0.05, it is considered as significant difference.

Anova: Single Factor						
SUMMARY						
Groups	Count	Sum	Average	Variance		
KLS	86	81.6794	0.94976	0.002189		
FCT (w=0)	86	80.6176	0.937414	0.002628		
ANOVA						
Source of Variation	SS	df	MS	F	P-value	F crit
Between Groups	0.006555	1	0.006555	2.72144	0.100855	3.896742
Within Groups	0.409456	170	0.002409			
Total	0.416011	171				

Table 5.12. Difference of Similarity achieved by KLS and FCT(w=0)

Table 5.12 shows that, when KLS segmentation method is performed on images, the average and variance of Similarity are 0.94976 and 0.002189, while in a case of FCT(w=0) segmentation, the average and variance of Similarity are 0.937414 and

0.002628 respectively. Anova test shows the difference of average and variance of similarity between these two groups by p-value. Since it is not equal or less than 0.05, it is considered as not significant difference, although there is improvement.

Anova: Single Factor						
SUMMARY						
Groups	Count	Sum	Average	Variance		
KLS	86	81.6794	0.94976	0.002189		
FCT (w=1)	86	59.5053	0.691922	0.031843		
ANOVA						
Source of Variation	SS	df	MS	F	P-value	F crit
Between Groups	2.858667	1	2.858667	167.9998	3.68E-27	3.896742
Within Groups	2.892702	170	0.017016			
Total	5.751368	171				

Table 5.13. Difference of Similarity achieved by KLS and FCT(w=1)

Table 5.13 shows that, when KLS segmentation method is performed on images, the average and variance of Similarity are 0.94976 and 0.002189, while in a case of FCT(w=1) segmentation, the average and variance of Similarity are 0.691922and 0.031843 respectively. Anova test shows the difference of average and variance of similarity between these two groups by p-value. Since it is equal or less than 0.05, it is considered as significant difference.

Hammoude Distance Metric:

Anova: Single Factor						
SUMMARY						
Groups	Count	Sum	Average	Variance		
LS	86	28.4607	0.330938	0.037492		
KLS	86	22.76151	0.264669	0.021937		
ANOVA						
Source of Variation	SS	df	MS	F	P-value	F crit
Between Groups	0.188842	1	0.188842	6.355242	0.012624	3.896742
Within Groups	5.051434	170	0.029714			
Total	5.240275	171				

Table 5.14. Difference of Hammoude Distance achieved by LS and KLS

Table 5.14 shows that, when LS segmentation method is performed on images, the average and variance of Similarity are 0.330938and 0.037492, while in a case of KLS segmentation, the average and variance of Similarity are 0.264669 and 0.021937

respectively. Anova test shows the difference of average and variance of Hammoude Distance between these two groups by p-value. Since it is equal or less than 0.05, it is considered as significant difference.

Anova: Single Factor						
SUMMARY						
Groups	Count	Sum	Average	Variance		
KLS	86	22.76151	0.264669	0.021937		
FCT (w=0)	86	26.4983	0.30812	0.035106		
ANOVA						
Source of Variation	SS	df	MS	F	P-value	F crit
Between Groups	0.081184	1	0.081184	2.846413	0.093412	3.896742
Within Groups	4.84864	170	0.028521			
Total	4.929824	171				

Table 5.15. Difference of Hammoude Distance achieved by LS and FCT(w=0)

Table 5.15 shows that, when KLS segmentation method is performed on images, the average and variance of Similarity are 0.264669 and 0.021937, while in a case of FCT(w=0) segmentation, the average and variance of Similarity are 0.30812and 0.035106 respectively. Anova test shows the difference of average and variance of Hammoude Distance between these two groups by p-value. Since it is not equal or less than 0.05, it is not considered as significant difference.

Anova: Single Factor						
SUMMARY						
Groups	Count	Sum	Average	Variance		
KLS	86	22.76151	0.264669	0.021937		
FCT (w=1)	86	48.6104	0.565237	0.073113		
ANOVA						
Source of Variation	SS	df	MS	F	P-value	F crit
Between Groups	3.884681	1	3.884681	81.73982	3.41E-16	3.896742
Within Groups	8.079241	170	0.047525			
Total	11.96392	171				

Table 5.16. Difference of Hammoude Distance achieved by LS and FCT(w=1)

Table 5.16 shows that, when KLS segmentation method is performed on images, the average and variance of Similarity are 0.264669 and 0.021937, while in a case of FCT(w=1) segmentation, the average and variance of Similarity are 0.565237 and 0.073113respectively. Anova test shows the difference of average and variance of

Hammoude Distance between these two groups by p-value.Since it is equal or less than 0.05, it is considered as significant difference.

Rms Error Metric:

Anova: Single Factor						
SUMMARY						
Groups	Count	Sum	Average	Variance		
LS	86	17.6871	0.205664	0.024423		
KLS	86	13.6519	0.158743	0.010251		
ANOVA						
Source of Variation	SS	df	MS	F	P-value	F crit
Between Groups	0.094668	1	0.094668	5.460539	0.020616	3.896742
Within Groups	2.947237	170	0.017337			
Total	3.041905	171				

Table 5.17. Difference of Rms Error achieved by LS and KLS

Table 5.17 shows that, when LS segmentation method is performed on images, the average and variance of Similarity are 0.205664and 0.024423, while in a case of KLS segmentation, the average and variance of Similarity are 0.158743and 0.010251respectively. Anova test shows the difference of average and variance of Rms Error between these two groups by p-value: 0.020616.Since it is equal or less than 0.05, it is considered as significant difference.

Anova: Single Factor						
SUMMARY						
Groups	Count	Sum	Average	Variance		
KLS	86	13.6519	0.158743	0.010251		
FCT (w=0)	86	16.3776	0.190437	0.012749		
ANOVA						
Source of Variation	SS	df	MS	F	P-value	F crit
Between Groups	0.043194	1	0.043194	3.756036	0.054274	3.896742
Within Groups	1.955	170	0.0115			
Total	1.998195	171				

Table 5.18. Difference of Rms Error achieved by KLS and FCT(w=0)

Table 5.18 shows that, when KLS segmentation method is performed on images, the average and variance of Rms Error are 0.158743and 0.010251, while in a case of FCT(w=0) segmentation, the average and variance of Rms Error are 0.190437and

0.012749 respectively. Anova test shows the difference of average and variance of Rms Error between these two groups by p-value. Since it is equal or less than 0.05, it is considered as significant difference.

Anova: Single Factor						
SUMMARY						
Groups	Count	Sum	Average	Variance		
KLS	86	13.6519	0.158743	0.010251		
FCT (w=1)	86	42.0231	0.488641	0.037323		
ANOVA						
Source of Variation	SS	df	MS	F	P-value	F crit
Between Groups	4.679796	1	4.679796	196.7396	3.44E-30	3.896742
Within Groups	4.043747	170	0.023787			
Total	8.723544	171				

Table 5.19. Difference of Rms Error achieved by KLS and FCT(w=1)

Table 5.19 shows that, when KLS segmentation method is performed on images, the average and variance of Rms Error are 0.158743 and 0.010251, while in a case of FCT(w=1) segmentation, the average and variance of Rms Error are 0.488641 and 0.037323 respectively. Anova test shows the difference of average and variance of Rms Error between these two groups by p-value. Since it is equal or less than 0.05, it is considered as significant difference.

The figure 5.13 shows the comparative view and difference of Border error, Similarity, Hammoude distance and Rms error achieved by “KLS and TLS”, “KLS and FCM (sw=0)”, and “KLS and FCM (sw=1)” using Anova test. The red lines in the middle of each area show the average in the figures.

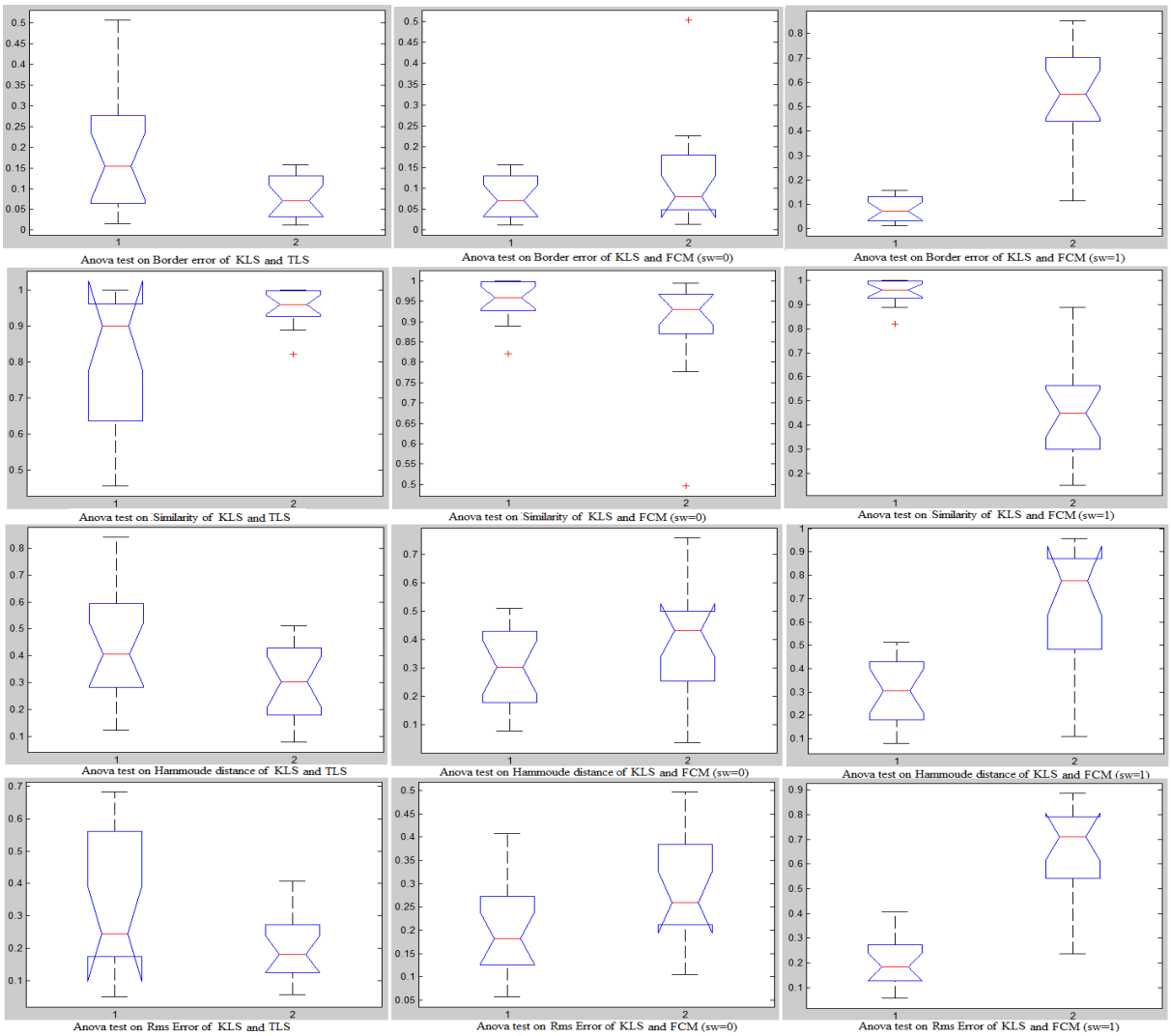

Figure 5.13. Difference of Border error, Similarity, Hammoude distance and Rms error of "KLS and TLS", "KLS and FCM (sw=0)", and "KLS and FCM (sw=1)".

As noticed before, another contribution achieved in this thesis is the computational cost which is significantly reduced in compare with TLS method. Table 5.20 indicate the comparison results.

Anova: Single Factor						
SUMMARY						
Groups	Count	Sum	Average	Variance		
LS	86	62.58818	0.727769	0.000424		
KLS	86	61.71328	0.717596	0.000372		
ANOVA						
Source of Variation	SS	df	MS	F	P-value	F crit
Between Groups	0.00445	1	0.00445	11.18839	0.001013	3.896742
Within Groups	0.067619	170	0.000398			
Total	0.072069	171				

Table 5.20. Difference of Computational cost achieved by LS and KLS

Table 5.20 shows that, the average of computational cost when LS is performed is 0.727769 while in a case of KLS segmentation, the average is 0.717596. Anova test shows the difference of average between these two groups by p-value: 0.001013.Since it is equal or less than 0.05, it is considered as significant difference.

Using the KLS hybrid algorithm, the results indicated that the proposed algorithm in skin cancer segmentation stage outperforms the commonly used algorithms of level set and Fuzzy c-means thresholding, in two cut off (sw=0, sw=1), in terms of accuracy.

5.4Feature Extraction and Selection

This step of thesis intends to rank the available extracted features by attention to their impact on skin cancer detection. As mentioned in section 4.3, 53 features have been extracted for 86 images.

The proposed "Smart IPSO-SVM" algorithm after 100 iterations had reported the selected features to the next step. The SVM type used is LIBSVM, this library is available at http://www.csie.ntu.edu.tw/~cjlin/libsvm.

The "Smart IPSO-SVM" algorithm introduced in section 4.5.1, and LIBSVM is used here as a common library for support vector machines. In this study, IPSO with 40 particles is chosen with c_1 and c_2 set to be 2.0. The threshold value for selecting a feature is set to be 0.5. In SVM, Radial basis function is considered as a kernel function. The 86 samples are divided into 3 sets as train, test, and validation. The first two sets are used by "Smart PSO-SVM", and the final Accuracy and F-score are obtained by detecting the validation sets. The experimental results of this section are reported in section 5.5 (together with classification results).

5.5 Classification

Here, the purpose is to classify the tumour to benign or melanoma. The selected subset of features using the proposed feature selection algorithm, "Smart IPSO-SVM", from previous stage is sent to classification stage. As Yashar et al,[256] proposed a new developed SVM ,SA-SVM, which has the higher accuracy than the traditional SVM, in

this thesis the SA-SVM is selected as a best candidate for the classification stage. The details of SA-SVM have been explained in section 4.5.2.1.

5.6 Results of Feature Selection and Classification

The results have been reported in two parts. In the first part, the Accuracy and F-score have been achieved by proposed algorithm, "Smart IPSO-SVM feature selection algorithm with SA-SVM classification" is experimented, and in the second part, the proposed algorithm is compared with 4 other algorithms.

5.6.1 Experimental Result by Smart IPSO-SVM Feature Selection Algorithm Followed By SA-SVM Classifier

Table 5.21 shows the average performance in each selected set of features to detect the melanoma by "the proposed feature selection algorithm followed by SA-SVM classifier". It should be noted that this results are achieved by the proposed "Smart IPSO-SVM" algorithm in 40 experiments.

	Accuracy	F-Score
Number of Observations	SA-SVM Classification with SFS-PSO-SVM Feature Selection	SA-SVM Classification with SFS-PSO-SVM Feature Selection
1	82.6299	0.8842
2	87.0455	0.9133
3	84.7944	0.9025
4	87.2294	0.9205
5	87.2294	0.9194
6	88.474	0.9273
7	87.1753	0.9167
8	87.1212	0.9142
9	86.1147	0.9086
10	84.9297	0.9041
11	86.039	0.9101
12	88.3036	0.9265
13	86.039	0.9088
14	88.5281	0.9285
15	88.5281	0.9285
16	84.8485	0.8986
17	88.3117	0.9255
18	86.0931	0.9097
19	87.3106	0.9199
20	87.2294	0.9184
21	88.4199	0.9255
22	86.0931	0.9104

23	88.1818	0.9264
24	86.0931	0.908
25	86.039	0.9101
26	87.1753	0.9136
27	88.4199	0.9264
28	85.4329	0.9077
29	88.4199	0.923
30	87.2294	0.9195
31	88.3658	0.9272
32	88.4091	0.923
33	87.2294	0.9181
34	87.0942	0.9156
35	88.2576	0.925
36	88.934	0.9294
37	88.3117	0.9251
38	87.1753	0.918
39	85.9578	0.9101
40	87.2294	0.9172

Table 5.21. Average performance of each set of features by proposed "Smart IPSO-SVM algorithm and SA-SVM classifier" for detecting the melanoma

Based on the results, average accuracy and F-score of "*the proposed approach"* are 87.0611 and 0.9395, respectively.

5.6.2 Comparison of the Proposed Algorithm with Different Algorithms

In this thesis to benchmark the proposed algorithm, different implementations and comparisons are performed.

- ***"SVM Classification without Feature Selection" & "SVM Classification with Sequential Feature Selection"***

In this section, it is intended to experiment that the use of feature selection algorithm increases the algorithm performance. For this purpose, firstly the SVM is trained with "original features" and compared the results with the SVM which has been trained by the subset of features obtained by "Sequential feature selection" algorithm. Table 5.22 shows the comparison of these two algorithms.

	Accuracy		F-score	
Number of Observations	SVM Classification without Feature Selection	SVM Classification with Sequential Feature Selection	SVM Classification without Feature Selection	SVM Classification with Sequential Feature Selection
1	81.3041	87.1591	0.875	0.9197
2	82.5457	85	0.8867	0.9074
3	81.3853	83.6851	0.8802	0.8959
4	80.276	87.1753	0.8654	0.9154
5	82.5	86.1147	0.8843	0.9109
6	79.6672	87.0942	0.8653	0.9122
7	81.2229	83.7662	0.8777	0.8961
8	81.5476	84.8485	0.8804	0.9024
9	83.2251	83.9015	0.8914	0.8999
10	79.1667	81.4935	0.8633	0.8785
11	82.5216	77.9221	0.8866	0.8566
12	79.1667	86.1472	0.8635	0.9106
13	81.3853	87.2511	0.8795	0.9168
14	82.5487	88.3658	0.8853	0.9256
15	82.5487	88.3658	0.8853	0.9256
16	81.3745	68.4794	0.8798	0.7563
17	81.2906	86.0931	0.8747	0.9077
18	81.2635	89.6104	0.8713	0.934
19	82.4269	86.1201	0.8809	0.9107
20	80.8523	87.1212	0.8728	0.914
21	82.6299	87.4188	0.8873	0.9185
22	80.211	87.2835	0.8694	0.9177
23	82.5487	84.7835	0.8854	0.9017
24	82.4838	82.5216	0.8822	0.8876
25	82.5108	79.1667	0.8846	0.8673
26	82.6299	87.1753	0.884	0.9161
27	81.3636	82.5216	0.8753	0.8858
28	81.4394	88.2305	0.8765	0.9256
29	81.9535	68.5335	0.8833	0.7563
30	81.4394	88.3658	0.8772	0.9236
31	80.322	88.4145	0.8699	0.9251
32	81.4665	72.0238	0.8795	0.7768
33	82.5108	83.631	0.8843	0.8924
34	82.6569	70.9253	0.8879	0.7694
35	79.1126	86.0931	0.8642	0.9097
36	75.5952	87.2835	0.8437	0.9197
37	83.6851	82.4675	0.8916	0.8833
38	81.4935	83.869	0.878	0.899
39	81.4394	84.8214	0.8774	0.9028
40	80.2273	85.9199	0.8683	0.9035

Table 5.22. Average performance of "SVM Classification without Feature Selection" and "SVM Classification with Sequential Feature Selection"

Based on the results, average accuracy and F-score of "*SVM Classification without Feature Selection"* are 81.3985 and 0.8775 and in "*SVM Classification with Sequential Feature Selection"* approach are 83.9291 and 0.8919 respectively. It is very obvious that using feature selection approaches can improve the result in compare with using the original data. The results would firmly confirm this hypothesis. For statistical evaluation between these two approaches, the pair t-test with a level of significance of α=0.05 is used, where the p value of t-test is 0.004 as shown in table 5.23.

t-Test: Paired Two Sample for Means		
	SVM Classification without Feature Selection	**SVM Classification with Sequential Feature Selection**
Mean	81.39847	83.9291
Variance	2.139318	28.62196
Observations	40	40
Pearson Correlation	-0.20956	
Hypothesized Mean Difference	0	
df	39	
t Stat	-2.74321	
P(T<=t) one-tail	0.004572	
t Critical one-tail	1.684875	
P(T<=t) two-tail	0.009144	
t Critical two-tail	2.022691	

Table 5.23. The T-test result between "SVM Classification without FS" and "SVM Classification with SFS"

These statistical tests show that the results achieved by these approaches are statistically different. Therefore, the *Sequential feature selection* is used since it has simpler structure and higher accuracy.

- ***"SVM Classification with Sequential Feature Selection" & "SA-SVM Classification with Sequential Feature Selection"***

In this section, the "SVM Classification with Sequential Feature Selection" & "SA-SVM Classification with Sequential Feature Selection" is compared to experience the performance of SA-SVM classification against SVM. The Sequential Feature Selection has been considered as a feature selection technique for both classifiers. Table 5.24 shows the comparison of these two algorithms.

	Accuracy		F-score	
Number of Observations	SVM Classification with Sequential Feature Selection	SA-SVM Classification with Sequential Feature Selection	SVM Classification with Sequential Feature Selection	SA-SVM Classification with Sequential Feature Selection
1	87.1591	87.2024	0.9197	0.9201
2	85	85.9848	0.9074	0.9134
3	83.6851	83.7662	0.8959	0.9006
4	87.1753	88.3658	0.9154	0.9263
5	86.1147	88.2197	0.9109	0.9264
6	87.0942	88.3117	0.9122	0.9253
7	83.7662	82.5	0.8961	0.8939
8	84.8485	82.6136	0.9024	0.8908
9	83.9015	83.8636	0.8999	0.9002
10	81.4935	82.5216	0.8785	0.8845
11	77.9221	82.5216	0.8566	0.8924
12	86.1472	87.7435	0.9106	0.9233
13	87.2511	84.8485	0.9168	0.9067
14	88.3658	89.5238	0.9256	0.9343
15	88.3658	89.5238	0.9256	0.9343
16	68.4794	81.3636	0.7563	0.8876
17	86.0931	87.2294	0.9077	0.9188
18	89.6104	87.2835	0.934	0.9202
19	86.1201	87.2781	0.9107	0.9201
20	87.1212	88.3117	0.914	0.9251
21	87.4188	87.2835	0.9185	0.9213
22	87.2835	87.2835	0.9177	0.9196
23	84.7835	82.5216	0.9017	0.8939
24	82.5216	86.6477	0.8876	0.9175
25	79.1667	81.3853	0.8673	0.8863
26	87.1753	88.2765	0.9161	0.9264
27	82.5216	87.1753	0.8858	0.9201
28	88.2305	87.1672	0.9256	0.9201
29	68.5335	81.3853	0.7563	0.8877
30	88.3658	87.1753	0.9236	0.9201
31	88.4145	87.1753	0.9251	0.9202
32	72.0238	82.5487	0.7768	0.8889
33	83.631	84.8864	0.8924	0.9056
34	70.9253	81.3853	0.7694	0.8876
35	86.0931	87.2727	0.9097	0.92
36	87.2835	86.2256	0.9197	0.9157
37	82.4675	87.1753	0.8833	0.9197
38	83.869	86.039	0.899	0.9134
39	84.8214	84.8214	0.9028	0.9036
40	85.9199	87.1212	0.9035	0.917

Table 5.24. Average performance of "SVM Classification without Feature Selection" and "SVM Classification with Sequential Feature Selection"

Based on the results, average accuracy and F-score of "*SVM Classification with Feature Selection"* are 83.9291 and 0.8919 and in "*SA-SVM Classification with Sequential Feature Selection"* approach are 85.7482 and 0.9112 respectively. The results show the better performance of SA-SVM versus SVM. The achieved results would firmly confirmed by the results achieved on the paper used as a reference, "Self-Advising SVM for Sleep Apnea Classification" by Yashar et al.[256]. Both the reference paper and the results show a same direction in performance of SVM and SA-SVM.

For statistical evaluation between these two approaches, the pair t-test is used with a level of significance of α=0.05, where the p value of t-test is 0.002.

t-Test: Paired Two Sample for Means		
	SVM Classification with Feature Selection	**SA-SVM Classification with Sequential Feature Selection**
Mean	83.9291025	85.748225
Variance	28.62195582	6.213365515
Observations	40	40
Pearson Correlation	0.764835891	
Hypothesized Mean Difference	0	
df	39	
t Stat	-3.028066611	
P(T<=t) one-tail	0.002174393	
t Critical one-tail	1.684875122	
P(T<=t) two-tail	0.004348785	
t Critical two-tail	2.02269092	

Table 5.25. The T-test result between "SVM Classification with Feature Selection" and "SA-SVM Classification with Sequential Feature Selection"

These statistical tests show that the results achieved by these approaches are statistically different. Therefore, the *SA-SVM* is used as a classifier of the algorithm because it helps to improve the performance.

- ***"SA-SVM Classification with Sequential Feature Selection" & "SA-SVM Classification with IPSO-SVM Feature Selection"***

In this section, it is going to compare the performance of two different feature selection algorithms, "Sequential Feature Selection "and "IPSO-SVM", which are followed by SA-SVM, separately. Table 5.26 shows the comparison of these two algorithms.

	Accuracy		F-score	
Number of Observations	SA-SVM Classification with Sequential Feature Selection	SA-SVM Classification with PSO-SVM Feature Selection	SA-SVM Classification with Sequential Feature Selection	SA-SVM Classification with PSO-SVM Feature Selection
1	87.2024	86.0931	0.9201	0.9098
2	85.9848	86.066	0.9134	0.9079
3	83.7662	87.2294	0.9006	0.9171
4	88.3658	86.931	0.9263	0.9111
5	88.2197	87.1753	0.9264	0.9157
6	88.3117	84.9567	0.9253	0.9027
7	82.5	88.3658	0.8939	0.9255
8	82.6136	87.1753	0.8908	0.917
9	83.8636	87.2294	0.9002	0.9148
10	82.5216	85.9307	0.8845	0.9066
11	82.5216	84.8674	0.8924	0.8987
12	87.7435	84.7944	0.9233	0.8962
13	84.8485	85.9578	0.9067	0.9039
14	89.5238	87.2294	0.9343	0.9173
15	89.5238	87.2294	0.9343	0.9173
16	81.3636	86.1147	0.8876	0.9104
17	87.2294	85.0325	0.9188	0.902
18	87.2835	87.3295	0.9202	0.9202
19	87.2781	82.5108	0.9201	0.8885
20	88.3117	87.2024	0.9251	0.9143
21	87.2835	87.0942	0.9213	0.914
22	87.2835	85.9199	0.9196	0.9059
23	82.5216	87.2294	0.8939	0.9178
24	86.6477	84.9567	0.9175	0.9036
25	81.3853	87.362	0.8863	0.918
26	88.2765	87.1753	0.9264	0.9161
27	87.1753	86.039	0.9201	0.9118
28	87.1672	88.934	0.9201	0.9309
29	81.3853	84.8485	0.8877	0.9003
30	87.1753	86.066	0.9201	0.908
31	87.1753	89.4481	0.9202	0.9291
32	82.5487	88.5227	0.8889	0.9285
33	84.8864	84.8674	0.9056	0.9004
34	81.3853	88.3658	0.8876	0.9272
35	87.2727	86.1472	0.92	0.9106
36	86.2256	86.0227	0.9157	0.9071
37	87.1753	85.0054	0.9197	0.902
38	86.039	88.3387	0.9134	0.9255
39	84.8214	87.1753	0.9036	0.914
40	87.1212	86.0931	0.917	0.9099

Table 5.26. Average performance of “SA-SVM Classification with Sequential Feature Selection” and “SA-SVM Classification with IPSO-SVM Feature Selection”

Based on the results, average accuracy and F-score of "*SA-SVM Classification with Sequential Feature Selection"* are 85.7482 and 0.9112 receptively and in "*SA-SVM Classification with IPSO-SVM Feature Selection"* approach are 86.5258 and 0.9119 respectively. The results show the better performance of "*SA-SVM with IPSO-SVM Feature Selection"*. For statistical evaluation between these two approaches, the pair t-test is used with a level of significance of α=0.05, where the p value of t-test is 0.05.

t-Test: Paired Two Sample for Means		
	SA-SVM Classification with Sequential Feature Selection	**SA-SVM Classification with PSO-SVM Feature Selection**
Mean	85.748225	86.52581
Variance	6.213365515	1.907148
Observations	40	40
Pearson Correlation	-0.116236369	
Hypothesized Mean Difference	0	
df	39	
t Stat	-1.646557024	
P(T<=t) one-tail	0.053842554	
t Critical one-tail	1.684875122	
P(T<=t) two-tail	0.107685107	
t Critical two-tail	2.02269092	

Table 5.27. The T-test result between "SA-SVM Classification with Sequential Feature Selection" and "SA-SVM Classification with IPSO-SVM Feature Selection"

Since, these statistical tests show that the results achieved by "*SA-SVM Classification with Sequential Feature Selection*" and "*SA-SVM Classification with IPSO-SVM Feature Selection*" are not statistically very different, it is intended to improve the performance of "*SA-SVM Classification with IPSO-SVM Feature Selection algorithm"* by proposing "*The proposed feature selection algorithm with SA-SVM classifier*". Then, it is compared with "*SA-SVM Classification with Sequential Feature Selection"* in next section to show the statistical difference appeared.

- ***"SA-SVM Classification with Sequential Feature Selection" & "SA-SVM Classification with IPSO-SVM Feature Selection"***

Since in previous section "*SA-SVM Classification with IPSO-SVM Feature Selection*" algorithm wasn't statistically different with the "*SA-SVM Classification with Sequential Feature Selection*" - as mentioned in previous section- it is going to improve its performance and accuracy by proposing the algorithm which has been described in section 4.5 and its results have been shown in section 5.5.1. In this section, the

performance of "SA-SVM Classification with Sequential Feature Selection" & the proposed algorithm of "SA-SVM Classification with Smart IPSO-SVM Feature Selection" are compared. Table 5.28 shows the comparison of these two algorithms.

	Accuracy		F-score	
Number of Observations	SA-SVM Classification with Sequential Feature Selection	SA-SVM Classification with SFS-PSO-SVM Feature Selection	SA-SVM Classification with Sequential Feature Selection	SA-SVM Classification with SFS-PSO-SVM Feature Selection
1	87.2024	82.6299	0.9201	0.8842
2	85.9848	87.0455	0.9134	0.9133
3	83.7662	84.7944	0.9006	0.9025
4	88.3658	87.2294	0.9263	0.9205
5	88.2197	87.2294	0.9264	0.9194
6	88.3117	88.474	0.9253	0.9273
7	82.5	87.1753	0.8939	0.9167
8	82.6136	87.1212	0.8908	0.9142
9	83.8636	86.1147	0.9002	0.9086
10	82.5216	84.9297	0.8845	0.9041
11	82.5216	86.039	0.8924	0.9101
12	87.7435	88.3036	0.9233	0.9265
13	84.8485	86.039	0.9067	0.9088
14	89.5238	88.5281	0.9343	0.9285
15	89.5238	88.5281	0.9343	0.9285
16	81.3636	84.8485	0.8876	0.8986
17	87.2294	88.3117	0.9188	0.9255
18	87.2835	86.0931	0.9202	0.9097
19	87.2781	87.3106	0.9201	0.9199
20	88.3117	87.2294	0.9251	0.9184
21	87.2835	88.4199	0.9213	0.9255
22	87.2835	86.0931	0.9196	0.9104
23	82.5216	88.1818	0.8939	0.9264
24	86.6477	86.0931	0.9175	0.908
25	81.3853	86.039	0.8863	0.9101
26	88.2765	87.1753	0.9264	0.9136
27	87.1753	88.4199	0.9201	0.9264
28	87.1672	85.4329	0.9201	0.9077
29	81.3853	88.4199	0.8877	0.923
30	87.1753	87.2294	0.9201	0.9195
31	87.1753	88.3658	0.9202	0.9272
32	82.5487	88.4091	0.8889	0.923
33	84.8864	87.2294	0.9056	0.9181
34	81.3853	87.0942	0.8876	0.9156
35	87.2727	88.2576	0.92	0.925
36	86.2256	88.934	0.9157	0.9294
37	87.1753	88.3117	0.9197	0.9251
38	86.039	87.1753	0.9134	0.918

39	84.8214	85.9578	0.9036	0.9101
40	87.1212	87.2294	0.917	0.9172

Table 5.28. Average performance of "SA-SVM Classification with Sequential Feature Selection" and "SA-SVM Classification with Smart IPSO-SVM Feature Selection"

Based on the results, average accuracy and F-score of "*SA-SVM Classification with Sequential Feature Selection"* are 85.7482 and 0.9112 and in "*SA-SVM Classification with Smart IPSO-SVM Feature Selection"* approach are 87.0611 and 0.9167 respectively. The results show the better performance of proposed algorithm of "*SA-SVM Classification with Smart IPSO-SVM Feature Selection"* than another algorithm. For statistical evaluation between these two approaches, the pair t-test is used with a level of significance of α=0.05, where the p value of t-test is 0.0009.

t-Test: Paired Two Sample for Means		
	SA-SVM Classification with Sequential Feature Selection	**SA-SVM Classification with SFS-PSO-SVM Feature Selection**
Mean	85.748225	87.06108
Variance	6.213365515	1.831366251
Observations	40	40
Pearson Correlation	0.282242507	
Hypothesized Mean Difference	0	
df	39	
t Stat	-3.350752558	
P(T<=t) one-tail	0.000899517	
t Critical one-tail	1.684875122	
P(T<=t) two-tail	0.001799033	
t Critical two-tail	2.02269092	

Table 5.29. The T-test result between "SA-SVM Classification with Sequential Feature Selection" and "SA-SVM Classification with Smart IPSO-SVM Feature Selection"

These statistical tests show that the results achieved by these approaches are statistically significance different. Therefore, according to achievement, the performance of the proposed algorithm is much better than the other compared algorithms.

5.7 Summary

This chapter reviewed the experimental results of proposed algorithms in different stages of skin cancer detection system. In pre-processing stage, the results show the better performance of Adaptive Median and Adaptive histogram Equalization among others. In segmentation stage, an algorithm is proposed based on K-mean and level set and the results compared with traditional Level set and Fuzzy c-means thresholding.

Four metrics of Border error, Similarity, Hammoude distance and Rms error were used for this purpose. The promoted results show the successful performance of proposed algorithm when compares to traditional level set segmentation method and Fuzzy c-means thresholding, in two cut off (sw=0, cut between the small and middle class, sw=1, cut between the middle and large class). To approve the improved results, ANOVA test has been applied for assurance. Additionally, the proposed algorithm can easily be retargeted to apply in other domains of interest. In next step, after extracting the different features of images, the proposed algorithm for feature selection (*Smart IPSO-SVM Feature Selection)* is performed to choose the best subset of features to feed the classification stage. In classification stage, the SA-SVM is compared with SVM and selected as a better classifier which has been used in this detection algorithm. This proposed algorithm is compared with 3 other algorithms and also the algorithm with no feature extraction. The experimental results show the better performance of proposed algorithm of "SA-SVM Classification with Smart IPSO-SVM Feature Selection" than the other algorithms. The average accuracy and F-score are estimated as 87.0611and 0.9167 respectively. The statistical evaluation using t-test also shows the superiority of proposed algorithm when compares with other algorithms employed in this thesis.

CHAPTER 6

SUMMARY AND FUTURE RESEARCH

6.1Introduction

During recent decades, the incident of malignant melanoma as the lethal form of skin cancer has been raised. This cancer can be cured successfully if it is detected in early stages. Therefore, this early diagnosis is an important factor to decrease the mortality rates. Although there are many developments in imaging technology like dermoscopy, this diagnosis suffers challenging subjectivity, especially in initial physicians' care that would be the primitive gateway of patients in dermatology community. Since the diagnosis of melanoma from benign is not an easy process in early stages, the dermatologist should be trained as an expert. Therefore, the computer-based diagnosis systems may be a beneficial tool for physicians with less experience. It can be useful to take the information achieved by computer into account for final and precise decision. For this purpose, physicians need a system to be more reliable and accurate than what it has been presented so far.

This thesis proposed creative and effective algorithms which can improve the performance of computer-aided diagnostic systems for melanoma detection. This chapter covers an overall review on this thesis with respect to the components of system, the proposed algorithms, contributions and experimental achievements. This chapter is finalized by pursuing the discussions on some directions for future work in the area.

6.2 Overall Review on This Thesis

An automatic detection system of melanoma includes several stages: image acquisition, image segmentation, feature extraction and selection, and classification.

In pre-processing stage, different comparisons were performed to select the suitable method for proposed algorithm. In order to dispossessing the noise, five noise removal filters were investigated. Gaussian, Median, Mean, Adaptive Median, Adaptive Wiener filters were compared in the noise removal part. The experimental results indicate that the Adaptive Median has better performance on skin cancer images. In the following of this step, three contrast enhancement techniques of "Histogram Equalization (HE) ","Adaptive Histogram Equalization (AHE) " and "Unsharp Masking (UM) "were compared. The experimental analysis show the better results when Adaptive Histogram Equalization (AHE) is applied. After enhancing the quality of an image in pre-processing stage, the algorithm is proposed to segment the skin image. In this proposed algorithm, the kmean algorithm is used as surface function or initial curve for level set algorithm. The level set algorithm starts evolving from this curve. This algorithm is compared with traditional Level set and Fuzzy c-means thresholding in two cut off (sw=0, cut between the small and middle class, sw=1, cut between the middle and large class). Four metrics of Border error, Similarity, Hammoude distance and Rms error are used for this purpose. The experimental results indicate the successful performance of proposed algorithm when compares to traditional level set and Fuzzy c-means thresholding algorithms. The proposed algorithm has less Border error, Hammoude distance and Rms error and more Similarity when compares with other mentioned algorithms. To determine the statistical difference of proposed algorithm with others, one-way analysis of variance (ANOVA) as a statistical inference is applied. Experimental results show the significant difference between KLS and TLS, while the mean values of "Border Error" and "Rms Error" show the significant difference between KLS and FCT (sw=0) and the other two metrics show although there are improvement, it is not significant. The mean values of third column show the significant difference between KLS and FCT (sw=1). On the other hand, the results show the reduction in computational cost. Increasing the performance and decreasing the computational cost would be considered as two beneficial contribution of segmentation section which can easily be retargeted to apply in other domains of interest. After separating the tumour from its background (skin) in segmentation stage, it is going to the next stage which is feature extraction.

In the studies related to skin cancer detection systems, many different features were used. One of the main disadvantages of previous works can be the few study on feature

selection algorithms. Another disadvantage is the lack of strong feature selection algorithms in most previous researches, and many of these studies did not provide enough information about their experimental settings and parameters. For adding the contribution to this area, after extracting 53 features from 86 images, the "Smart IPSO-SVM" feature selection algorithm is proposed to choose the best subset of features to feed the classification stage. In this algorithm, IPSO include 40 particles in each population. In first population of IPSO, the first particle is initialized smartly using Sequential feature selection. The other particles are initialized randomly. The threshold value is set to 0.5. The weights more than this threshold are selected as a chosen features. To compute the fitness of each particle; SVM algorithm is trained by the training set and the selected features from the corresponding particle and the performance of the SVM on the test set with the corresponding feature set is considered as the fitness of that particle. The accuracy of each particle is compared with other particles to determine the best fitness. The best accuracy in a population is considered as "gbest" and the best accuracy in the history of that particle is "pbest". The particles in next populations are generated according to the velocity and particles' position which the formulas have been described in 4.4.2. After generating the next population the same process happens. Apparently, in the first population "pbest" and "gbest" are same. By reaching to 100th iteration the process is stopped and the obtained "pbest" with its corresponding features is considered as best solution candidate. The best selected subset of features is sent to classifiers to find out whether it is melanoma or not.

Most of researchers in skin cancer detection systems have used the SVM as a classifier in their studies. One of the main disadvantages of previous works can be the lack of study on SA-SVM which is a new and developed classifier. For adding another contribution to this area, the SA-SVM is selected as classifier in classification stage. This classifier generates further information from misclassified data in training phase. The details have been explained in section 4.5.2.1. However, it is compared with SVM in the study as well and the results confirm the better performance of this classifier versus SVM in skin cancer detection system.

The proposed "Smart IPSO-SVM feature selection algorithm with SA-SVM classifier" is compared with 4 other algorithms including, "Sequential feature selection with SVM classifier", "Sequential feature selection with SA-SVM classification",

"IPSO-SVM feature selection with SA-SVM classification" and when there is no feature selection in the algorithm. The results compared according to the average of Accuracy and F-score in 100 iterations with 40 particles. For statistical analysis of the proposed algorithm, t-Test is performed in 40 observations to determine whether the results are statistically different or not. The average accuracy and F-score are estimated as 87.0611and 0.9167 respectively. The statistical evaluation using t-test also shows the superiority of proposed algorithm when compares with other algorithms in this thesis.

To sum up, the objective of this thesis to investigate and experiment the different steps of detection system has been achieved completely and the other objective to propose an algorithm for classifying the lesion as malignant or benign satisfied successfully.

6.3 Directions for Future Work

This research indicated new ideas and approaches to address the key components in a computer-based system for diagnosis of melanoma. Now, various possible directions which may be pursued for further advance of this study are drawn.

To develop a reliable real-world computer-based diagnosis system of skin cancer, it is required to test the system rigorously with a large number of images in different conditions, for example on thousands of lesions from people. This would entail a well-organised take parting of different medical institutions. This system has to meet the necessity of (i) expert gainers, like dermatologists who are demanding a second opinion for their clinical diagnosis on the given lesion (ii) non-expert gainers, like general practitioners who are demanding to amend their diagnosis accuracy to have more confidence. This system may be designed to be considered as a training tool for medical students as well. The final purpose is to make people able to do primitive analysis on their skin and based on the results taken would pursue a medical doctor for advice and treatment. This will save the time and cost and earlier diagnosis.

It could be beneficial to provide a large dataset include different images of the same lesion. These similar images can be taken from different imaging modalities such as ultra sound, dermoscopy and etc. to consider the various aspect of lesion. This can appeal the different information about the same tumour such as depth of lesion, or surface of the lesion and other criteria. Thus, the acquired information would be useful

to estimate and predict more accurately. On the other hand, in some cases the sequential images taken in a period of time would be a good option for detection.

Further research on the line of this thesis may be done by going through different segmentation methods for improving the traditional ones and make them more consistent with the skin cancer images in diagnosis systems. Moreover, the SA-SVM as a new developed classification technique is capable to be investigated and improved. Also, it can be feed with other advance techniques in feature extraction to improve its accuracy. Finally, another contribution in the area can be the investigation on pathologist images with the same or improved algorithms. The hybrid segmentation algorithms maybe applied on pathologist images to improve the segmentation results.

6.4Limitation of the Study

Although the current thesis generate great findings in the area, it can be confirmed that the present research have the capability to be improved more in respect to solving the limitations. A limitation of this research it just used digital camera skin image and did not used pathologist images or other type of images. Based on using digital images, the research had not considered the depth of the melanoma and just used two dimension images. The propose system also did not consider a set of continue capturing images, it was limited to individual image testing.

The proposed system is applicable in the specific area of skin cancer detection and can be modified to be used in other similar systems.

REFERENCES

1. American cancer society, cancer facts and figures 2010. Available at: http://www.cancer.org/Research/CancerFactsFigures/CancerFactsFigures/cancer-facts-and-figures-2010.
2. Australia skin cancer facts and figures. Available at: http://www.cancer.org.au/cancersmartlifestyle/SunSmart/Skincancerfactsandfigures.htm .
3. Australia skin cancer facts and figures. Available at: http://www.cancer.org.au/Healthprofessionals/cancertypes/melanoma.htm.
4. A. C. Geller, S. M. Swetter, K. Brooks, M. Demierre, and A. L. Yaroch. Screening, early detection, and trends for melanoma: Current status (2000-2006) and future directions. Journal of the American Academy of Dermatology, 57:555–572, 2007.
5. R. P. Braun, L. E. French, and J. H. Saurat. Dermoscopy of pigmented lesions: a valuable tool in the diagnosis of melanoma. Swiss Medical Weekly, 134:83–90, 2004.
6. C. M. Balch, A. C. Buzaid, S. J. Soong, N. Cascinelli M. B. Atkins, D. G. Coit, I. D. Fleming, J. E. Gershenwald, A. J. Houghton, J. M. Kirkwood, K. M. McMasters, M. F. Mihm, D. L. Morton, D. S. Reintgen, M. I. Ross, A. Sober, J. A. Thompson, and J. F. Thompson. Final version of the american joint committee on cancer staging system for cutaneous melanoma. Journal of Clinical Oncology, 19:3635–3648, 2001.
7. C. M. Balch, S. J. Soong, J. E. Gershenwald, J. F. Thompson, D. S. Reintgen, and N. Cascinelli et al. Prognostic factors analysis of 17,600 melanoma patients: validation of the american joint committee on cancer melanoma staging system. Journal of Clinical Oncology, 19:3622–3634, 2001.
8. R. Braun, H. Rabinovitz, M. Oliviero, A. Kopf, and J. Saurat. Dermoscopy of pigmented lesions. Journal of the American Academy of Dermatology, 52(1):109– 121, 2005.
9. I. Maglogiannis and C. Doukas. Overview of advanced computer vision systems for skin lesions characterisation. IEEE Transaction on Information Technology in Biomedicine, 13(5):721–733, 2009.
10. R. J. Pariser and D. M. Pariser. Primary care physicians' errors in handling cutaneous disorders: A prospective survey. Journal of the American Academy of Dermatology, 17:239–245, 1987.
11. H. Pehamberger, A. Steiner, and K. Wolff. In vivo epiluminescence microscopy of pigmented skin lesions. I: Pattern analysis of pigmented skin lesions. Journal of the American Academy of Dermatology, 17:571–583, 1987.
12. S. W. Menzies, C. Ingvar, and W. H. McCarthy. A sensitivity and specificity analysis of the surface microscopy features of invasive melanoma. Melanoma Research, 6(1):55–62, February 1996.
13. J. Henning, S. Dusza, S.Wang, A. Marghoob, H. Rabinovitz, D. Polsky, and A. Kopf. The CASH (colour, architecture, symmetry, and homogeneity) algorithm for dermoscopy. Journal of the American Academy of Dermatology, 56(1):45–52, 2007.
14. W. Stolz, A. Riemann, A. B. Cognetta, L. Pillet, W. Abmayr, D. Holzel, P. Bilek, F. Nachbar, M. Landthaler, and O. Braun-Falco. ABCD rule of dermatoscopy: A new practical method for early recognition of malignant melanoma. European Journal of Dermatology, 4:521–527, 1994.

15. G. Argenziano, G. Fabbrocini, P. Carli, V. De Giorgi, E. Sammarco, and M. Delfino. Epiluminescence microscopy for the diagnosis of doubtful melanocytic skin lesions: Comparison of the ABCD rule of dermatoscopy and a new 7-point checklist based on pattern analysis. Archives of Dermatology, 134:1563–1570, 1998.
16. G. Argenziano, H. P. Soyer, S. Chimenti, R. Talamini, R. Corona, F. Sera, M. Binder, L. Cerroni, G. De Rosa, G. Ferrara, R. Hofmann-Wellenhof, M. Landthaler, S. W. Menzies, H. Pehamberger, D. Piccolo, H. S. Rabinovitz, R. Schiffner, S. Staibano, W. Stolz, I. Bartenjev, A. Blum, R. Braun, H. Cabo, P. Carli, V. De Giorgi, M. G. Fleming, J. M. Grichnik, C. M. Grin, A. C. Halpern, R. Johr, B. Katz, R. O. Kenet, H. Kittler, J. Kreusch, J. Malvehy, G. Mazzocchetti, M. Oliviero, F. Ozdemir, K. Peris, R. Perotti, A. Perusquia, M. A. Pizzichetta, S. Puig, B. Rao, P. Rubegni, T. Saida, M. Scalvenzi, S. Seidenari, I. Stanganelli, M. Tanaka, K. Westerhoff, I. H. Wolf, O. Braun-Falco, H. Kerl, T. Nishikawa, K.Wolff, and A.W. Kopf. Dermoscopy of pigmented skin lesions: Results of a consensus meeting via the Internet. Journal of the American Academy of Dermatology, 48:679–693, 2003.
17. W. Stolz, O. Braun-Falco, P. Bilek, M. Landthaler, W. H. C. Burgdorf, and A. B. Cognetta. colour Atlas of Dermatoscopy, volume 1. Blackwell, Berlin, 2 edition, March 2002.
18. http://www.google.com.au/url?sa=t&rct=j&q=&esrc=s&frm=1&source=web&cd=5&cad=rja&uact=8&ved=0CEQQFjAE&url=http%3A%2F%2Fwww.cancer.gov%2Fcancertopics%2Fwyntk%2Fskin.pdf&ei=JDpNU62GLc2kkQXLp4HgAw&usg=AFQjCNFtArZpRpoADXrrU5BK4l3YeZpOmA&bvm=bv.64764171,d.dGI.
19. American Cancer Society. Cancer Facts & Figures 2013, in: Annual Report. (Atlanta, GA: American Cancer society) (2013). Available from: http://www.cancer.org/acs/groups/content/@epidemiologysurveilance/documents/document/acspc-036845.pdf.
20. Skin Cancer: Basal and Squamous Cell. www.cancer.org.
21. Arul N, Cho YY," A Rising Cancer Prevention Target of RSK2 in Human Skin Cancer", 2013 Aug 5; 3:201. doi: 10.3389/fonc.2013.00201. eCollection 2013.
22. American Cancer Society. Skin Cancer Prevention and Early Detection, in: Annual Report. (Atlanta, GA: American Cancer society) (2013). Available from: http://www.cancer.org/cancer/cancercauses/sunanduvexposure/skincancerpreventionandearlydetection/skin-cancer-prevention-and-early-detection-intro.
23. Caroline M Owen, Nicholas R Telfer, "Skin Cancer", Medicine, Volume 33, Issue 1, 1 January 2005, Pages 64-67.
24. Randy Gordon," Skin Cancer: An Overview of Epidemiology and Risk Factors", Seminars in Oncology Nursing, Vol 29, No 3 (August), 2013: pp 160-169.
25. Australian Institute of Health and Welfare 2010. Cancer in Australia 2010: An overview. Cancer Series No. 60. Cat. no. CAN 56. Canberra: AIHW. Retrieved from http://www.aihw.gov.au/publication-detail/?id=6442472459 on October 1, 2011
26. Australian Institute of Health and Welfare. Health system expenditures on cancer and other neoplasms in Australia 2000-2001. Health and Welfare Expenditure Series Number 22. Canberra: AIHW 2005.
27. Dhawan Ap, Dalessandro B, Patwardhan S,Mullani N," Multispectral optical imaging of skin-lesions for detection of malignant melanomas", Annual International Conference of Engineering in Medicine and Biology Society, EMBC, 2009.
28. Eggert Stockfleth, Ted Rosen, Steven Schumaak,"Managing Skin Cancer", Springer, 2010.
29. Ascierto P.A. , P.G.B.G., Early Diagnosis of MAlignant MElanoma: Proposal of a working formulation for the Management of Cutaneous Pigmented Lesions for the melanoma Coorperative Group. International Journal of Oncology, 2003. 22(6): p. 1209-1215.
30. Fleming, M.G., et al., Techniques for a structural analysis of dermatoscopic imagery. Computerized Medical Imaging and Graphics, 1998. 22(5): p. 375-389.

31. B.Salah, M.Alshraideh, R.Beidas and F.Hayajneh.” Skin Cancer Recognition by Using a Neuro-Fuzzy System”.2011.
32. A.N. Hoshyar, A.Al- Jumaily, R.Sulaiman.” Review on Automatic Early Skin Cancer Detection”, International Conference on Computer Science and Service System (CSSS), IEEE. 2011.
33. Nachbar, F.S., Wilhelm Merkle, Tanja Cognetta, Armand B. Vogt, Thomas Landthaler, Michael and P.B.-F. Bilek, Otto Plewig, Gerd, The ABCD rule of dermatoscopy: High prospective value in the diagnosis of doubtful melanocytic skin lesions. Journal of the American Academy of Dermatology, 1994. 30(4): p. 551-559.
34. G. Di Leo, A. Paolillo, P. Sommella, G. Fabbrocini, O. Rescigno,” A software tool for the diagnosis of melanomas, Automatic Implementation of the 7-Point Check List Method”, IEEE,2010.
35. Soyer HP, A.G., Zalaudek I, Corona R, Sera F, Talamini R, Barbato F, Baroni A, Cicale L, Di Stefani A, Farro P, Rossiello L, Ruocco E, Chimenti S, Three-Point Checklist of Dermoscopy. Dermatology, 2004. 208(1): p. 27-31.
36. Crowson, A.N., C.M. Magro, and M.C. Mihm, Prognosticators of melanoma, the melanoma report, and the sentinel lymph node. Modern Pathology, 2006. 19: p. S71-S87.
37. WH., C.J., A classification of malignant melanoma in man correlated with histogenesis and biological behaviour. . Advances in the Biology of the Skin, 1967. VIII: p. 621-647.
38. Clark Jr WH, From L, and B. EA., Histogenesis and biologic behavior of primary human malignant melanomas of the skin. Cancer Res, 1969. 29: p. 705-726.
39. Breslow, A., Thickness, cross-sectional areas and depth of invasion in the prognosis of cutaneous melanoma. Ann Surg, 1970. 172: p. 902-908.
40. Crowson, A., et al., The pathology of melanoma. Cutaneous Melanoma, 4th edn. Quality Medical Publishers Inc.: St Louis, 2003: p. 171-206.
41. M. Naresh Babu, Vamsi K. Madasu, M. Hanmandlu, S. Vasikarla,” Histo-pathological Image Analysis using OS-FCM and Level Sets”, 39th IEEE Applied Imagery Pattern Recognition Workshop (AIPR),2010.
42. A. Tabesh, M. Teverovskiy, H.-Y. Pang, V. Kumar, D. Verbel, A. Kotsianti, and O. Saidi. Multifeature prostate cancer diagnosis and gleason grading of histological images. IEEE Trans. Medical Imaging, 26(10):1366–78, 2007.
43. S. Park, D. Sargent, R. Lieberman, and U. Gustafsson. Domain-specific image analysis for cervical neoplasia detection based on conditional random fields. IEEE Trans. Medical Imaging, 30(3):867 –78, 2011.
44. A. Esgiar, R. Naguib, B. Sharif, M. Bennett, and A. Murray. Fractal analysis in the detection of colonic cancer images. IEEE Transaction on Information Technology in Biomedicine, 6(1):54–58, 2002.
45. A. Madabhushi. Digital pathology image analysis: opportunities and challenges. Imaging in Medicine, 1(1):7–10, 2009.
46. Rubin R, Strayer D, Rubin E, McDonald J. Rubin's pathology: clinicopathologic foundations of medicine. Lippincott Williams & Wilkins; 2007.
47. Weind KL, Maier CF, Rutt BK, Moussa M. Invasive carcinomas and fibroadenomas of the breast: comparison of microvessel distributions--implications for imaging modalities. Radiology. 1998 Aug; 208:477–83.
48. Bartels PH, Thompson D, Bibbo M, Weber JE. Bayesian belief networks in quantitative histopathology. Anal Quant Cytol Histol. 1992 Dec; 14:459–73.
49. Hamilton PW, Anderson N, Bartels PH, Thompson D. Expert system support using Bayesian belief networks in the diagnosis of fine needle aspiration biopsy specimens of the breast. J Clin Pathol. 1994 Apr; 47:329–36.
50. http://dermnetnz.org/lesions/melanoma.html.
51. Phillip H. McKee and Eduardo Calonje, “Diagnostic Atlas of Melanocytic Pathology”, Elsevier, UK, 2009.

52. Clark, W.H. and M.C. Mihm, Lentigo maligna and lentigo maligna melanoma. Am J Pathol, 1969. 55: p. 39-54.
53. Reed, R.J., Acral lentiginous melanoma. In: New Concepts in Surgical Pathology of the Skin. Wiley: New York, 1976: p. 89-90.
54. Clark Jr WH, D.E. Elder, and D. Guerry, Model predicting survival in stage I melanoma based on tumor progression. Natl Cancer Inst, 1989. 81: p. 1893-1904.
55. Koh, H.K., E. Michalik, and A.J. Sober, Lentigo maligna melanoma has no better prognosis than other types of melanoma.blogsome.com. J Clin Oncol 1984. 2: p. 994-1001.
56. Vollmer, R.T., Malignant melanoma. A multivariate analysis of prognostic factors. . Pathol Annu, 1989. 24: p. 383-407.
57. Barnhill, R.L., J.A. Fine, and G.C. Roush, Predicting fiveyear outcome for patients with cutaneous melanoma in a population-based study. Cancer. Cancer, 1996. 78: p. 427-432.
58. Balch, C.M., T.M. Murad, and S.J. Soong, A multlifactorial analysis of melanoma: prognostic histopathological features comparing Clark's and Breslow's staging methods. . Ann Surg, 1978. 188: p. 732-742.
59. Balch, C.M., S.J. Soong, and T.M. Murad, A multifactorial analysis of melanoma. II. Prognostic factors in patients with stage I (localized) melanoma. . Surgery, 1979. 86: p. 343-351.
60. Cascinelli, N., A. Morabito, and R. Bufalino, Prognosis of stage I melanoma of the skin. Int J Cancer, 1980. 26: p. 733-739.
61. Sondergaard, K. and G. Schou, Survival with primary cutaneous malignant melanoma, evaluated from 2012 cases. A multivariate regression analysis. . Virchows Arch A Pathol Anat Histopathol, 1985. 406: p. 179-195.
62. Rigel, D.S., R.J. Friedman, and A.W. Kopf, Factors influencing survival in melanoma. . Dermatol Clin, 1991. 9: p. 631-642.
63. Stidham, K.R., J.L. Johnson, and H.F. Seigler, Survival superiority of females with melanoma. A multivariate analysis of 6383 patients exploring the significance of gender in prognostic outcome. . Arch Surg, 1994. 129: p. 316-324.
64. Garbe, C., P. Buttner, and J. Bertz, Primary cutaneous melanoma. Identification of prognostic groups and estimation of individual prognosis for 5093 patients. Cancer 1995. 75: p. 2484-2491.
65. Balch, C.M., S. Soong, and M.I. Ross, Long-term results of a multi-institutional randomized trial comparing prognostic factors and surgical results for intermediate thickness melanomas (1.0 to 4.0 mm). . Intergroup Melanoma Surgical Trial. Ann Surg Oncol, 2000. 7: p. 87-97.
66. Retsas, S., K. Henry, and M.Q. Mohammed, Prognostic factors of cutaneous melanoma and a new staging system proposed by the American Joint Committee on Cancer (AJCC): validation in a cohort of 1284 patients. Eur J Cancer, 2002. 38: p. 511-516.
67. Jade Homsi, MD, Mohammed Kashani-Sabet, MD, Jane L. Messina, MD, Adil Daud, MD," Cutaneous Melanoma: Prognostic Factors", Cancer Control: Journal of the Moffitt Cancer Center.
68. Day CL Jr, Harrist TJ, Gorstein F, et al. Malignant melanoma. Prognostic significance of "microscopic satellites" in the reticular dermis and subcutaneous fat. Ann Surg. 1981;194:108-112.
69. Leon, P., J.M. Daly, and M. Synnestvedt, The prognostic implications of microscopic satellites in patients with clinical stage I melanoma. . Arch Surg, 1991. 126: p. 1461-1468.
70. Rao, U.N., J. Ibrahim, and L.E. Flaherty, Implications of microscopic satellites of the primary and extracapsular lymph node spread in patients with high-risk melanoma: pathology corollary of Eastern Cooperative Oncology Group Trial E1690. J Clin Oncol, 2002. 20: p. 2053-2057.
71. http://www.uptodate.com/contents/pathologic-characteristics-of-melanoma.

72. R. Marks, “Epidemiology of melanoma”, Clin. Exp. Dermatology, Vol. 25, pp. 459-463, 2000.
73. U. Leiter, P. G. Buttner et alii, “Prognostic factors of thin cutaneous melanoma: an analysis of the central malignant melanoma registry of the German Dermatological Society”, Journal of Clinical Oncology, Vol. 22, pp. 3660-3667, 2004.
74. Fikret Ercal, Anurag Chawla, William V. Stoecker, Hsi-Chieh Lee, and Randy H. Moss.” Neural Network Diagnosis of Malignant Melanoma From Color Images”, IEEE Transactions on Biomedical Engineering. Vol. 41, No. 9,1994.
75. I.M. Ariel, "Malignant Melanoma", Appleton- Century-Crofts, New York, 1981.
76. A.J. Sober, "Diagnosis and management of skin-cancer", Cancer, vol. 51, pp. 2448-2452, 1983.
77. Hall, P.N., E. Claridge, and J.D.M. Smith, Computer screening for early detection of melanoma—is there a future? British Journal of Dermatology, 1995. 132(3): p. 325-338.
78. Rajpara, S.M., et al., Systematic review of dermoscopy and digital dermoscopy/ artificial intelligence for the diagnosis of melanoma. British Journal of Dermatology, 2009. 161(3): p. 591-604.
79. Rosado B, M.S., Harbauer A et al., Accuracy of computer diagnosis of melanoma: a quantitative meta-analysis. Archives of Dermatology, 2003. 139: p. 361-367.
80. Bauer, P.C., P. Boi, S. Burroni, M. Dell'Eva, G. Micciolo, R. Cristofolini, M., Digital epiluminescence microscopy: usefulness in the differential diagnosis of cutaneous pigmentary lesions. A statistical comparison between visual and computer inspection. Melanoma Research, 2000. 10(4): p. 345-349.
81. Friedman Rj, G.-K.D.F.M.J. and et al., THe diagnostic performance of expert dermoscopists vs a computer-vision system on small-diameter melanomas. Archives of Dermatology, 2008. 144(4): p. 476-482.
82. Blum, A., I. Zalaudek, and G. Argenziano, Digital Image Analysis for Diagnosis of Skin Tumors. Seminars in Cutaneous Medicine and Surgery, 2008. 27(1): p. 11-15.
83. Joaquim Mesquita da Cunha Viana,” Classification of Skin Tumours through the Analysis of Unconstrained Images”, De Montfort University Leicester, UK, 2008.
84. S.S. Al-amri, N.V. Kalyankar, and S.D. Khamitkar, “Linear and Non-linear Contrast Enhancement Image”, IJCSNS International Journal of Computer Science and Network Security, VOL.10 No.2, pp. 139, February 2010.
85. S.S. Agaian, K.P. Lentz, and A.M. Grigoryan, “A New Measure of Image Enhancement”, International Conference on Signal Processing & Communication, 2000.
86. L. Reginald, L. Lagendijk, and J. Biemond, “Basic Methods for Image Restoration and Identification”, International Conference on Image and Graphics, 1999.
87. R.C. Gonzalez, and R.E. Woods, “Digital Image Processing”, 3rd Edn., Prentice- all, Inc., New Jersey, ISBN: 10: 013168728x, pp: 594, 2008.
88. M.J. Ogorzaáek, G. Surówka, L. Nowak, and C. Merkwirth, “New Approaches for Computer-Assisted Skin Cancer Diagnosis”, The Third International Symposium on Optimization and Systems Biology (OSB’09), China, 2009.
89. A. Chiem, A. Al-Jumaily , R.N. Khushaba,” A Novel Hybrid System for Skin Lesion Detection”, 3rd International Conference on Intelligent Sensors, Sensor Networks and Information, ISSNIP, 2007.
90. Ho Tak Lau, Adel Al-Jumaily,” Automatically Early Detection of Skin Cancer: Study Based on Nueral Netwok Classification”, International Conference of Soft Computing and Pattern Recognition, 2009.
91. Lindelöf B, Hedblad M-A. Accuracy in the clinical diagnosis and pattern of malignant melanoma at a dermatological clinic. The Journal of Dermatology. 1994;21(7):461–464.[PubMed].
92. Morton CA, Mackie RM. Clinical accuracy of the diagnosis of cutaneous malignant melanoma. British Journal of Dermatology. 1998;138(2):283–287. [PubMed].

93. Argenziano G, Soyer HP. Dermoscopy of pigmented skin lesions—a valuable tool for early diagnosis of melanoma. *The Lancet Oncology*. 2001;2(7):443–449. [PubMed].
94. Menzies SW, Bischof L, Talbot H, et al. The performance of SolarScan: an automated dermoscopy image analysis instrument for the diagnosis of primary melanoma. *Archives of Dermatology*. 2005;141(11):1388–1396. [PubMed].
95. Binder M, Schwarz M, Winkler A, et al. Epiluminescence microscopy: a useful tool for the diagnosis of pigmented skin lesions for formally trained dermatologists. *Archives of Dermatology*. 1995;131(3):286–291.
96. Pehamberger H, Binder M, Steiner A, Wolff K. *In vivo* epiluminescence microscopy: improvement of early diagnosis of melanoma. *Journal of Investigative Dermatology*.1993; 100(3).
97. Dhawan AP, Gordon R, Rangayyan RM. Nevoscopy: three-dimensional computed tomography of nevi and melanomas in situ by transillumination. *IEEE Transactions on Medical Imaging*. 1984;3(2):54–61.
98. Zouridakis G, Duvic MDM, Mullani NA. 2005. Houston, Tex, USA: Biomedical Imaging Lab, Department of Computer Science, University of Houston; Transillumination imaging for early skin cancer detection.
99. C.Demir and B.Yener," Automated cancer diagnosis based on histopathological images: a systematic survey", Technical Report, Rensselaer Polytechnic Institute, Department Of Computer Science, TR-05-09.
100. D.N.Ponraj, M.E.Jenifer, P.Poongodi, J.S.Manoharan," A Survey on the Preprocessing Techniques of Mammogram for the Detection of Breast Cancer", Journal of Emerging Trends in Computing and Information Sciences, VOL. 2, NO. 12, December 2011.
101. S. Alina, C. Mihai Ciuc, T. Radulescu, L. Wanyu, D.Petrache, "Preliminary Work on Dermatoscopic Lesion Segmentation," 20th European Signal Processing Conference (EUSIPCO 2012)".
102. D. Chang, W. Wu, "Image Contrast Enhancement Based on a Histogram Transformation of Local Standard Deviation", IEEE Transactions on Medical Imaging, Vol. 17, No. 4, 1998.
103. R.Garnavi, M.Aldeen, M.E.Celebi, A.Bhuiyan, C.Dolianitis, and G.Varigos,"Automatic Segmentation of Dermoscopy Images Using Histogram Thresholding on Optimal Color Channels", International Journal of Biological and Life Sciences, 2012.
104. K. N. Plataniotis and A. N. Venetsanopoulos, Color Image Processing and Applications. Springer, 2000.
105. G.Wyszecki, WS.Stiles: Color Science: Concepts and Methods, Quantitative Data and Formulae. New York: John Wiley and Sons, 1982.
106. Dr. J. Abdul Jaleel, Sibi Salim, Aswin.R.B," Artificial Neural Network Based Detection of Skin Cancer", International Journal of Advanced Research in Electrical, Electronics and Instrumentation Engineering, 2012.
107. R.D. Fiete," Modeling the Imaging Chain of Digital Cameras ", Image Enhancement Processing book, SPIE Digital Library, Chapter 9, 35 pages,2010.
108. J.Lu," Contrast Enhancement of Medical images using Multiscale Edge Representation", Optical Enineering, 2012.
109. K. Madhankuma, and P. Kumar, "Characterization of Skin Lesions", Proceedings of the International Conference on Pattern Recognition, Informatics and Medical Engineering , March 21-23, 2012.
110. K.A. Norton, H. Iyatomi, M. Emre Celebi, G. Schaefer, M. Tanaka, and K. Ogawa, "Development of a Novel Border Detection Method for Melanocytic and Non-Melanocytic Dermoscopy Images", 32nd Annual International Conference of the IEEE EMBS Buenos Aires, Argentina, 2010.
111. D.H. Chung, G. and Sapiro, "Segmenting Skin Lesions with Partial-Differential-Equations-Based Image Processing Algorithms", IEEE Transactions on Medical Imaging, Vol. 19, No. 7, 2000.

112. P.Patida , M.Gupta , S.Srivastava , A. K.Nagawa ,"Image De-noising by Various Filters for Different Noise", International Journal of Computer Applications (0975 – 8887) Volume 9– No.4, November 2010.
113. N. Radhika, T. Antony,"Image Denoising Techniques Preserving Edge", ACEEE Int. J. on Information Technology, Vol. 01, No. 02, Sep 2011.
114. MC. Motwani, M.C. Gadiya, R. C. Motwani, Jr .Harris," Survey of Image Denoising Techniques", Proceedings of GSPX, Citeseer, 2004.
115. D.H. Rao, P.P. Panduranga, ," A Survey on Image Enhancement Techniques: Classical Spatial Filter, Neural Network, Cellular Neural Network, and Fuzzy Filter", IEEE International Conference on Industrial Technology, 2006.
116. B.Shinde, D.Mhaske, M.Patare, A.R. Dani," Apply Different Filtering Techniques to Remove the Speckle Noise Using Medical Imag es",International Journal of Engineering Research and Applications (IJERA), Vol. 2, Issue 1,Jan-Feb 2012.
117. L.Hargaš, M.Hrianka, A.Duga," Noise Image Restoration By Spatial Filters", Department of Electronics and Electrotechnology ,University of Žilina, Slovaki, 2007. http://www.urel.feec.vutbr.cz/ra2007/archive/ra2003/papers/376.pdf.
118. H.R. Myler, A.R.Weeks," The pocket of handbook of image processing Algorithms in C", Department of Electical and Computer Engineering"University of Central Florida, Orlando, Florida, 1993.
119. A.K. Kanithi,"Study of Spatial and Transform Domain Filters for Efficient Noise Reduction", Department of Electronics and Communication Engineering, National Institute of Technology, Rourkela, India, 2011.
120. N.Bhoi," Spatial-Domain and Transform-Domain Digital Image Filters", Department of Electronics and Communication Engineering National Institute of Technology, Rourkela, India, 2009.
121. S. Sookpotharom," Border Detection of Skin Lesion Images Based on Fuzzy C-Means Thresholding", 3rd International Conference on Genetic and Evolutionary Computing, 2009.
122. D. Ruiz, Member, IEEE, V.J. Berenguer, A. Soriano, J. Martin," A cooperative approach for the diagnosis of the melanom", 30th Annual International IEEE EMBS Conference Vancouver, British Columbia, Canada, 2008.
123. M.Nourmohamadi, H.Pourghassem," Dermoscopy Image Segmentation Using a Modified Level Set Algorithm", Fourth International Conference on Computational Intelligence and Communication Network, 2012.
124. Y.Chen, J.Hua,"Image Restoration Algorithm Research on Local Motion-blu", Information Engineering and Electronic Business", 3, 23-2, 2011.
125. C.Khare, K.Kumar Nagwanshi," Implementation and Analysis of Image Restoration Techniques", International Journal of Computer Trends and Technology- May to June Issue 2011.
126. I. Aizenberg, C. Butakoff, V. Karnaukhov, N. Merzlyakov, and O.Milukova, "Blurred image restoration using the type of blur and blur parameters identification on the neural network," SPIE Proc.,vol. 4667, Image Processing: Algorithms and Systems, pp. 460–471, 2002.
127. J. M. Blackledgey and D. A.Dubovitskiyz," Texture Classification using Fractal Geometry for the Diagnosis of Skin Cancers", EG UK Theory and Practice of Computer Graphics, pp. 1–8, 2009.
128. M.K. Mahmoud, A. Al-Jumaily, A. "Segmentation of skin cancer images based on gradient vector flow (GVF) snake", International Conference on Mechatronics and Automation, 2011.
129. M. S. Ahmed, K. K. Tahbou," Recursive Wiener Filtering for Image Restoration", IEEE Transactions on acoustics, Speech, and Signal Processing, vol. asp -34, No. 4, 1986.
130. Z.Zhang, W.V. Stoecker, and R.H. Moss," Border Detection on Digitized Skin Tumor Images",IEEE Transaction Medical Imaging, 19(11): 1128–1143,2000.

131. M. Fiorese, E. Peserico, A. Silletti," VirtualShave: automated hair removal from digital dermatoscopic images", 33rd Annual International Conference of the IEEE EMBS Boston, Massachusetts USA, 2011.
132. P. Schmid, "Segmentation of digitized dermatoscopic images by two-dimensional color clustering", IEEE Trans Medical Imaging, 1999.
133. H. Zhou, M. Chen, R. Gass, J. M. Rehg, L. Ferris, J. Ho and L. Drogowski, "Feature Preserving Artifact Removal from Dermoscopy Images", Proc. of SPIE Medical Imaging: Image Processing, vol. 6914, 46, 2008.
134. Lee T, Ng V, Gallagher R, Coldman A, McLean D. DullRazor: A software approach to hair removal from images. Computers in Biology and Medicine 1997;27: 533-543.
135. M. E. Celebi, H. Iyatomi, G. Schaefer, and W. V. Stoecker. Lesion border detection in dermoscopy images. Computerised Medical Imaging and Graphics, 33(2):148–153, 2009.
136. H. Iyatomi, H. Oka, M. Saito, A. Miyake, M. Kimoto, J. Yamagami, S. Kobayashi, A. Tanikawa, M. Hagiwara, K. Ogawa, G. Argenziano, H. P. Soyer, and M. Tanaka. Quantitative assessment of tumour extraction from dermoscopy images and evaluation of computer-based extraction methods for an automatic melanoma diagnostic system. Melanoma Research, 16(2):183–190, 2006.
137. T. K. Lee, V. Ng, D. McLean, A. Coldman, R. Gallagherand, and J. Sale. A multi-stage segmentation method for images of skin lesions. In IEEE Pacific Rim Conference on Communications, Computers, and Signal Processing, pages 602–605, 1995.
138. M. Hintz-Madsen, L. K. Hansen, J. Larsen, and K. Drzewiecki. A probabilistic neural network framework for detection of malignant melanoma. In Artificial Neural Networks in Cancer Diagnosis, Prognosis and Patient Management, pages 141–183.CRC Press, 2001.
139. A. Sbonera, E. Blanzieria, C. Ecchera, P. Bauerb, M. Cristofolinib, G. Zumianib, and S. Fortia. A knowledge based system for early melanoma diagnosis support. In Proceedings of the 6th Intelligent Data Analysis in Medicine and Pharmacology (IDAMAP) Workshop, 2001.
140. A. J. Round, A. W. Duller, and P.J. Fish. Colour segmentation for lesion classification. In 19th International Conference - IEEE/EMBS, pages 582–585, 1997.
141. J. Gao, J. Zhang, and M. G. Fleming. Segmentation of dermatoscopic images by stabilised inverse diffusion equations. In IEEE International Conference on Image Processing (ICIP 1998), volume 3, pages 823–827, 1998.
142. E. Zagrouba and W. Barhoumi. A preliminary approach for the automated recognition of malignant melanoma. Image Analysis and Stereology Journal, 23:121–135,2004.
143. E. Zagrouba and W. Barhoumi. An accelerated system for melanoma diagnosis based on subset feature selection. Journal of Computing and Information Technology, 1:69–82, 2005.
144. M. E. Celebi, Y. A. Aslandogan, W. V. Stoecker, H. Iyatomi, H. Oka, and X. Chen. Unsupervised border detection in dermoscopy images. Skin Research and Technology,13: 454–462, 2007.
145. M. E. Celebi, H. A. Kingravi, H. Iyatomi, Y. A. Aslandogan, W. V. Stoecker, R. H. Moss, J. M. Malters, J. M. Grichnik, A. A. Marghoob, H. S. Rabinovitz, and S. W. Menzies. Border detection in dermoscopy images using statistical region merging. Skin Research and Technology, 14:347–353, 2008.
146. W. E. Denton, A. W. G Duller, and P. J. Fish. Boundary detection for skin lesions: an edge focusing algorithm. In 5th IEEE International Conference on Image Processing and its Applications, pages 399–403, 1995.
147. Y. V. Haeghen, J. M. Naeyaert, and I. Lemahieu. Development of a dermatological workstation: preliminary results on lesion segmentation in cie l*a*b* colour space. In International Conference on colour in Graphics and Image Processing, volume 1, pages 6572–6575, 2000.

148. B. Erkol, R. Moss, R. Stanley, W. Stoecker, and E. Hvatum. Automatic lesion boundary detection in dermoscopy images using gradient vector flow snakes. Skin Research and Technology, 11:17–26, 2005.
149. T. Mendonca, A. Marcal, A. Vieira, J. C. Nascimento, M. Silveira, J. S. Marques, and J. Rozeira. Comparison of segmentation methods for automatic diagnosis of dermoscopy images. In 29th IEEE EMBS Annual International Conference, volume 1,pages 6572–6575, 2007.
150. W. Stoecker, R. Moss, J. Stanley, X. Chen, K. Gupta, R. Narayana, B. Shrestha, and P. Jella. Automatic detection of critical dermoscopy features for malignant melanoma diagnosis, 2006. Patent Number: 11/421031, United States.
151. P. Schmid. Lesion detection in dermatoscopic images using anisotropic diffusion and morphological flooding. In IEEE International Conference on Image Processing (ICIP 1999), volume 3, pages 449–453, 1999.
152. G. A. Hance, S. E. Umbaugh, R. H. Moss, and W. V. Stoecker. Unsupervised colour image segmentation: With application to skin tumor borders. IEEE Engineering in Medicine and Biology Magazine, 15:104–111, 1996.
153. P. Schmid. Segmentation of digitised dermatoscopic images by two-dimensional colour clustering. IEEE Transactions on Medical Imaging, 18(2):164–171, 1999.
154. R. Cucchiara, C. Grana, S. Seidenari, and G. Pellacani. Exploiting colour and topological features for region segmentation with recursive fuzzy c-means. Machine Graphics and Vision, 11:169–182, 2002.
155. H. Galda, H. Murao, H. Tamaki, and S. Kitamura. Skin image segmentation using a self-organising map and genetic algorithms. Transactions of the Institute of Electrical Engineers of Japan-Part C, 123:2056–2062, 2002.
156. P. Schmid-Saugeon, J. Guillod, and J. P. Thiran. Towards a computer-aided diagnosis system for pigmented skin lesions. computerised Medical Imaging and Graphics, 27(2):69–72, January 2003.
157. R. Melli, C. Grana, and R. Cucchiara. Comparison of colour clustering algorithms for segmentation of dermatological images. In SPIE Medical Imaging, volume 6144, pages 3S1–3S9, 2006.
158. D. Delgado, C. Butakoff, B. K. Ersboll, and W. V. Stoecker. Independent histogram pursuit for segmentation of skin lesions. IEEE transactions on biomedical engineering, 55:157–161, 2008.
159. H. Zhou, M. Chen, L. Zou, R. Gass, L. Ferris, L. Drogowski, and J. M. Rehg. Spatially constrained segmentation of dermoscopy images. In 5th IEEE International Symposium on Biomedical Imaging, pages 800–803, 2008.
160. T. Donadey, C. Serruys, and A. Giron. Boundary detection of black skin tumors using an adaptive radial-based approach. In SPIE Medical Imaging, volume 3379, pages 810–6, 2000.
161. S. Na, L. Xumin, G. yong," Research on k-means Clustering Algorithm", Third International Symposium on Intelligent Information Technology and Security Informatics, 2010.
162. Guanglei Xiong, Xiaobo Zhou, and Liang Ji," Automated Segmentation of Drosophila RNAi Fluorescence Cellular Images Using Deformable Models", IEEE Transactions on Circuits and Systems, Vol.53, No.11, 2006.
163. Ng, H. P., Ong, S. H., et al, Medical Image Segmentation Using K-Means Clustering and Improved Watershed Algorithm. IEEE Southeast Symposium on Image Analysis and Interpretation, 61-5, 2006.
164. Vamsi K. Madasu & Brian C. Lovell," Blotch detection in pigmented skin lesions using Fuzzy Co-Clustering and Texture Segmentation", Digital Image Computing: Techniques and Applications, 2009.
165. Yefen Wu,Fengying Xie, Zhiguo Jiang, Rusong Meng," Automatic skin lesion segmentation based on supervised learning", Seventh International Conference on Image and Graphics, 2013.

166. Ammara Masood, Adel Ali Al Jumaily, Omama Masood," Automated Segmentation of Skin Lesions: Modified Fuzzy C mean Thresholding Based Level Set Method", 16th International Multi Topic Conference (INMIC), 2013.
167. Zhou H, Schaefer G, Sadka A, Celebi M. Anisotropic mean shift based fuzzy c- means segmentation of dermoscopy images. IEEE Journal of Selected Topics in Signal Processing 2009; 3(1): 26–34.
168. Mete M, Kockara S, Aydin K. Fast density-based lesion detection in dermoscopy images. Computerized Medical Imaging and Graphics 2011;35(2):128–36.
169. Liu Z, Sun J, Smith M, Smith L, Warr R. Unsupervised sub-segmentation for pigmented skin lesions. Skin Research and Technology 2012;18(2):77–87.
170. Friedman R, Rigel D, Kopf A. Early detection of malignant melanoma: the role of physician examination and self-examination of the skin. CA: A Cancer Journal for Clinicians 1985;35(3):130‑51.
171. M. Kamali, G. Samei, "Border preserving skin lesion segmentation", in Proceedings of SPIE 6915, Medical Imaging 2008: Computer-Aided Diagnosis, 2008.
172. K. Ahmed, T. Jesmin, Md. Zamilur Rahman," Early Prevention and Detection of Skin Cancer Risk using Data Mining", International Journal of Computer Applications (0975 – 8887) Volume 62– No.4, January 2013.
173. G.Subramanya Nayak, Ottolina Davide, Puttamadappa C," Classification of Bio Optical signals using K- Means Clustering for Detection of Skin Pathology", International Journal of Computer Applications (0975 – 8887) Volume 1 – No. 2, 2010.
174. R. T. Whitaker." Volumetric deformable models: Active blobs. In Visualization in Biomedical Computing" (1994), pp. 122–134.
175. A. Masood, A. A. Al-Jumaily, "Fuzzy C mean Thresholding based Level Set for Automated Segmentation of Skin Lesions", Journal of Signal and Information Processing, Vol. 4, No. 3B, ISSN: 2159-4465, August 2013, pp. 66-71.
176. A. Lefohn, J. E.Cates, R. T .Whitaker. "Interactive, GPU-based level sets for 3D segmentation". In Proc. Of Medical Image Computing and Computer Assisted Intervention (MICCAI ‟03 (2003), pp. 564–572.
177. J. Cates, A. Lefohn, and R. Whitaker, "GIST: an interactive, GPU-based level set segmentation tool for 3D medical images". Medical Image Analysis 8, 3 (2004), 217–231.
178. Li, B.N., et al.: Integrating spatial fuzzy clustering with level set methods for automated medical image segmentation. Computers in Biology and Medicine 41, 1–10 (2011).
179. Q. Abbas, I. Fondón, M. Rashid. Unsupervised skin lesions border detection via two-dimensional image analysis. Computer Methods and Programs in Biomedicine 104, 1–15 (2011).
180. J. Tang, "A multi-direction GVF snake for the segmentation of skin cancer images," Pattern Recognition 42(6), 1172–1179 (2009).
181. J. E. Golston, W. V. Stoecker, R. H. Moss, and I. P. S. Dhillon, "Automatic detection of irregular borders in melanoma and other skin tumors," Comp. Med. Imaging Graphics 16(3), 199–203 (1992).
182. P. Pagadala. Tumor border detection in epiluminescence microscopy images. Master's thesis, Department of Electrical and Computer Engineering, University of Missouri-Rolla, Sweden, August 1998.
183. H. Ganster, A. Pinz, R. Rohrer, E. Wildling, M. Binder, and H. Kittler. Automated melanoma recognition. IEEE Transactions on Medical Imaging, 20:233–239, March 2001.
184. T. Donadey, C. Serruys, A. Giron, and W. Woelker. Image segmentation based on adaptive 3-d-analysis of the cie-l*a*b colour space. In SPIE Visual Communications and Image Processing, volume 2727, pages 1197–1203, 1996.

185. Abbasi N, Shaw H, Rigel D, Friedman R, McCarthy W, Osman I, et al. Early diagnosis of cutaneous melanoma: revisiting the ABCD criteria. Journal of the American Medical Association 2004;292(22):2771‑6.
186. Mackie R, Doherty V. Seven-point checklist for melanoma. Clinical and Experimental Dermatology 1991;16(2):151‑2.
187. Malvehy J, Puig S, Argenziano G, Marghoob AA, Soyer HP. Dermoscopy report: proposal for standardization: results of a consensus meeting of the International Dermoscopy Society. Journal of the American Academy of Dermatology 2007;57(1):84‑95.
188. K. M. Clawson, P. J. Morrow, B. W. Scotney, D. J. McKenna, and O. M. Dolan. Determination of optimal axes for skin lesion asymmetry quantification. In IEEE International Conference on Image Processing (ICIP 2007), volume 2, pages 453– 456, 2007.
189. Y. Chang, R. Joe Stanley, R. H. Moss, and W. V. Stoecker. A systematic heuristic approach for feature selection for melanoma discrimination using clinical images. Skin Research and Technology, 11:165–178, 2005.
190. Z. She, Y. Liu, and A. Damatoa. Combination of features from skin pattern and ABCD analysis for lesion classification. Skin Research and Technology, 13:25–33, 2007.
191. V. Ng, B. Fung, and T. K. Lee. Determining the asymmetry of skin lesion with fuzzy borders. Computers in Biology and Medicine, 35:103–120, December 2005.
192. W. V. Stoecker, W. Weiling Li, and R. H. Moss. Automatic detection of asymmetry in skin tumors. computerised Medical Imaging and Graphics, 16(3):191–197, 1992.
193. I. Maglogiannis and D. I. Kosmopoulos. Computational vision systems for the detection of malignant melanoma. Oncology Reports, 15:1027–1032, 2006.
194. S. Seidenari, G. Pellacani, and C. Grana. Asymmetry in dermoscopic melanocytic lesion images: A computer description based on colour distribution. Acta Dermato-Venereologica, 86(2):123–128, March 2006.
195. L. Andreassi, R. Perotti, M. Burroni, G. Dell 'Eva, and M. Biagioli. Computerised image analysis of pigmented lesions. Chronica Dermatologica, 5:11–24, 1995.
196. V. Ng and D. Cheung. Measuring asymmetries of skin lesions. In IEEE International Conference on Systems, Man, and Cybernetics, volume 5, pages 4211–4216, October 1997.
197. A. Bono, S. Tomatis, C. Bartoli, G. Tragni, G. Radaelli, A. Maurichi, and R. Marchesini. The ABCD system of melanoma detection: A spectrophotometric analysis of the asymmetry, border, colour, and dimension. Cancer, 85(1):72–77, January 1999.
198. A. G. Manousaki, A. G. Manios, E. I. Tsompanaki, J. G. Panayiotides, D. D. Tsiftsis, A. K. Kostaki, and A. D. Tosca. A simple digital image processing system to aid in melanoma diagnosis in an everyday melanocytic skin lesion unit. A preliminary report. International Journal of Dermatology, 45:402–410, April 2006.
199. H. Zabrodsky, S. Peleg, and D. Avnir. Continuous symmetry measures. Journal of the American Chemical Society, 114(20):7843–7851, November 1992.
200. H. Zabrodsky, S. Peleg, and D. Avnir. A measure of symmetry based on shape similarity. In IEEE Computer Society Conference on Computer Vision and Pattern Recognition (CVPR 92), pages 703–706, June 1992.

201. S. Seidenari, G. Pellacani, and C. Grana. Pigment distribution in melanocytic lesion images: A digital parameter to be employed for computer-aided diagnosis. Skin Research and Technology, 11:236–241, 2005.
202. T. K. Lee, M. S. Atkins, R. Gallagher, C. E. Macaulay, A. Coldman, and D. I. McLean. Describing the structural shape of melanocytic lesions. In SPIE Medical Imaging, volume 3661, pages 1170–1179, 1999.
203. T. K. Lee and M. S. Atkins. New approach to measure border irregularity for melanocytic lesions. In SPIE Medical Imaging, volume 3979, pages 668–675, 2000.
204. T. K. Lee, D. I. McLeanc, and M. S. Atkins. Irregularity index: A new border irregularity measure for cutaneous melanocytic lesions. Medical Image Analysis, 7:47–64, 2003.
205. M. Celebi, H. Kingravi, B. Uddin, H. Iyatomi, Y. A. Aslandogan, W. V. Stoecker, and R. H. Moss. A methodological approach to the classification of dermoscopy images. computerised Medical Imaging and Graphics, 31:362–373, 2007.
206. Y. Cheng, R. Swamisai, S. E. Umbaugh, R. H. Moss, W. V. Stoecker, S. Teegala, and S. K. Srinivasan. Skin lesion classification using relative colour features. Skin Research and Technology, 14:53–64, 2008.
207. R.M. Haralick, K. Shanmugam, and I. Dinstein, ”Textural Features for Image Classification”, IEEE Trans. on Systems, Man and Cybernetics, Vol. SMC-3, pp. 610-621, 1973.
208. R.M. Haralick and K. Shanmugam, ”Computer Classification of Reservoir Sandstones”, IEEE Trans. on Geo. Eng., Vol. GE-11, pp. 171-177, 1973.
209. J.S. Weszka, C.R. Dyer, and A. Rosenfeld, “A comparative Study of Texture Measures for Terrain Classification”, IEEE Trans. on Systems, Man and Cybernetics, Vol. SMC-6, pp. 269-285, 1976.
210. D.C. He, L.Wang, and J. Juibert, ”Texture Feature Extraction”, Pattern Recognition Letters, Vol. 6, pp. 269-273, 1987.
211. M.M. Trivedi, R.M. Haralick, R.W. Conners, and S. Goh, ”Object Detection based on Gray Level Coocurrence”, Computer Vision, Graphics, and Image Processing, Vol. 28, pp. 199-219, 1984.
212. R.W. Conners, M.M. Trivedi, and C.A. Harlow, ”Segmentation of a High-Resolution Urban Scene Using Texture Operators”, Computer Vision, Graphics, and Image Processing, Vol. 25, pp. 273-310, 1984.
213. M. Iizulca, ”Quantitative evaluation of similar images with quasi-gray levels”, Computer Vision, Graphics, and Image Processing, Vol. 38, pp. 342-360, 1987.
214. L.H. Siew, R.H. Hodgson, and E.J. Wood, ”Texture Measures for Carpet Wear Asessment”, IEEE Trans. on Pattern Analysis and Machine Intell., Vol. PAMI-10, pp. 92-105, 1988.
215. R.W. Conners and C.A. Harlow, ”A theoretical comparison of texture algorithms”, IEEE Trans. on Pattern Analysis and Machine Intell., Vol. PAMI-2, pp. 204- 222, 1980.
216. Aribisala B, Claridge E. A border irregularity measure using Hidden Markov Models as a malignant melanoma predictor. In: Proc. Int. Conf. biomedical engineering. 2005.
217. Ma L, Qin B, Xu W, Zhu L. Multi-scale descriptors for contour irregularity of skin lesion using wavelet decomposition. In: Proc. Int. Conf. biomedical engineering and informatics (BMEI), vol. 1. Piscataway, NJ: IEEE Press; 2010.p. 414‑8.
218. Umbaugh S, Moss R, Stoecker W. Applying artificial intelligence to the identification of variegated coloring in skin tumors. IEEE Engineering in Medicine and Biology 1991;10(4):57‑62.
219. Claridge E, Cotton S, Hall P, Moncrieff M. From colour to tissue histology: physics based interpretation of images of pigmented skin lesions. In: Dohi T, Kikinis R, editors. Proc. Int. Conf. medical image computing and computerassisted intervention (MICCAI), vol. 2488 of LNCS. Berlin: Springer; 2003. p. 730‑8.
220. She Z, Excell PS. Skin pattern analysis for lesion classification using local isotropy. Skin Research and Technology 2011;17(2):206‑12.

221. Zhou Y, Smith M, Smith L, Warr R. A new method describing border rregularity of pigmented lesions. Skin Research and Technology 2010;16(1):66‐76.
222. M. Dash and H. Liu. Feature selection for classification. Intelligent Data Analysis, 1:679–693, 1997.
223. H. Liu and H. Motoda. Feature Selection for Knowledge Discovery and Data Mining. Kluwer Academic, Boston, 1998.
224. P. Langley. Selection of relevant features in machine learning. In AAAI Fall Symposium on Relevance, pages 140–144, 1994.
225. H. Liu and L. Yu. Toward integrating feature selection algorithms for classification and clustering. IEEE Transactions on Knowledge and Data Engineering, 17:491–502, 2005.
226. Rohrer R, Ganster H, Pinz A, Binder M. Feature selection in melanoma recognition. In: Proc. Int. Conf. pattern recognition (ICPR), vol. 2. Los Alamitos, CA: IEEE Computer Society Press; 1998. p. 1668‐70.
227. Celebi M, Aslandogan Y. Content-based image retrieval incorporating models of human perception. In: Proc. Int. Conf. information technology: coding and computing (ITCC), vol. 2. Los Alamitos, CA: IEEE Computer Society Press; 2004. p. 241‐5.
228. Situ N, Yuan X, Wadhawan T, Zouridakis G. Computer-aided skin cancer screening: feature selection or feature combination. In: Proc. IEEE Int. Conf. image processing (ICIP). Piscataway, NJ: IEEE Press; 2010. p. 273‐6.
229. R. Walvick, K. Patel, S. Patwardhan, and A. Dhawan. Classification of melanoma using wavelet-transform-based optimal feature set. In SPIE Medical Imaging 2002: Image Processing, volume 5370, pages 944–951, 2004.
230. T. Ro_, H. Handels, J. Kreusch, H. Busche, H. Wolf, and S. Poppl. Automatic classification of skin tumours with high resolution surface profiles. In V. Hlavac and R. Sara, editors, Computer Analysis of Images and Patterns, volume 970 of Lecture Notes in Computer Science, pages 368–375. Springer Berlin / Heidelberg, 1995.
231. A. Nimunkar, A. Dhawan, P. Relue, and S. Patwardhan. Wavelet and statistical analysis for melanoma. In SPIE Medical Imaging 2002: Image Processing, volume 4684, pages 1346–1352, 2002.
232. Firpi, H. and Goodman,E., ESwarmed feature selectionE Proceedings of the 33rd applied imagery pattern recognition workshop, pp. 112–118, 2004.
233. Liu, Y. et al., Feature Selection with Particle SwarmsE LNCS Vol 3314, pp 425–430, 2005.
234. Wang, X. et al., EFeature Selection based on Rough Sets and Particle Swarm OptimizationE Pattern Recognition Letter, Vol 28, issue 4, pp. 459–471,March 2007.
235. Tu, C. J. et al.,EFeature Selection using PSO-SVME Proceedigs of International Multiconference Engineers and Computer scientist, Hong Kong, pp.138–143, 2006.
236. Lee, T. F. et al,EFeature Selection of SVM and ANN using Particle Swarm Optimization for Power Transformers Incipient Fault Symptom DiagnosisE International Journal of Computational Intelligence Research, Vol 3, No. 1, pp. 50–65, 2007.
237. Amonchanchaigul, T. and Kreesuradej,W., EInput Selection using Binary Particle Swarm OptimizationE International Conference on Computational intelligence for Modelling Control and Automation , 2006.
238. Chakraborty, B., Feature Subset Selection by Particle Swarm Optimization with Fuzzy Fitness FunctionE in Proc.ISKE 2008 (3rd. International Conference on Intelligent Systems and Knowledge Engineering), pp. 1038–1042, Nov. 2008.
239. Chakraborty, B., Binary Particle Swarm Optimization based Algorithm for Feature Subset SelectionE Proc ICAPR09. pp. 145–148, Feb. 2009.
240. Chakraborty, B.," Feature Subset Selection Using Hybrid Particle Swarm Optimization", ICIC Express Letters, Vol. 4, No. 5, October 2010.

241. Yashar Maali, Adel Al-Jumaily," Hierarchical Parallel PSO-SVM Based Subject-Independent Sleep Apnea Classification", ICONIP 2012, Part IV, LNCS 7666, pp. 500–507, 2012.
242. A. Unler and A. Murat, "A discrete particle swarm optimization method for feature selection in binary classification problems," Eur. J. Oper. Res.,vol. 206, no. 3, pp. 528–539, Nov. 2010.
243. Y. Liu, G. Wang, H. Chen, and H. Dong, "An improved particle swarm optimization for feature selection," J. Bionic Eng., vol. 8, no. 2, pp. 191– 200, Jun. 2011.
244. A. Mohemmed, M. Zhang, and M. Johnston, "Particle swarm optimization based AdaBoost for face detection," in Proc. IEEE CEC, 2009, pp. 2494–2501.
245. Pablo G. Cavalcanti, Jacob Scharcanski, Gladimir V.G. Baranoski," A two-stage approach for discriminating melanocytic skin lesions using standard cameras", Expert Systems with Applications 40 (2013) 4054–4064.
246. I. Maglogiannis, S. Pavlopoulos, and D. Koutsouris. An integrated computer supported acquisition, handling, and characterisation system for pigmented skin lesions in dermatological images. IEEE Transactions on Information Technology in Biomedicine, 9:86–98, March 2005.
247. A. Green, N. Martin, J. Pfitzner, MO'Rourke, and N. Knight. Computer image analysis in the diagnosis of melanoma. Journal of the American Academy of Dermatology, 31:958–964, 1994.
248. G. Pellacani, M. Martini, and S. Seidenari. Digital videomicroscopy with image analysis and automatic classification as an aid for diagnosis of spitz nevus. Skin Research and Technology, 5:266–272, 1999.
249. M. Burroni, R. Corona, G. Dell'Eva, F. Sera, R. Bono, P. Puddu, R. Perotti, F. Nobile, L. Andreassi, and P. Rubegni. Melanoma computer-aided diagnosis: Reliability and feasibility study. Clinical Cancer Research, 10:1881–1886, March 2004.
250. S. Dreiseitl, L. Ohno-Machado, H. Kittler, S. Vinterbo, H. Billhardt, and M. Binder. A comparison of machine learning methods for the diagnosis of pigmented skin lesions. Journal of Biomedical Informatics, 34:28–36, 2001.
251. S. E. Umbaugh, R. H. Moss, and W. V. Stoecker. Applying artificial intelligence to the identification of variegated colouring in skin tumors. IEEE engineering in medicine and biology magazine, 10:57–62, 1991.
252. I. Maglogiannis, E. Zafiropoulos, and C. Kyranoudis. Intelligent segmentation and classification of pigmented skin lesions in dermatological images. In Advances in Artificial Intelligence, volume 3955 of Lecture Notes in Computer Science, pages 214–223. Springer Berlin, 2006.
253. T. Tommasi, E. La Torre, and B. Caputo. Melanoma recognition using representative and discriminative kernel classifiers. In Computer Vision Approaches to Medical Image Analysis, volume 4241 of Lecture Notes in Computer Science, pages 1–12. Springer Berlin, 2006.
254. A. Kjoelen, M. J. Thompson, S. E. Umbaugh, R. H. Moss, and W. V. Stoecker. Performance of ai methods in detecting melanoma. IEEE Engineering in Medicine and Biology Magazine, 14:411–416, 1995.
255. M. Wiltgen, A. Gergerb, and J. Smolle. Tissue counter analysis of benign common nevi and malignant melanoma. International Journal of Medical Informatics, 69:17–28, 2003.
256. Yashar Maali, Adel Al-Jumaily, "Self-Advising Support Vector Machine", Knowledge-Based Systems Journal, 52 (2013) 214–222.
257. Jin, H. and C.X. Ling, Using AUC and accuracy in evaluating learning algorithms. IEEE Transactions on Knowledge and Data Engineering,, 2005. 17(3): p. 299-310.
258. Ling, C.H., Jin Zhang, Harry, AUC: A Better Measure than Accuracy in Comparing Learning Algorithms Advances in Artificial Intelligence, Y.C.-d. Xiang, Brahim, Editor 2003, Springer Berlin / Heidelberg. p. 991-991.

259. Sboner, A., et al., A multiple classifier system for early melanoma diagnosis. Artificial Intelligence in Medicine, 2003. 27(1): p. 29-44.
260. Goutte, C. and E. Gaussier, A probabilistic interpretation of precision, recall and F-score, with implication for evaluation, in Advances in Information Retrieval, D.E. Losada and J.M. FernandezLuna, Editors. 2005. p. 345-359.
261. Gath, I., C. Feuerstein, and A. Geva, unsupervised classification and adaptive definition of sleep patterns. Pattern Recognition Letters, 1994. 15(10): p. 977-984.
262. M M Puranik, S Krishnan," Segmentation of Image Using Watershed and Fast Level set methods", International Conference and Workshop on Emerging Trends in Technology (ICWET 2011) – TCET, Mumbai, India.
263. B. Chen, C. Tai Phang, R. Harrison and Y. Pan," Novel Hybrid Hierarchical-k-means Clustering Method (H-k-means) for Microarray Analysis", Workshops and Poster Abstracts, IEEE Computational Systems Bioinformatics Conference, 2005.
264. M. Silveira , "Comparison of Segmentation Methods for Melanoma Diagnosis in Dermoscopy Images," IEEE Journal of Selected Topics in Signal Processing, Vol. 3, pp. 35-45, 2009.
265. J. MacQueen, Some methods for classification and analysis of multivariate observations. Proc: 5th Berkeley Symp. Math. Statist, Prob, 1:218-297, 1967.
266. L. Li, P. Ross, M. Kruusmaa, X. Zheng," A Comparative Study of Ultrasound Image Segmentation Algorithms for Segmenting Kidney Tumors", ISABEL '11,ACM, October 26-29, Barcelona, Spain.
267. N. Hema Rajini, R.Bhavani," Enhancing K-means and Kernelized Fuzzy C-means Clustering with Cluster Center Initialization in Segmenting MRI brain images", 2011 3rd International Conference on Eectronics Computer Technology(ICECT),2011.
268. S.J. Osher, J.A. Sethian: Fronts propagation with curvature dependent speed: Algorithms based on hamilton-jacobi formulations. Journal of Computational Physics, 12–49 (1988).
269. J.A. Sethian: Level set Methods and Fast Marching Methods, 2nd edn. Cambridge University Press, Cambridge (1999).
270. I. Guyon and A. Elisseeff, "An introduction to variable and feature selection," J. Mach. Learn. Res., vol. 3, pp. 1157–1182, Mar. 2003.
271. Pudil, P., Novoviovca, J. and Kittler, J. (1994) Floating search methods in feature selection. Pattern Recognition Letters, 15, 1119-1125.
272. Eberhart, R. and J. Kennedy. A new optimizer using particle swarm theory. in Micro Machine and Human Science, 1995. MHS '95., Proceedings of the Sixth International Symposium on. 1995.
273. Kennedy, J., R. Eberhart, and Ieee, Particle swarm optimization. 1995 Ieee International Conference on Neural Networks Proceedings, Vols 1-61995. 1942-1948.
274. Bing Xue, Mengjie Zhang, and Will N. Browne," Particle Swarm Optimization for Feature Selection in Classification: A Multi-Objective Approach", IEEE Transactions On Cybernetics, Vol. 43, NO. 6, 2013.
275. Y. Shi and R. Eberhart, "A Modified Particle Swarm Optimizer," in Proc. of the IEEE Congress on Evolutionary Computation, 1998, pp. 69–73.
276. G.Pranava, P.V.Prasad," Constriction Coefficient Particle Swarm Optimization for Economic Load Dispatch with Valve Point Loading Effects", 2013 International Conference on Power, Energy and Control (ICPEC).
277. P. Sajda. Machine learning for detection and diagnosis of disease. Biomedical Engineering, 8:537–565, 2006.
278. Vapnik, V., Statistical Learning1998: Wiley.
279. B. E. Boser, I. M. Guyon, and V. N. Vapnik. A training algorithm for optimal margin classifiers. In Proceedings of the fifth annual workshop on Computational Learning Theory, pages 144–152, 1992.

280. Wencai Zeng, Jiong Jiay, Zhonglong Zhengz, Chenmao Xie and Li Guo," A Comparison Study: Support Vector Machines for Binary Classification in Machine Learning", 2011 4th International Conference on Biomedical Engineering and Informatics (BMEI).
281. V. Kecman, Learning and Soft Computing, The MIT Press London, 2001.
282. S. S. Keerthi and C-J. Lin. Asymptotic behaviors of support vector machines with gaussian kernel. Neural Computtation, 15:1667–1689, 2003.
283. C. J. C. Burges. A tutorial on support vector machines for pattern recognition. Data mining and knowledge discovery, 2:121–167, 1998.
284. J. Platt. Fast training of support vector machines using sequential minimal optimisation. pages 185–208, 1999.
285. Sokolova, M., N. Japkowicz, and S. Szpakowicz, Beyond accuracy, F-Score and ROC: A family of discriminant measures for performance evaluation, in AI 2006: Advances in Artificial Intelligence, Proceedings, A. Sattar and B.H. Kang, Editors. 2006. p. 1015-1021.
286. Alain H, Djemel Z," Image quality metrics: PSNR vs. SSIM", International Conference on Pattern Recognition, 2010.